# SYNTHESIS, CHARACTERIZATION, AND PARAMETERIZATION OF ANIONIC AND NEUTRAL MONODENTATE LIGANDS AND THE ADDITION OF A PYRROLE LIGAND TO A SURFACE

By

Nicholas Alexander Maciulis

A THESIS

Submitted to
Michigan State University
in partial fulfillment of the requirements
for the degree

MASTERS OF SCIENCE

Chemistry

2012

ABSTRACT

**SYNTHESIS, CHARACTERIZATION, AND PARAMETERIZATION OF ANIONIC AND NEUTRAL MONODENTATE LIGANDS AND THE ADDITION OF A PYRROLE LIGAND TO A SURFACE**

By

Nicholas Alexander Maciulis

The main body of this thesis concerns determining the donor ability of ligands bound to a $d^0$ chromium center. Synthetic protocols and characterization data for a variety of chromium(VI) nitrido compounds of the general formula $NCr(NPr^i_2)_2X$ are reported, where X is a variety of mono-anionic ligands. Using spin saturation transfer or line shape analysis, the free energy barriers for diisopropylamido rotation were studied. It is proposed that the estimated enthalpic barriers, Ligand Donor Parameters (LDPs), for amido rotation can be used to parameterize the donor abilities of this diverse set of anionic ligands toward transition metal centers in low *d*-electron counts.

The last chapter of the thesis is devoted to placing the 5,5-dimethyldipyrrolylmethane (dmpm) ligand on a surface. The dmpm ligand was protected and coupled to a borylated polystyrene resin. The straight-forward route to placing a ligand on a surface has been developed. A detail on the synthesis and characterization is also discussed.

# ACKNOWLEDGEMENTS

I first would like to thank my parents Algimantas and Margarethe Maciulis for supporting my interests and encouraging me to pursue my dreams.

I also want to thank the Chemistry Faculty at Alma College, especially Dr. Nancy Dopke for giving me the chance to work in her lab and Dr. Sean Mo for nurturing my curiosities in chemistry. My experience with them was wonderful and I will never forget them.

Aaron, thank you for giving me a chance to work in your lab and learn about synthetic inorganic chemistry. The lessons and techniques I learned will always be with me for the rest of my life.

I would also like to thank my committee members for being patient, understanding and for providing insight and guidance in my research.

To Dan Holmes and Kermit Johnson: I would not have been as successful with my research if it wasn't for you. You were always helpful, whether it was fixing problems with the NMR instrument or interpretation of data or teaching me kinetic experiments I will always be thankful.

To my lab mates: Steve DiFranco, may you find peace and happiness when you get your PhD. Without your synthetic skills, this chromium project would not be as complete as it is. Amila, may you find a job that pays you lots and lots of money.

To Sebastian Jesberg for being a true friend and who was always ready to talk about life's problems and support my decisions.

To Allison Brown for keeping me sane during my time at graduate school.

To everyone else that I have associated with I thank all of you for support and moral. In these last few months I have gotten to know many of you and I am sad that I am leaving because I am saying goodbye to some very amazing people. I hope you all are successful and happy with your lives.

TABLE OF CONTENTS

LIST OF TABLES

LIST OF FIGURES

LIST OF SCHEMES

# LIST OF ABBREVIATIONS

LDP = Ligand Donating Parameter

SSMT = Spin Saturation Magnetization Transfer

CLSA = Complete Line Shape Analysis

NMR = Nuclear Magnetic Resonance

NOE = Nuclear Overhauser Effect

AOM = Angular Overlap Model

EPR = Electronic Paramagnetic Resonance

$\%V_{bur}$ = Percent Buried Volume

DMAP = 4-Dimethylaminopyridine

HMPA = Hexamethylphosphoramide

OBn = Benzyloxy

OPth = κ(O)-*N*-oxy-phthalimide

OAd = Admantoxide

$O^tBuF_6$ = Hexafluoroterbutoxide

OTf = Trifluoromethanesulfonoxide

THF = Tetrahydrofuran

BOC = *N*-*tert*-butoxycarbonyl

HBPin = Pinacoleborane

TBAF = Tetrabutyl Ammonium Fluoride

TPP = Tetraphenylporhinato Dianion

OEP = Octaethylporphinato Dianion

DMA = *N*,*N*-dimethylacetamide

DME = 1,2-Dimethoxyethane (glyme)

NHC = *N*-heterocyclic Carbene

dmpm = 5,5-dimethyldipyrrolylmethane

$^{t}$Bu = *tert*-Butyl

Me = Methyl

Ph = Phenyl

$^{i}$Pr = Isopropyl

## Chapter 1: Metal Centers and their Ligands

### 1.1 Introduction

Many everyday products that we depend on, such as plastics and fuels, were created or modified using a catalyst. Humanity truly benefits from these products without realizing how much effort was put into researching them. From plastic bags to Tupperware to "O"-rings used in space shuttles, the physical properties of polymers are dependent on the molecular weight and tacticity. This, in some respects, is determined by the catalyst. It is the ligands bound to the metal that affect the reactivity of the catalyst that ultimately determines the tacticity and molecular weight, which determines the physical properties of the polymer.[1]

Another area of interest that is dependent on the activity of a catalyst is generating fuels for future use. Currently, oil refinement and "cracking" use catalysts[2,3] to improve the gas performance and reduce pollution. But there is a push for moving towards a hydrogen economy.[4] Nocera published papers[5] discussing a new cobalt complex that splits water into $H_2$ gas and $O_2$ gas. This gives a promising outlook for a cleaner future because the conditions for $H_2$ generation using the reported methods are at ambient conditions, while previous routes used the water-gas shift reaction to generate $H_2$ that was energy intensive and produced $CO_2$ as an unwanted by-product.[6]

In regards to sustainability, another area of immense importance is nitrogen fixation. Fritz Haber discovered a route to generate ammonia by mixing $N_2$ and $H_2$ but it is energy intensive and requires harsh conditions.[7] Studies of enzymes[8] that naturally reduce $N_2$ to $NH_3$ have led to

break-through designs in transition metal complexes that coordinate $N_2$ and hydrogenate the unsaturated dinitrogen molecule.[9] Only once the most promising catalytic system is found and the correct ligand set is identified will the issues of sustaining a growing society be met.

A long time goal in the world of academics and industry has been controlling the reactivity of a catalyst. There is no doubt whether a transition metal center is $d^0$, such as Schrock's Catalyst,[10] or $d^8$ as in Wilkinson's catalyst,[11] that the activity of both systems rely heavily on the ancillary ligands. It is the electronic and steric effects of the ligand that play a role in determining the activity and selectivity of the metal center.

Part of the difficulty in designing a catalyst is deciding on which ligands to choose for a system and how their donor ability affects reactivity. Typically, the choice of ligand is dependent on 1) analogy to a similar reaction in the literature, 2) picking ancillary ligands already available in the lab, and 3) an educated guess based on experience in the field. If there was a way to know the donor ability of a ligand, one could tune the catalytic system to meet the needs of the catalyst without as much trial and error. This would speed up progress in science to meet the needs of a society in the 21$^{st}$ century.

A famous study in gauging donor properties of ligands is the study of phosphine ligands by Tolman.[12] He looked at the how the electronic and steric factors of the R groups on phospine ligands affected the donor ability of the phosphorous atom bound to Nickel by observing the CO stretches in the IR.[12,13] Figure 1.1 shows some different resonance forms of CO bound to an electron rich metal center.

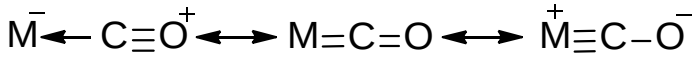

**Figure 1.1:** CO stretch and back-bonding effects on measurements

In the case of Tolman's system, a strong phophine donor will push more electron density on the metal favoring the resonance form on the left and result in a high stretching frequency that is similar to the normal range of free CO stretching frequencies. While a poor donor or electron-withdrawing ligand will favor the form on the right and cause a lower CO stretching frequency. This effect is seen throughout the different $Ni(CO)_3PR_3$ complexes.

Another key factor that affects the reactivity of many ligand complexes is the sterics. In Tolman's original study, he looked at homo-leptic phosphines that formed a cone shape. By treating the metal center as the apex of the cone, the sides of the cone were determined by the van der Waals radii of the outermost atoms. Combining the steric and electronic parameters produces the graph in Figure 1.2.

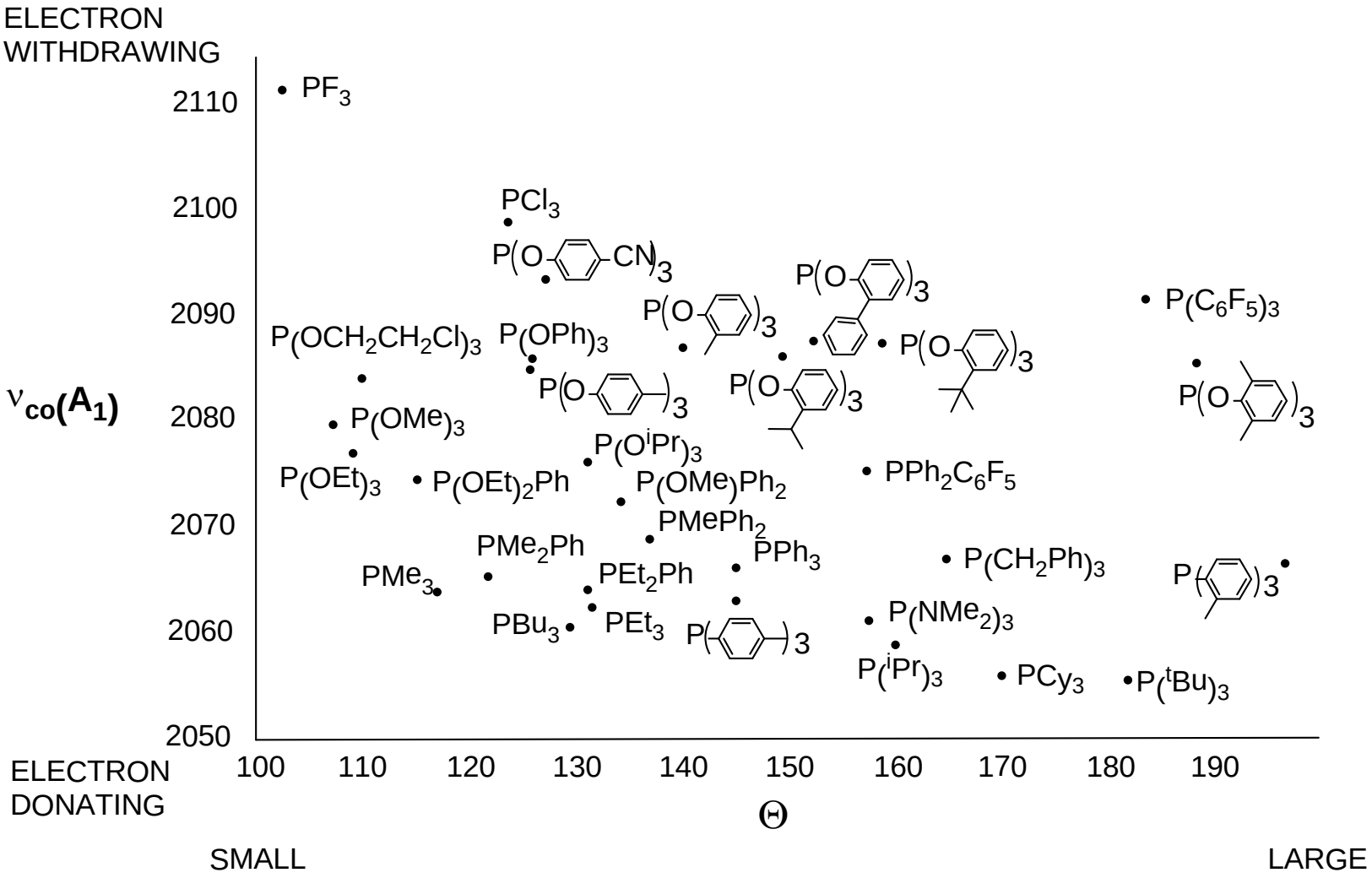


**Figure 1.2:** Tolman Map[13]

This study gave insight into choosing ligands with specific properties that dictate the reactivity of a catalytic system and has contributed to the development of chemistry for late transition metal systems. One can even see these steric and electronic effects explaining reactions and mechanisms found in the literature. No where in the literature has these parameters been more important than in homogeneous catalysis. For example, hydrogenation reactions involving the $RhClL_3$ catalyst increases in the following order where L = $P(p\text{-}C_6H_4F)_3$ < $PPh_3$ < $P(p\text{-}C_6H_4OCH_3)_3$.[14] This can be explained by the fact that increasing the donor ability of the group in the *para*-position increases the reactivity of the catalyst.

Even the sterics of the phosphines has a huge influence on the reaction. As an example, product distribution of propylene dimerization in a $Ni(C_3H_5)L{\cdot}AlCl_3$ system changes with increasing size of L ligand for the order of $PMe_3$, $PEt_3$, and $P(^iPr)_3$.[15] These are only a few examples, but the point is that Tolman's study of the electronic and steric components of phosphines ligands has made an important impact on how chemists approach the design of their catalysts.

Although, this has been immensely useful for later transition metals, early transition metal catalysts in higher oxidation states prefer anionic ligands over ligands with dative interactions to stabilize the high positive charge.[16] A common method has been to base donor strength of a ligand on its $pK_a$. One can rationalize that the resonance forms and electronegativity of the substituents bound to the ligand will either increase or decrease the donor ability but to what extent is unknown. To this date there has not been a study in determining donor ability of anionic ligands for early transition metal centers.

## 1.2: Investigation of the Probe for Donors Bound to a $d^0$ Chromium Center

As in Tolman's system, the donor ability of one ligand had an effect on the other ligands bound to it. So adding a ligand that has a feature that would be easy to measure would allow us to put a number to it and compare donor ability of different ligands. Searching through the literature one finds that amides have been exhaustively studied using NMR.[17] An interesting study[17f,g] looked at the effects of electronegativity of the R substituents bound to the carbonyl carbon on the barrier of rotation of the amide (see Figure 1.3).

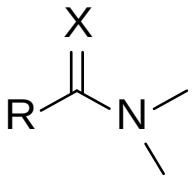


X = O, S

R = $CH_3O$, $CH_3S$, CN, EtCO, $CH_3C{\equiv}C$

**Figure 1.3:** Amides with different R and X substituents

As the R substituents increase in electron donation from CN to $CH_3O$, the barrier of rotation of the amide lowers. This study showed that the barrier of rotation of an amide can be used as a way to rate the donor ability of the R substituents. We could adopt this concept and apply it to a metal system to determine the donor ability of ligands bound to a metal center. Amido ligands show some of the interesting features when bound to transition metals in higher oxidation states. They can form both $\sigma$- and $\pi$- bonds that have different contributing resonance forms based on the Lewis acidity of the metal center.[18] The left form in Figure 1.4 is an amido but if there is an

open orbital with the correct symmetry then the lone pair can donate forming a pseudo-imido shown on the right.

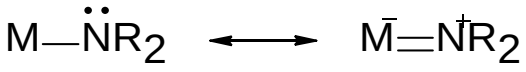

**Figure 1.4:** Amido resonance forms

The imido resonance structure contributes to bonding in nitrodo complexes of the formula $NCr(N^{i}Pr_2)_2X$. Thus, a series of compounds were synthesized in which the X ligand was varied with different anionic ligands. All of the orbitals on chromium and the ligands involved in bonding are shown in Figure 1.5. The lone pairs on the three ligands will compete for the two empty *p*-orbitals on chromium, although there will be some mixing with the $d_{x2-y2}$ and $d_{xy}$ orbitals due to symmetry. As shown in Figure 1.5, there is competition for the empty orbitals on chromium. A strong X donor will compete stronger with the lone pairs on the amido ligand resulting in a lower barrier of rotation about the chromium nitrogen bond, whereas a poor X donor will compete poorly with the amido, giving a higher barrier of rotation.

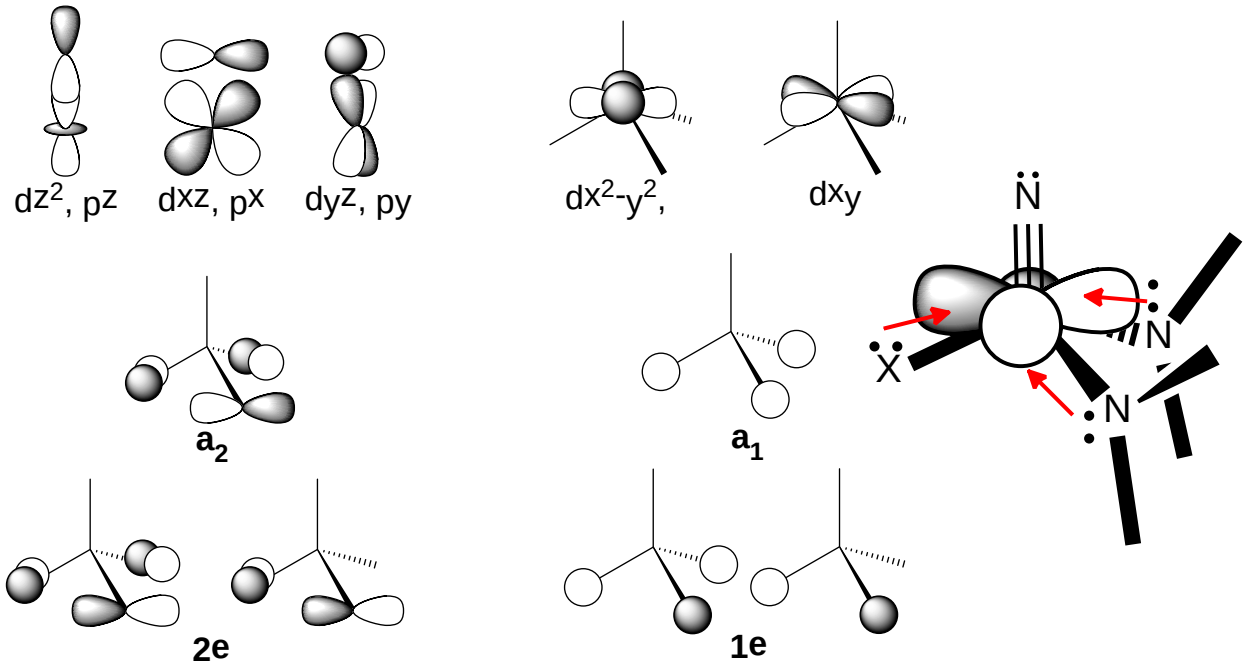


**Figure 1.5**: Bonding and antibonding orbitals available on chromium and ligands. The isopropyl groups on the amido ligands have been replaced by methyl groups for clarity. For interpretation of the references to color in this and all other figures, the reader is referred to the electronic version of this dissertation.

Since the $d_{x2\text{-}y2}$, $d_{xy}$, $p_x$, and $p_y$ orbitals on chromium have similar symmetry, there will be mixing. Therefore, barrier of rotation of the amido ligands will also be influenced by donors without lone pairs such as a $sp^3$ carbon with $\alpha$-hydrogens (X type) or neutral donors (L type) that only bind to the metal center through dative interactions. The latter requires the formation of a cationic chromium complex. Figure 1.6 shows the X, LX, and L type ligands[19] studied on the chromium system.

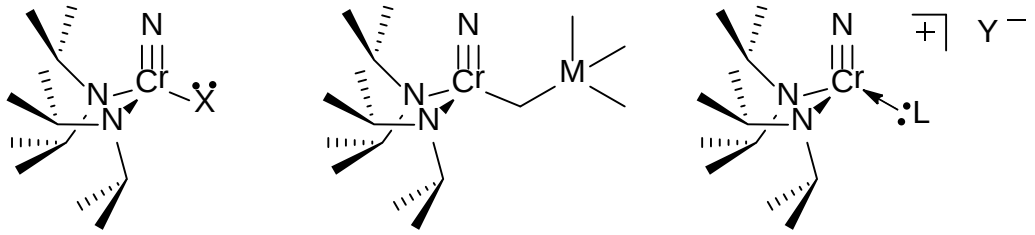


**Figure 1.6:** Three types of donors bound to chromium

X = I, Br, Cl, F, NCS, NCO, $O_2CPh$, CN, $OC_6F_5$, SPh, $NO_3$, $PyrC_6H_3(CF_3)_2$, $PyrC_6F_5$, Pyrrolyl, $O^tBuF_6$, Indolyl, F, Ph, OPth, $OSiPh_3$, $CC^tBu$, $CCSi^iPr_3$, O-*p*-$(CF_3)C_6H_4$, O-*p*-$(Cl)C_6H_4$, O-*p*-$(F)C_6H_4$, O-*p*-$(SMe)C_6H_4$, OPh, O-*p*-$(OMe)C_6H_4$, O-*p*-$(^tBu)C_6H_4$, Carbazolyl, OBn, $N^iPr_2$, OAd, N(Me)Ph, $NMe_2$

M = C, Si; L= HMPA, DMAP; Y= $BF_4$, $PF_6$

The beauty of our system is that we can investigate anionic and neutral donor ligands. This will allow us to determine the overlap between some other famous studies such as the Tolman map. The barrier is then measured using Spin Saturation Magnetization Transfer (SSMT)[20] or Complete Line Shape Analysis (CLSA)[21] techniques.

It has been shown that knowing the donor ability of phosphines through Tolman's electronic parameter improves the selectivity and reactivity of the catalyst. Knowing the donor ability of anionic ligands will help our understanding of reactivity in earlier high-valent transition metals. Knowing the donor abilities for both neutral and anionic ligands will allow for a faster development of catalysts and improvement of designs that will speed up the process for discovery eventually benefiting the standard of life for humanity.

REFERENCES

REFERENCES


1) (a) Flook, M. M.; Ng, V. W. L.; Schrock, R. R. *J. Am. Chem. Soc.* **2011**, *133*, 1784-1786 (b) Shaver, M. P.; Cameron, D. J. A. *Biomacromolecules* **2010**, *11*, 3673-3679 (c) Takeuchi, D.; Matsuura, R.; Park, S. Osakada, K. *J. Am. Chem. Soc*. **2007**, *129*, 7002-7003 (d) Bierwagen, E. P.; Bercaw, J. E.; Goddard III, W. A. *J. Am. Chem. Soc.* **1994**, *116*, 1481-1489

2) Schwarzenbeck, E. F. *Origin and Refining of Petroleum*, Chapter 5, **1971**, 94-112, *Advances in Chemistry* Vol. *113*

3) (a) Zaera, F. *J. Phys. Chem. Lett.* **2010**, *1*, 621-627 (b) Zaera, F. *J. Phys. Chem. B* **2002**, *106*, 4043-4052 (c) Martens, J. A.; Tielen, M.; Jacobs, P. A. *Catal. Today* **1987**, *1*, 435 (d) Martens, J. A. Jacobs, P. A.; Weithkamp, J. *J. Appl. Catal.* **1986**, *20*, 239-281 (e) Weitkamp, J. *Ind. Eng. Prod. Res. Dev.* **1982**, *21*, 550-558

4) Gregoire-Padró, G. E. *Energy Fuels* **1998**, *12*, 1-2

5) (a) Surendranath, Y.; Dincă, M.; Nocera, D. G. *J. Am. Chem. Soc.* **2009**, *131*, 2615-2620 (b) Kanan, M. W.; Nocera, D. G. *Science* **2008**, *321*, 1072-1075

6) (a) Dufour, J.; Serrano, D. P.; Galvez, J. L.; Moreno, J., Gonzalez, A. *Energy Fuels* **2011**, *25*, 2194-2202 (b) Wang, L.; Murata, K.; Inaba, M. *Ind. Eng. Chem. Res.* **2004**, *43*, 3228-3232 (c) Wang, D.; Czernik, S.; Chornet, E. *Energy Fuels* **1998**, *12*, 19-24

7) Haber, F.; van Oordt, G. Z. *Anorg. Chem.* **1905**, *47*, 42-44

8) (a) Barney, B. M.; McClead, J.; Lukoyanov, D.; Laryukhin, M.; Yang, T.-C.; Dean, D. R.; Hoffman, B. M.; Seefeldt, L. C. *Biochemistry* **2007**, *46*, 6784-6794 (b) Dos Santos, P. C.; Igarashi, R. Y.; Lee, H. I.; Hoffman, B. M.; Seefeldt, L. C.; Dean, D. R. *Acc. Chem. Res.* **2005**, *38*, 208-214 (c) Igarashi, R. Y.; Laryukhin, M.; Dos Santos, P. C.; Lee, H. I.; Dean, D. R.; Seefeldt, L. C.; Hoffman, B. M. *J. Am. Chem. Soc.* **2005**, *127*, 6231-6241 (d) Duyvis, M. G.; Wassink, H.; Haaker, H. *Biochemistry* **1998**, *37*, 17345-17354 (e) Burgess, B. K.; Lowe, D. J. *Chem. Rev.* **1996**, *96*, 2983-3012

9) (a) Kimura, T.; Koiso, N.; Ishiwata, K.; Kuwata, S.; Ikariya, T. *J. Am. Chem. Soc.* **2011**, *133*, 8880-8883 (b) Reithofer, M. R.; Schrock, R. R.; Müller, P. *J. Am. Chem. Soc.* **2010**, *132*, 8349-8358 (c) McNaughton, R. L.; Roemelt, M.; Chin, J. M.; Schrock, R. R.; Neese, F.;

Hoffman, B. M. *J. Am. Chem. Soc.* **2010**, *1321*, 8645-8656 (d) Schrock, R. R. *Chem. Commun.* **2003**, *19*, 23899-2391 (e) Shaver, M. P.; Fyzuk, M. D. *Adv. Synth. Catal.* **2003**, *345*, 1061-1076 (f) Yandulov, D. V.; Schrock, R. R. *Science* **2003**, *301*, 76-78 (g) Birk, T.; Bendix, J. *Inorg. Chem.* **2003**, *42*, 7608-7615 (h) Leung, S. K. Y.; Haung, J. S.; Liang, J. L.; Che, C. M.; Zhou, Z. Y. *Angew. Chem., Int. Ed.* **2003**, *42*, 340-343 (i) O'Donoghue, M. B.; Zanetti, N. C.; Davis, W. M.; Schrock, R. R. *J. Am. Chem. Soc*. **1997**, *119*, 2753-2754

10) (a) Schrock, R. R.; Murdzek, J. S.; Bazan, G. C.; Robbins, J.; DiMare, M.; O'Regan, M. *J. Am. Chem. Soc.* **1990**, *112*, 3875-3886 (b) Thorn-Csányi, E.; Zilles, J. U. *J. Molec. Catal. A* **2002**, *190*, 85-100 (c) Schrock, R. R.; DePue, R. T.; Feldman, J.; Yap, K. B.; Yang, D. C.; Davis, W. M.; Park, A. DiMare, M.; Schofield, M. *Organometallics* **1990**, *9*, 2262-2275

11) Osborn, J. A.; Jardine, F. H.; Young, J. F.; Wilkinson, G. *J. Chem. Soc. A* **1966**, 1711-1732

12) Tolman, C. A. *J. Am. Chem. Soc.* **1970**, *92*, 2953-2956

13) Tolman, C. A. *Chem. Rev.* **1977**, *77*, 313-347

14) (a) Montelactici, S.; van der Ent, A.; Osborn, J. A.; Wilkinson, G. *J. Chem. Soc. A.* **1968**, 1054-1058 (b) Tolman, C. A.; Meakin, P. Z.; Lindner, D. L.; Jesson, J. P. *J. Am. Chem. Soc.* **1974**, *96*, 2762-2774

15) Bogdanovic, B.; Henc, B.; Karmann, H.-G.; Nüssel, H.-G.; Walter, D.; Wilke, G. *Ind. Eng. Chem.* **1970**, *62*, 34-44

16) Sanderson, R. T. *Inorg. Chem.* **1986**, *25*, 3518-3522

17) (a) Kemnitz, C. R.; Loewen, M. J. *J. Am. Chem. Soc.* **2007**, *129*, 2521-2528 (b) Rablen, P. R.; Miller, D. A.; Bullock, V. R.; Hutchinson, P. H.; Gorman, J. A. *J. Am. Chem. Soc.* **1999**, *121*, 218-226 (c) Perrin, C. L.; Thoburn, J. D.; Kresge, J. A. *J. Am. Chem. Soc.* **1992**, *114*, 8800-8807 (d) Mann, B. E. *J. Magn. Reson.* **1977**, *25*, 91-94 (e) Drakenberg, T.; Dahlqvist, K.-I.; Forsén, S. *J. Phys. Chem.* **1972**, *76*, 2178-2183 (f) Sandström, J. *J. Phys. Chem.* **1967**, *71*, 2318-2325 (g) Fryer, C. W.; Conti, F.; Franconi, C. *Ric. Sci., Parte 2, Sez. A.* **1965**, *35*, 788-793

18) Crabtree, R. H. The Organometallic Chemistry of the Transition Metals $5^{th}$ Ed. New Jersey: John Wiley and Sons, Inc. **2009**

19) Green, M. L. H. J. *Organomet. Chem.* **1995**, *500*, 127-148

20) (a) Dahlquist, F. W.; Longmuir, K. J.; Du Vernet, R. B. *J. Magn. Reson.* **1975**, *17*, 406-410 (b) Jarek, R. L.; Flesher, R. J.; Shin, S. K. *J. Chem. Edu.* **1997**, *74*, 978-982

21) (a) Binsch, G. *J. Am. Chem. Soc.* **1969**, *96*, 1304-1309 (b) Allerhand, A.; Gutowsky, H. S.; Meinzer, R. A. *J. Am. Chem. Soc.* **1966**, *88*, 3185-3194 (c) McConnell, H. M. *J. Chem. Phys.* **1958**, *28*, 430-431

## Chapter 2: Synthesis of the Chromium Nitrido Complexes

### 2.1: Synthesis of $NCr(N^iPr_2)_3$ (**1**)

Development of nitrido transition metal complexes has been growing due to interest in NACM catalysis,[1] nitrogen fixation,[2] and atom transfer reactions.[3] Compared to other transition metal nitrido moieties, few examples of chromium nitrido complexes exist. Previous synthetic routes included oxidation of chromium in the presence of ammonia,[4] decomposition of sodium azide,[3c] and photolysis of chromium azido complexes.[5] An interesting approach developed in the Cummins' lab, involved oxidative cleavage of nitric oxide on chromium(II) nitrosyl compounds by $V(THF)(Mes)_3$, yielding chromium(VI) nitrido complexes.[6]

In the beginning of this chapter, I present a convenient and efficient synthesis of our chromium(VI) nitrido starting material, $NCr(N^iPr_2)_3$ (**1**), through atom transfer.[3] The red-brown $Cr(N^iPr_2)_3$ complex with $D_3$ symmetry was synthesized by mixing 3 equivalents of $LiN^iPr_2$ to a heterogeneous solution of $CrCl_3$ in ether.[7] $NCr(O^tBu)_3$ was synthesized using common starting materials.[8] To $(NH_4)_2Cr_2O_7$ in 1,2-dimethoxyethane was added $Me_3SiCl$, $HN(SiMe_3)_2$, and $NEt_3$. The reaction then stirred for one day with an excess of $^tBuOH$. After twelve hours of stirring, $^tBuOH$ was removed *in vacuo*, and the canary yellow product was sublimed at 40 $^oC$ under vacuum. $NCr(O^tBu)_3$ is light sensitive and should be stored in a dark container and in the freezer.

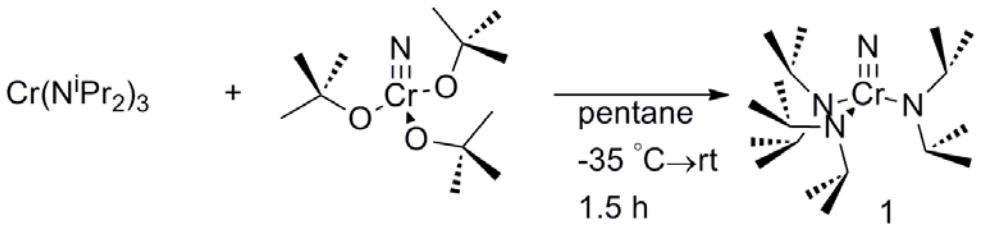


**Scheme 2.1:** Synthesis of $NCr(N^{i}Pr_2)_3$ (**1**)

Addition of solid $NCr(O^{t}Bu)_3$ to $Cr(N^{i}Pr_2)_3$ in pentane with stirring for two hours induced a three-electron, atom-transfer reaction affording $NCr(N^{i}Pr_2)_3$ (**1**) in high yield.

Atom transfer reactions resulting in chromium nitrido complexes were first reported in 1985,[9] reaction of $NMn^{V}$(TTP) with $Cr^{II}$(TTP) in THF cleanly generated $NCr^{V}$(TTP). An investigation by Bottomley and Neely[10,11] on substituent effects on porphyrins in intermetal transfer reactions provided an explanation for the driving force.

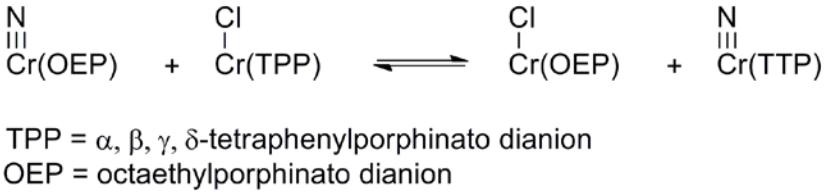


**Scheme 2.2:** Intermetal atom transfer reaction

In the reversible reaction shown in Scheme 2.2, exchange between the chloro and nitrido axial ligands resulted in a net two electron, atom transfer. Their rate data suggest that the addition of electron donor groups to the porphyrin[12,13] on the chromium(III) acceptor shifted the reaction towards the right. Stronger donating ligands are required to stabilize the higher positive charge on chromium. This is seen in our atom transfer reaction, shown in Scheme 2.1, that produces the robust compound, $NCr(N^{i}Pr_2)_3$.

## 2.2: Synthesis using Protonolysis

### 2.2.1: Protonolysis using Lutidinium Salts

Protonolysis of **1** with the appropriate 2,6-lutidinium halide ([HLut][X]), where X is Br or Cl in $CHCl_3$ at mild temperatures affords complexes **3** and **4**. This method is similar to the published procedure[15,16] for making $NCr(N^iPr_2)_2I$ (**2**). [HLut][Cl] and [HLut][Br] can be conveniently prepared by addition of HCl or HBr to 2,6-lutidine in THF under a nitrogen atmosphere.

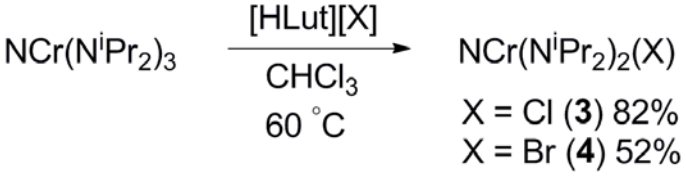


**Scheme 2.3:** Protonolysis using lutidinium salts

### 2.2.2: Protonolysis using HX

Alkoxides are common ligands found in the literature for high-valent metals. Changes in the electronics of the group bound to the oxygen in an alkoxide can have a significant impact on its donor properties. For example, by replacing a methyl group in $O^tBu$ with a $CF_3$ group, molybdenum and tungsten nitrido complexes increased reactivity in NACM reactions.[1a] Knowing the donor ability of different alkoxides may explain the reactivity of catalytic systems that rely on alkoxides, and discover an overlooked ligand.

Following a similar procedure[16] to make **9** and **10**, addition of one equivalent of the corresponding alcohol, silanol, carboxylate, and thiolate to **1** generated fifteen complexes cleanly

with relatively high yields. In most cases, HX compounds were added to a near frozen solution of **1** in toluene and allowed to warm to room temperature and stir for 1.5 hours. In the case of triflic acid, a near frozen solution of DME/pentane was required to generate **5** cleanly. In other cases, longer reaction times and higher temperatures were required; for example reaction of 1-adamantanol with **1** required heating at 90 $^{o}$C for three days. Removal of solvent and diisopropylamine *in vacuo* and crystallization from pentane gave compounds **5**, **6**, **7**, **8**, **11**, **12**, **13**, **14**, **15**, **16**, **17**, **18** and **19** in 52-94% yields.

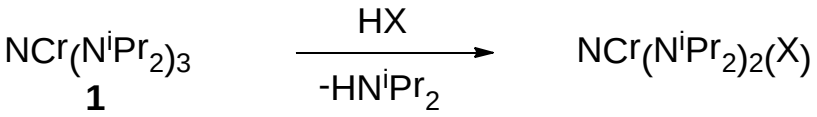


X = OTf (**5**), 70%
OAd (**6**), 70%
$OSiPh_3$ (**7**), 72%
$O_2CPh$ (**8**), 88%
$O^tBuF_6$ (**9**)
OPh (**10**)
O-*p*-(OMe)$C_6H_4$ (**11**), 87%
O-*p*-(SMe)$C_6H_4$ (**12**), 92%
O-*p*-($^t$Bu)$C_6H_4$ (**13**), 94%
O-*p*-(F)$C_6H_4$ (**14**), 88%
O-*p*-(Cl)$C_6H_4$ (**15**), 85%
O-*p*-($CF_3$)$C_6H_4$ (**16**), 82%
$OC_6F_5$ (**17**), 76%
SPh (**18**), 75%

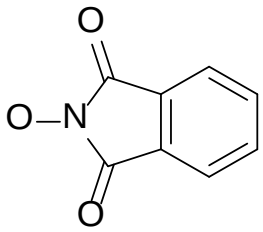

(OPth, **19**), 52%

**Scheme 2.4:** Protonolysis using HX compounds

### 2.3: Synthesis using Salt Metathesis

#### 2.3.1: Salt Metathesis using Thallium Salts

Although thallium is toxic and has a lack of stability with some X substituents, it avoided unwanted reduction seen with other reagents (vide infra), and the thallium reagents are easy to prepare. Following literature procedures,[18] addition of thallium ethoxide to the corresponding HX substituents generated TlX and ethanol that were easily removed by filtration and distillation. Unfortunately, obtaining $^{1}H$ and $^{13}C$ NMR data on the thallium pyrroles was not possible due to insolubility.

Substituted pyrroles $HPyr^{C6F5}$ and $HPyr^{C6H3(CF3)2}$ were prepared to study substitution effects on pyrrole-based ligands on hydroamination rates.[19] Their results indicated that electron withdrawing groups present on the pyrrole made the nitrogen a worse donor to titanium. With our system we can determine the donor abilities of pyrrole and substituted pyrroles and show that electron-withdrawing groups do in fact make pyrrole a worse donor.

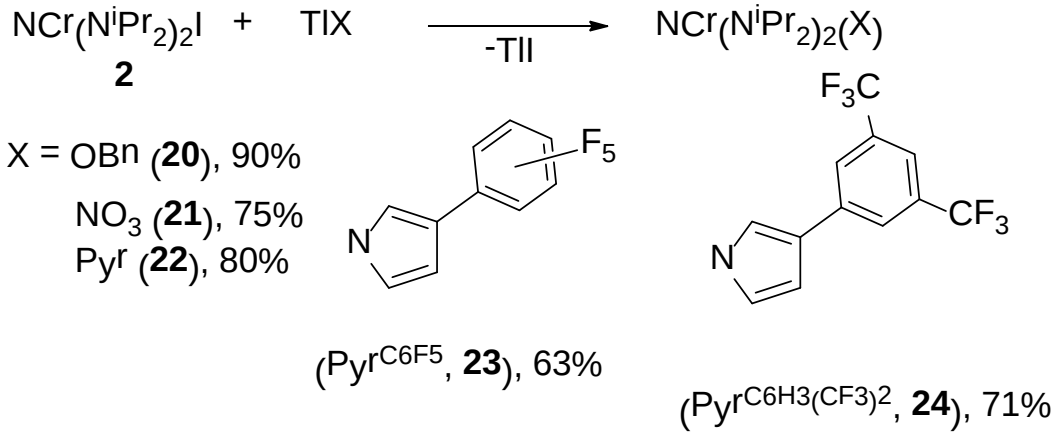


**Scheme 2.5:** Salt metathesis using thallium salts

Reaction of TlX with **2** led to precipitation of yellow TlI in hexanes or toluene, which was easily removed by filtration. The reaction cleanly gave new $NCr(N^iPr_2)_2(X)$ complexes **20-24**. In the production of $NCr(N^iPr_2)_2(NO_3)$ (**21**), tetrahydrofuran (THF) was used as the solvent due to low solubility of thallium nitrate in other organic solvents.

### 2.3.2: Salt Metathesis using Sodium Salts

The three complexes $NCr(N^iPr_2)_2(X)$, where X = NCO (**28**), NCS (**29**), and CN (**30**) were prepared using commercially available sodium salts and $NCr(N^iPr_2)_2I$ (Scheme 2.6). Long reaction times and mild heating were required due to low solubility of the sodium salts in organic solvents, even in acetonitrile. The use of 1,4-dioxane in the preparation of **28** and **29** helped the reaction to proceed. The use of cyclic ethers has been known to help sodium salts dissociate and increase solubility of the complex in solution.[17] In the case of using NaCN, reaction only occurred within the presence of one equivalent of 15-crown-5 ether.

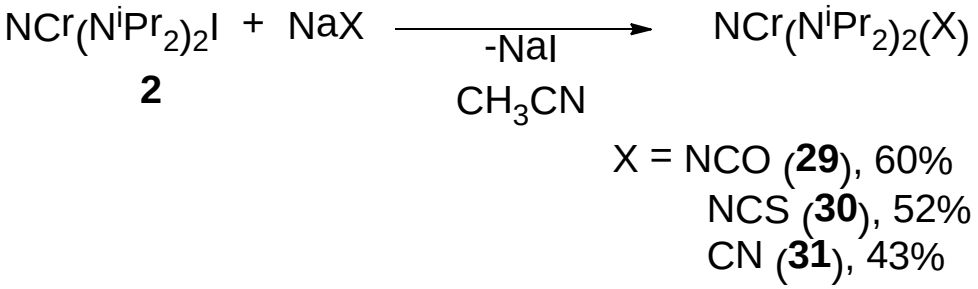


**Scheme 2.6:** Synthesis using sodium salts

**2.4: Synthesis using Ligand Exchange with Lithium Salts**

Reaction of lithium reagents with **2** has been shown to result in reduction to the known nitrido chromium(V) dimer.[15,16] Transmetalation using phenoxide **10** proved to be a viable route in preparing indolyl (**25**), carbazolyl (**26**), *N*-methylanilide (**27**), $CH_2Si(Me)_3$ (**35**) $CCSi^iPr_3$ (**39**), and $CC^tBu$ (**40**).

The syntheses of **25** and **26** compares their donor abilities with pyrrole, as the lone pair on the nitrogen is known to be less involved in the conjugation of the ring.[21,22] Preparation of carbon bound donors was of keen interest because the absence of lone pairs on the $\alpha$-carbon might allow us to distinguish between $\sigma$- and $\pi$-effects. As shown in Scheme 2.7, the lithium salts were added to a cold stirring solution of **10** in hexanes with short reaction times.

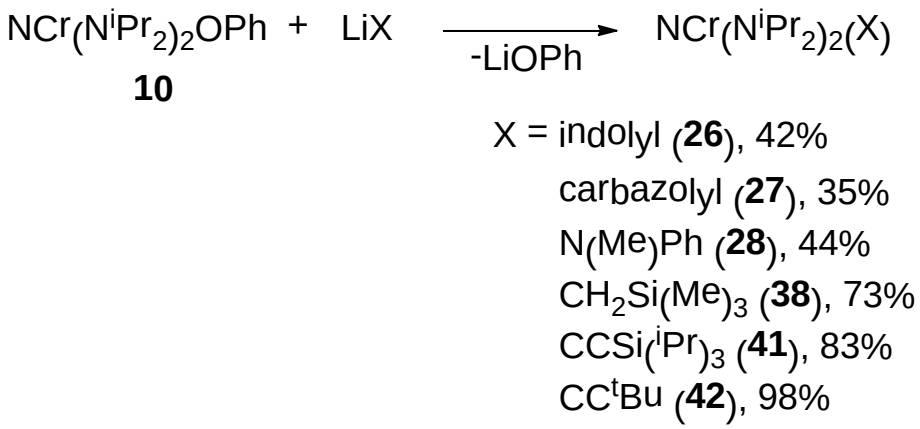


**Scheme 2.7:** Synthesis using ligand exchange with lithium salts

In the case of neopentyl (**38**), adamantoxide (**6**) was used as the transmetalation partner, because the reaction with **10** only resulted in reduction. The alkynyls **39** and **40** are stable at room temperature, while the alkyl complexes **35** and **38** need to be covered and stored in the fridge.

## 2.5: Synthesis using Ligand Exchange with Lithium to Zinc Transmetalation

To study the effect of sterics in the barrier of rotation in amides, dimethylamido (**31**) was synthesized. Shown in Scheme 2.8, treating $ZnCl_2$ with an excess amount of $LiNMe_2$ in DME/THF mixture presumably generates an amido zincate complex.[23] Addition of this mixture to **10** cleanly produces $NCr(N^iPr_2)_2NMe_2$ **31**, while addition of the $LiNMe_2$ direct to **2** only resulted in reduction.

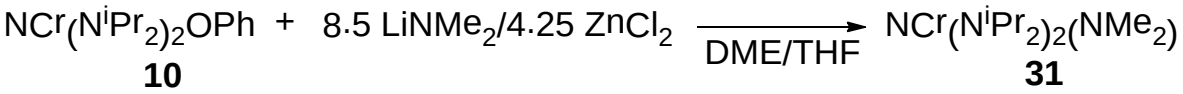


**10** **31**

**Scheme 2.8:** Synthesis using ligand exchange with lithium to zinc transmetalation

## 2.6: Synthesis using Ligand Exchange with $MgR_2$

One of the earliest chromium(VI) alkyl complexes reported in the literature was $NCr(N^iPr_2)_2CH_2SiMe_2Ph$ (**36**). We wondered if neophyl analogue would have different donor properties than **36**. Using conditions[15] similar to those used to prepare **36**, 0.7 equivalents of the $Mg(CH_2C(Me)_2Ph)_2$[24] was added to 1 equivalent of **2** in ether, affording the $\sigma$–complex, $NCr(N^iPr_2)_2CH_2C(Me)_2Ph$ (**37**).

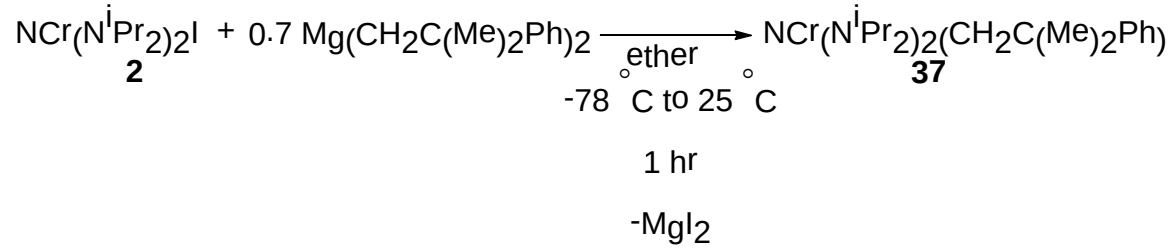


**2** **37**

**Scheme 2.9:** Synthesis using ligand exchange with $MgR_2$ compounds

Reaction of the Grignard reagent, $BrMgCH_2C(Me)_2Ph$ instead of the dialkyl magnesium compound only resulted in halide exchange between I and Br. It was observed that the addition of $MgBr_2$ or $MgCl_2$ to **2** also resulted in halide exchange. As with all $\sigma$-complexes, they are stable at room temperature for short periods of time and slowly decompose in the presence of light forming a black solid, free amine, and the imine $Me_2C{=}N^iPr$ (vida infra). It is likely this occurs as a $\beta$–H abstraction by the leaving alky group.[15, 25]

In an attempt to synthesize $NCr(N^iPr_2)_2CH_2SnMe_3$ (**42**), 0.5 equivalents of $Mg(CH_2SnMe_3)_2$, prepared from two equivalents of $ClMg(CH_2SnMe_3)$[26] and dioxane, was added to a cold, stirring solution of **10** in cold ether. To our surprise, the product was $NCr(N^iPr_2)(OPh)_2$ (**41**), which matched the $^1H$ NMR spectrum reported in the literature.[16] Browsing through the literature provides some clues as to what may have happened. Tin(IV) alkyl complexes display a varied reactivity ranging from being a coupling partner in Stille Coupling,[27] a catalyst,[28] and stabilization of cationic radicals on the carbons bound to tin.[29] Further investigation is warranted to understand this phenomenon and determine by what mechanism the bisphenoxide was generated.

### 2.7: Synthesis of $[NCr(N^iPr_2)_2DMAP][BF_4]$ and $[NCr(N^iPr_2)_2HMPA][PF_6]$

The desire to see how neutral donors compare to anionic donors fueled the route for cationic complexes. This result might overlap with the neutral members commonly found in the Tolman map.[30] Addition of a mixture of $AgBF_4$ and DMAP or $AgPF_6$ and HMPA in acetonitrile

to a stirring solution of **2** in chloroform yielded the corresponding cationic complexes. Unfortunately, the cationic complexes are only stable at room temperature for short periods of time (< 4 hours) and must be stored in the refrigerator.

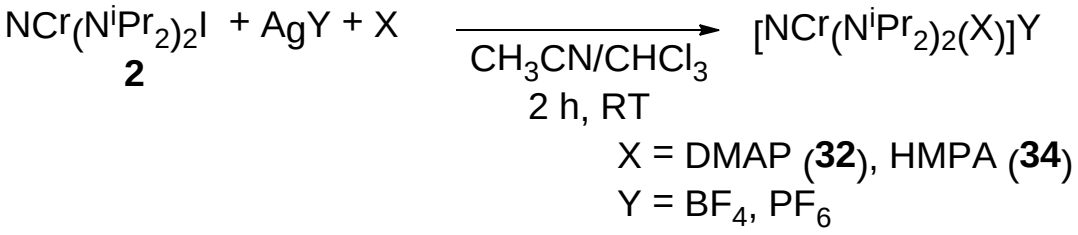


**Scheme 2.10:** Synthesis of neutral donors

### 2.8: Synthesis using Tin(IV)-Catalyzed Decomposition of Cationic $BF_4$ Salt

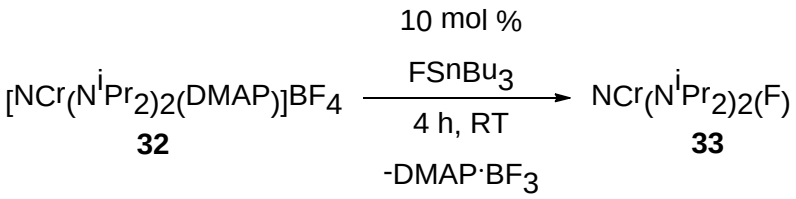


**Scheme 2.11:** Synthesis of $NCr(N^iPr_2)_2F$ (**33**)

Many attempts to synthesis the fluoride (**33**) were made. The only successful route was catalytic decomposition of the cationic complex $[NCr(N^iPr_2)_2(DMAP)]BF_4$ (**33**) using $FSnBu_3$ at room temperature. The expected byproduct, $DMAP{\cdot}BF_3$, was detected in the $^{19}F$ NMR spectrum of a reaction to form **33**.

The uniqueness of our system is that a diversity of $NCr(N^iPr_2)_2X$ compounds can be synthesized. If anyone who would want to place their ligands on our system they can use any of the selected synthetic routes to do so. Also, we have found conditions to put difficult ligands, such as alkyls that are known to be prone to reduction, onto the chromium or for other high

oxidation state metals. Also, we have discovered that for our system Sn(IV) complexes are catalytically active by doing ligand swap with free compounds in solution or with ligands on chromium.

## 2.9: Experimental Section

### 2.9.1 General Procedure:

All reactions and manipulations were carried out in a MBraun glovebox under nitrogen atmosphere and/or using standard Schlenk techniques. Ethereal solvents, pentane, hexanes, toluene, and benzene were purchased from Aldrich Chemical Co. and purified through alumina columns to remove water after sparging with dinitrogen to remove oxygen. HCl in diethyl ether was purchased from Aldrich Chemical Co. and used as received. All NMR solvents were purchased from Cambridge Isotopes Laboratories, Inc. Deuterated toluene and benzene was distilled from sodium benzophenone ketyl. Deuterated chloroform was distilled from calcium hydride under dry dinitrogen atmosphere. The NMR solvents were stored in the glovebox in glass containers with a stopcock. The reagent 15-crown-5 was dried by making a toluene solution and refluxing with a Dean-Stark trap overnight. $ClMgCH_2C(Me)_2Ph$ and trimethylsilylmethyl lithium were purchased from Sigma Aldrich and were used as received. (Tri*iso*propylsilyl) acetylene and *tert*-butyl acetylene were purchased from Sigma Aldrich and were distilled under nitrogen and freeze-pump-thawed before being brought into the dry box. Lutidinium iodide was prepared using the literature procedures.[16] Compounds $NCr(N^iPr_2)_2I$ **2**, $NCr(N^iPr_2)_2OPh$ **9**, $NCr(N^iPr_2)_2O^tBuF_6$ **10**, and $NCr(N^iPr_2)_2CH_2Si(Me)_2Ph$ **36** were made following literature procedure.[15,16] The 3-substituted pyrroles, $Hpyr^{C6F5}$ and $Hpyr^{C6H3(CF3)2}$,

where prepared as previously reported.[19] (Pyrrolyl)thallium(I) was prepared similar to the literature procedure[18] using 1.1 equivalents of freshly filtered TlOEt in ether, which was added to cold pyrrole in ether. The product precipitates as a colorless solid with low solubility in common organic solvents. This same procedure was used to generate $TlPyr^{C6H3(CF3)2}$ and $TlPyr^{C6F5}$. $Mg(CH_2C(Me)_2Ph)_2$,[24] $Mg(CH_2Si(Me)_2Ph)_2$,[31] and neopentyl lithium[32] were made following literature procedures. Spectra were taken on Varian instruments located in the Max T. Rogers Instrumentation Facility at Michigan State University. These include a UNITYplus 500 spectrometer equipped with a 5 mm Pulsed-Field-Gradient (PFG) switchable broadband probe and operating at 499.955 MHz ($^1$H) and 125.77 ($^{13}$C), and a UNITYplus 300 spectrometer operating at 299.976 MHz ($^1$H). Complete Line Shape Analysis (CLSA) was performed on gNMR, available as a free download.[35] $^1$H NMR chemical shifts are reported relative to residual $CHCl_3$ in $CDCl_3$ as 7.24 ppm. $^{13}$C NMR chemical shifts are reported relative to $^{13}CDCl_3$ as 77.0 ppm. $^{19}$F NMR chemical shifts are relative to external, neat $FC_6H_5$ as –113.15 ppm. Silicon NMR was taken on a 600 MHz instrument operating at 119.16 MHz ($^{29}$Si) and referenced with $SiMe_4$ at 0.00 ppm. The quaternary carbons in the CN, NCS and NCO compounds in $^{13}$C NMR have very long relaxation times, requiring the delay time to be set to 15 seconds for the acquisition. Melting points are uncorrected.

**2.9.2 Synthesis of NCr($N^iPr_2$)$_3$ (1):** Under an inert $N_2$ atmosphere, a 250 mL Erlenmeyer flask was loaded with Cr($N^iPr_2$)$_3$ (1.15 g, 3.26 mmol, 1 equiv.) and pentane (~25 mL). In a separate flask, a pentane solution (50 mL) of freshly sublimed NCr($O^tBu$)$_3$ (0.931 g, 3.26 mmol, 1 equiv.) was prepared. The yellow solution of NCr($O^tBu$)$_3$ was added slowly in portions over ~10 min to the rapidly stirring Cr($N^iPr_2$)$_3$ solution. The solution rapidly turned beet red, and stirring was continued for 1.5 h after addition was complete. The volatiles were removed in vacuo, and acetonitrile (100 mL) was added. After stirring for 5 min, the mixture was filtered through a fritted glass funnel, and the solids were washed with acetonitrile (2 × 10 mL). The solids were transferred to a vial and dried in vacuo yielding the title compound as dark red microcrystals (1.06 g, 2.90 mmol, 89% yield). If necessary, **1** can be further purified by recrystallization from concentrated pentane solution at −35 °C. $^1$H NMR (500 MHz, $CDCl_3$, −30 °C): 4.33 (br sept, 3H, C*H*($CH_3$)$_2$), 3.42 (br sept, 3H, C*H*($CH_3$)$_2$), 1.43 (br d, 14H, CH(C*H*$_3$)$_2$), 1.05 (br d, 14H, CH(C*H*$_3$)$_2$). Melting point and room temperature NMR spectroscopy were in agreement with literature values.[16]

**2.9.3 Synthesis of NCr($N^iPr_2$)$_2$(Cl) (3):** Under an inert atmosphere a pressure tube was loaded with **1** (0.400 g, 1.09 mmol, 1 equiv.), 2,6-lutidinium chloride (0.392 g, 2.73 mmol, 2.5 equiv.), and a stirbar. $CHCl_3$ (~35 mL) was added. The tube was sealed and removed from the drybox. The tube was set in a 60 °C oil bath, and the reaction was stirred for 12 h. The tube was taken back into the drybox, and the volatiles were removed *in vacuo*. The residue was extracted with

pentane and filtered. The solvent was removed yielding **3** as an orange powder (0.270 g, 0.895 mmol, 82% yield). Diffraction quality crystals were obtained from a concentrated pentane solution at −35 °C. $^{1}$H NMR (500 MHz, $CDCl_3$, 25 °C): 5.24 (sept, $J_{HH}$ = 6.61, 2H, C*H*$(CH_3)_2$), 3.82 (sept, $J_{HH}$ = 6.21, 2H, C*H*$(CH_3)_2$), 1.91 (d, $J_{HH}$ = 6.42, 6H, CH(C*H*$_3)_2$), 1.49 (d, $J_{HH}$ = 6.28, 6H, CH(C*H*$_3)_2$), 1.25 (d, $J_{HH}$ = 6.33, 6H, CH(C*H*$_3)_2$), 1.13 (d, $J_{HH}$ = 6.57, 6H, CH(C*H*$_3)_2$). $^{13}$C{$^{1}$H} NMR (125 MHz, $CDCl_3$, 0 °C): 59.20, 57.10, 30.36, 29.92, 21.45, 19.90. Mp: 157-158 °C.

**2.9.4 Synthesis of NCr(N$^{i}$Pr$_2)_2$(Br) (4):** Under an inert atmosphere, a pressure tube was loaded with **1** (0.120 g, 0.328 mmol, 1 equiv.), 2,6-lutidinium bromide (0.092 g, 0.49 mmol, 1.5 equiv.), and a stirbar. $CHCl_3$ (~25 mL) was added. The tube was sealed and removed from the drybox. The tube was set in a 60 °C oil bath and stirred for 12 h. The tube was moved back into the drybox, and the volatiles were removed in vacuo. The residue was extracted with pentane and filtered through Celite. The solvent was removed in vacuo yielding **4** as an orange powder (0.060 g, 0.17 mmol, 52% yield). Diffraction quality crystals were obtained from a concentrated pentane solution at −35 °C. $^{1}$H NMR (500 MHz, $CDCl_3$, 25 °C): 5.28 (sept, $J_{HH}$ = 6.51, 2H, C*H*$(CH_3)_2$), 3.81 (sept, $J_{HH}$ = 6.31, 2H, C*H*$(CH_3)_2$), 1.89 (d, $J_{HH}$ = 6.31, 6H, CH(C*H*$_3)_2$), 1.50 (d, $J_{HH}$ = 6.26, 6H, CH(C*H*$_3)_2$), 1.28 (d, $J_{HH}$ = 6.40, 6H, CH(C*H*$_3)_2$), 1.14 (d, $J_{HH}$ = 6.64, 6H, CH(C*H*$_3)_2$). $^{13}$C{$^{1}$H} NMR (125 MHz, $CDCl_3$, −5 °C): 59.34, 57.40, 30.20, 29.54, 21.29, 19.78. Mp: 160-164 °C.

**2.9.5 Synthesis of NCr(N$^{i}$Pr$_2$)$_2$(OTf) (5):** Under an inert atmosphere, a scintillation vial was loaded with **1** (0.30 g, 0.82 mmol, 1 equiv.), pentane (10 mL), and a stir bar. The solution was cooled to near frozen in a liquid nitrogen cooled cold well. To the rapidly stirring solution, 1.55 M triflic acid in a DME (533 μL, 0.826 mmol, 1.01 equiv.) was added dropwise. The reaction was allowed to come to room temperature and stirred for 4 h. The volatiles were removed in vacuo, and the residue was taken up in a minimal amount of pentane (2 × 10 mL) and filtered through Celite. The filtrate was concentrated in vacuo. Cooling the pentane solution to −35 °C yielded **5** as red-orange crystals (0.238 g, 0.573 mmol, 70% yield). $^{1}$H NMR (300 MHz, $CDCl_3$, 25 °C): 5.31 (sept, $J_{HH}$ = 6.66, 2H, C*H*$(CH_3)_2$), 3.94 (sept, $J_{HH}$ = 6.35, 2H, C*H*$(CH_3)_2$), 2.02 (d, $J_{HH}$ = 6.35, 6H, CH(C*H*$_3)_2$), 1.48 (d, $J_{HH}$ = 6.35, 6H, CH(C*H*$_3)_2$), 1.31 (d, $J_{HH}$ = 6.35, 6H, CH(C*H*$_3)_2$), 1.16 (d, $J_{HH}$ = 6.35, 6H, CH(C*H*$_3)_2$). $^{19}$F NMR (564 MHz, $CDCl_3$, 25 °C): −76.65. Mp: 198 °C (sub).

**2.9.6 Synthesis of NCr(N$^{i}$Pr$_2$)$_2$(OAd) (6):** Under an inert atmosphere, a pressure tube was loaded with 1-adamantanol (0.042 g, 0.27 mmol, 1 equiv.), toluene (10 mL), and a stirbar. To this solution, **1** (0.10 g, 0.27 mmol, 1 equiv.) in toluene (8 mL) was added. The pressure tube was sealed and placed in a 90 °C oil bath. The reaction stirred at this temperature for 3 d. The tube was taken back into the glove box, and the volatiles were removed in vacuo. The residue was extracted with pentane and filtered through Celite. The solution was concentrated to ~5 mL and placed in a −35 °C freezer yielding red-orange crystals of **6** (0.080 g, 0.191 mmol, 70% yield). $^{1}$H NMR (500 MHz, $CDCl_3$, −40 °C): 4.75 (br sept, 2H, C*H*$(CH_3)_2$), 3.54 (br sept, 2H,

C*H*($CH_3$)$_2$), 2.08 (app s, 3H, Ad C*H*), 1.71 (d, $J_{HH}$ = 2.5 Hz, 6H, Ad C$H_2$), 1.63 (d, $J_{HH}$ = 5.5 Hz, 6H, CH(C$H_3$)$_2$), 1.54 (app s, 6H, Ad C$H_2$), 1.40 (d, $J_{HH}$ = 5.5 Hz, 6H, CH(C$H_3$)$_2$), 1.07-1.02 (m, 12H, CH(C$H_3$)$_2$). $^{13}C\{^1H\}$ NMR (125 MHz, $CDCl_3$, −35 °C): 74.0, 57.4, 53.4, 47.0, 36.2, 31.0, 30.0, 29.3, 21.0, 19.5. Mp: 120-125 °C.

**2.9.7 Synthesis of NCr(N$^i$Pr$_2$)$_2$(OSiPh$_3$) (7):** Under an inert atmosphere, a scintillation vial was loaded with **1** (0.70 g, 0.19 mmol, 1 equiv.), toluene (~5 mL), and a stirbar. A solution of $HOSiPh_3$ (0.053 g, 0.19 mmol, 1 equiv.) in toluene (5 mL) was added slowly. As the reaction stirred it gradually turned from the beet color of the starting material to orange. After 16 h, the solution was dried in vacuo. The residue was extracted with pentane and filtered through Celite. The filtrate was concentrated (~5 mL) in vacuo. The pentane solution yielded orange crystals of **7** (0.075 g, 0.14 mmol, 72% yield) at −35 °C. $^1H$ NMR (500 MHz, $CDCl_3$, 0 °C): 7.64 (d, $J_{HH}$ = 6.34, 6H Ar-C-*H*), 7.49-7.26 (m, 9H Ar-C-*H*), 5.01 (sept, $J_{HH}$ = 6.61, 2H, C*H*($CH_3$)$_2$), 3.63 (sept, $J_{HH}$ = 6.20, 2H, C*H*($CH_3$)$_2$), 1.60 (d, $J_{HH}$ = 6.39, 6H, CH(C$H_3$)$_2$), 1.39 (d, $J_{HH}$ = 6.29, 6H, CH(C$H_3$)$_2$), 1.09 (d, $J_{HH}$ = 6.53, 6H, CH(C$H_3$)$_2$), 1.00 (d, $J_{HH}$ = 6.29, 6H, CH(C$H_3$)$_2$). $^{13}C\{^1H\}$ NMR (125 MHz, $CDCl_3$, 25 °C): 138.7, 135.3, 128.9, 127.2, 58.4, 55.4, 30.2, 29.5, 21.4, 20.6. Mp: 115-120 °C.

**2.9.8 Synthesis of NCr(N$^i$Pr$_2$)$_2$(O$_2$CPh) (8):** Under an inert atmosphere a scintillation vial was loaded with **1** (0.150 g, 0.409 mmol, 1 equiv.), a stir bar, and toluene (8 mL), and placed in a liquid nitrogen cooled cold well until nearly frozen. Benzoic acid (0.050 g, 0.41 mmol, 1 equiv.)

in toluene (1 mL) was added. The reaction was allowed to warm to room temperature and was stirred for 6 h. Over that time the solution changed from the beet color of the starting material to dark orange. The volatiles were removed in vacuo, and the residue was extracted with pentane (2 × 5 mL) and filtered through Celite. Concentrated solutions cooled to −35 °C yielded **8** as red-orange crystals (0.140 g, 0.360 mmol, 88% yield). $^{1}$H NMR (500 MHz, $CDCl_3$, 0 °C): 8.02-8.00 (m, 2H Ar-*o*-C-*H*), 7.45-7.41 (m, 1H Ar-*p*-C-*H*), 7.37-7.34 (m, 2H Ar-*m*-C-*H*), 5.60 (sept, $J_{HH}$ = 6.29, 2H, C*H*$(CH_3)_2$), 3.86 (sept, $J_{HH}$ = 6.47, 2H, C*H*$(CH_3)_2$), 1.94 (d, $J_{HH}$ = 6.31, 6H, CH(C*H*$_3)_2$), 1.53 (d, $J_{HH}$ = 6.37, 6H, CH(C*H*$_3)_2$), 1.18 (d, $J_{HH}$ = 6.40, 6H, CH(C*H*$_3)_2$), 1.13 (d, $J_{HH}$ = 6.46, 6H, CH(C*H*$_3)_2$). $^{13}$C{$^{1}$H} NMR (125 MHz, $CDCl_3$, 0 °C): 171.5, 133.5, 131.4, 129.9, 127.9, 58.2, 57.0, 30.7, 30.1, 22.2, 21.7. Mp: 121 °C (dec).

**2.9.9 Synthesis of NCr(N$^{i}$Pr$_2$)$_2$(O-*p*-(OMe)C$_6$H$_4$)** (**11**)**:** Under an inert atmosphere, a scintillation vial was loaded with **1** (0.15 g, 0.41 mmol, 1 equiv.), toluene (5 mL), and a stirbar. The solution was frozen in a liquid nitrogen cooled cold well, then removed to a stir plate. To the thawing solution of **1** was added a solution of HO-*p*-(OMe)$C_6H_4$ (0.051 g, 0.41 mmol, 1 equiv.) in toluene (5 mL) over 5 min. The reaction was stirred and was allowed come to room temperature. After 1.5 h, the orange solution was dried in vacuo. The residue was extracted with pentane and filtered through Celite. The filtrate was concentrated (~5 mL) in vacuo. Cooling concentrated pentane solutions to −35 °C yielded dark orange crystals of **11** (0.139 g, 0.356 mmol, 87% yield). $^{1}$H NMR (500 MHz, $CDCl_3$, −38 °C): 6.89 (d, $J_{HH}$ = 8.50, 2H, Ar-*m*-C-*H*), 6.71 (d, $J_{HH}$ = 9.00, 2H, Ar-*o*-C-*H*), 4.99 (sept, $J_{HH}$ = 6.50, 2H, C*H*$(CH_3)_2$), 3.72 (s, 3H, Ar-*p*-

OC$H_3$), 3.71 (sept, $J_{HH}$ = 6.50, 2H, C$H$($CH_3$)$_2$), 1.82 (d, $J_{HH}$ = 6.00, 6H, CH(C$H_3$)$_2$), 1.43 (d, $J_{HH}$ = 6.00, 6H, CH(C$H_3$)$_2$), 1.15-1.13 (m, 12H, CH(C$H_3$)$_2$). $^{13}$C{$^1$H} NMR (125 MHz, $CDCl_3$, −35 °C): 161.3, 152.3, 117.6, 113.5, 58.0, 55.5, 54.9, 30.3, 29.9, 21.3, 21.0. Mp: 102-104 °C.

**2.9.10 Synthesis of NCr(N$^i$Pr$_2$)$_2$(O-*p*-(SMe)C$_6$H$_4$) (12):** Under an inert atmosphere, a scintillation vial was loaded with **1** (0.15 g, 0.41 mmol, 1 equiv.), toluene (5 mL), and a stirbar. The solution was frozen in a liquid nitrogen cooled cold well, then removed to a stir plate. To the thawing solution was added HO-*p*-(SMe)$C_6H_4$ (0.057 g, 0.41 mmol, 1 equiv.) in toluene (5 mL) over 5 minutes. The reaction was stirred and allowed to come to room temperature. After 1.5 h the orange solution was dried in vacuo. The residue was extracted with pentane and filtered through Celite. The filtrate was concentrated (~5 mL) in vacuo. Cooling concentrated pentane solutions to −35 °C yielded dark orange crystals of **12** (0.153 g, 0.376 mmol, 92% yield). $^1$H NMR (500 MHz, $CDCl_3$, −10 °C): 7.14 (d, $J_{HH}$ = 8.64, 2H, Ar-*m*-C-*H*), 6.88 (d, $J_{HH}$ = 8.64, 2H, Ar-*o*-C-*H*), 5.02 (sept, $J_{HH}$ = 6.21, 2H, C$H$($CH_3$)$_2$), 3.73 (sept, $J_{HH}$ = 6.09, 2H, C$H$($CH_3$)$_2$), 2.40 (s, 3H SC$H_3$), 1.83 (d, $J_{HH}$ = 6.08, 6H, CH(C$H_3$)$_2$), 1.44 (d, $J_{HH}$ = 6.18, 6H, CH(C$H_3$)$_2$), 1.14 (d, $J_{HH}$ = 6.00, 12H, CH(C$H_3$)$_2$). $^{13}$C{$^1$H} NMR (125 MHz, $CDCl_3$, −10 °C): 165.7, 130.2, 125.7, 118.2, 58.2, 55.3, 30.3, 30.0, 23.3, 21.3, 21.0, 18.6. Mp: 112-115 °C.

**2.9.11 Synthesis of NCr(N$^i$Pr$_2$)$_2$(O-*p*-($^t$Bu)C$_6$H$_4$) (13):** Under an inert atmosphere, a scintillation vial was loaded with **1** (0.15 g, 0.41 mmol, 1 equiv.), toluene (5 mL), and a stirbar.

The solution was frozen in a liquid nitrogen cooled cold well, then removed to a stir plate. To the thawing solution was added HO-*p*-($^{t}$Bu)$C_6H_4$ (0.061 g, 0.41 mmol, 1 equiv.) in toluene (5 mL) over 5 min. The reaction was stirred and allowed to come to room temperature. After 1.5 h, the orange solution was dried in vacuo. The residue was extracted with pentane and filtered through Celite. The filtrate was concentrated (~5 mL) in vacuo. Cooling concentrated pentane solutions to −35 °C yielded dark orange crystals of **13** (0.16 g, 0.385 mmol, 94% yield). $^{1}$H NMR (500 MHz, $CDCl_3$, −25 °C): 7.16 (d, $J_{HH}$ = 8.62, 2H, Ar-*m*-C-*H*), 6.88 (d, $J_{HH}$ = 8.62, 2H, Ar-*o*-C-*H*), 5.00 (sept, $J_{HH}$ = 6.35, 2H, C*H*$(CH_3)_2$), 3.71 (sept, $J_{HH}$ = 6.23, 2H, C*H*$(CH_3)_2$), 1.82 (d, $J_{HH}$ = 6.18, 6H, CH(C*H*$_3)_2$), 1.44 (d, $J_{HH}$ = 6.35, 6H, CH(C*H*$_3)_2$), 1.24 (s, 9H C(C*H*$_3)_3$), 1.13 (d, $J_{HH}$ = 6.35, 12H, CH(C*H*$_3)_2$). $^{13}$C{$^{1}$H} NMR (125 MHz, $CDCl_3$, −35 °C): 164.4, 141.3, 125.5, 116.5, 58.1, 58.0, 55.0, 33.9, 31.5, 30.3, 30.0, 21.2, 20.9. Mp: 188-190 °C.

**2.9.12 Synthesis of NCr(N$^{i}$Pr$_2$)$_2$(O-*p*-(F)$C_6H_4$) (14):** Under an inert atmosphere, a scintillation vial was loaded with **1** (0.15 g, 0.41 mmol, 1 equiv.), toluene (5 mL), and a stirbar. The solution was frozen in a liquid nitrogen cooled cold well, then removed to a stir plate. To the thawing solution was added HO-*p*-(F)$C_6H_4$ (0.046 g, 0.41 mmol, 1 equiv.) in toluene (5 mL) over 5 min. The reaction was stirred and was allowed to come to room temperature. After 1.5 h, the orange solution was dried in vacuo. The residue was extracted with pentane and filtered through Celite. The filtrate was concentrated (~5 mL) in vacuo. Cooling concentrated pentane solutions to −35 °C yielded dark orange crystals of **14** (0.136 g, 0.360 mmol, 88% yield). $^{1}$H NMR (500 MHz, $CDCl_3$, −30 °C): 7.38 (d, $J_{HH}$ = 8.63, 2H, Ar-*m*-C-*H*), 6.95 (d, $J_{HH}$ = 8.63, 2H, Ar-*o*-C-*H*), 5.06

(sept, $J_{HH}$ = 6.48, 2H, C*H*($CH_3$)$_2$), 3.75 (sept, $J_{HH}$ = 6.42, 2H, C*H*($CH_3$)$_2$), 1.84 (d, $J_{HH}$ = 6.35, 6H, CH(C*H*$_3$)$_2$), 1.45 (d, $J_{HH}$ = 6.43, 6H, CH(C*H*$_3$)$_2$), 1.16-1.11 (m, 12H, CH(C*H*$_3$)$_2$). $^{13}$C{$^1$H} NMR (125 MHz, $CDCl_3$, 0 °C): 163.2, 157.3, 117.9 (d, $J_{CF}$ = 7.8), 114.9 (d, $J_{CF}$ = 22.4), 58.3, 55.3, 30.3, 30.0, 21.3, 21.1. $^{19}$F NMR (564 MHz, $CDCl_3$, 25 °C): –126.8. Mp: 81 °C (dec).

**2.9.13 Synthesis of NCr(N$^i$Pr$_2$)$_2$(O-*p*-(Cl)C$_6$H$_4$) (15):** Under an inert atmosphere, a scintillation vial was loaded with **1** (0.15 g, 0.41 mmol, 1 equiv.), toluene (5 mL), and a stirbar. The solution was frozen in a liquid nitrogen cooled cold well, then removed to a stir plate. To the thawing solution was added HO-*p*-(Cl)$C_6H_4$ (0.053 g, 0.41 mmol, 1 equiv.) in toluene (5 mL) over 5 min. The reaction was stirred and was allowed to come to room temperature. After 1.5 h, the orange solution was dried in vacuo. The residue was extracted with pentane and filtered through Celite. The filtrate was concentrated (~5 mL) in vacuo. Cooling concentrated pentane solutions to −35 °C yielded dark orange crystals of **15** (0.137 g, 0.348 mmol, 85% yield). $^1$H NMR (500 MHz, $CDCl_3$, −40 °C): 7.06 (d, $J_{HH}$ = 8.99, 2H, Ar-*m*-C-*H*), 6.84 (d, $J_{HH}$ = 8.76, 2H, Ar-*o*-C-*H*), 5.01 (sept, $J_{HH}$ = 6.26, 2H, C*H*($CH_3$)$_2$), 3.73 (sept, $J_{HH}$ = 6.26, 2H, C*H*($CH_3$)$_2$), 1.82 (d, $J_{HH}$ = 6.29, 6H, CH(C*H*$_3$)$_2$), 1.42 (d, $J_{HH}$ = 6.04, 6H, CH(C*H*$_3$)$_2$), 1.12 (d, $J_{HH}$ = 6.57, 6H, CH(C*H*$_3$)$_2$), 0.996 (d, $J_{HH}$ = 6.18, 6H, CH(C*H*$_3$)$_2$). $^{13}$C{$^1$H} NMR (125 MHz, $CDCl_3$, −20 °C): 165.3, 128.5, 123.1, 118.7, 58.3, 55.4, 44.8, 30.3, 30.1, 23.2, 21.3, 21.0. Mp: 124-125 °C.

**2.9.14 Synthesis of NCr(N$^i$Pr$_2$)$_2$(O-*p*-(CF$_3$)C$_6$H$_4$) (16):** Under an inert atmosphere, a scintillation vial was loaded with **1** (0.15 g, 0.41 mmol, 1 equiv.), toluene (5 mL), and a stirbar.

The solution was frozen in a liquid nitrogen cooled cold well, then removed to a stir plate. To the thawing solution was added HO-*p*-($CF_3$)$C_6H_4$ (0.066 g, 0.41 mmol, 1 equiv.) in toluene (5 mL) over 5 min. The reaction was stirred and was allowed to come to room temperature. After 1.5 h, the orange solution was dried in vacuo. The residue was extracted with pentane and filtered through Celite. The filtrate was concentrated (~5 mL) in vacuo. Cooling concentrated pentane solutions to −35 °C yielded dark orange crystals of **16** (0.143 g, 0.336 mmol, 82% yield). $^1$H NMR (500 MHz, $CDCl_3$, 3 °C): 7.37 (d, $J_{HH}$ = 8.58, 2H, Ar-*m*-C-*H*), 6.95 (d, $J_{HH}$ = 8.58, 2H, Ar-*o*-C-*H*), 5.07 (sept, $J_{HH}$ = 6.29, 2H, C*H*($CH_3$)$_2$), 3.76 (sept, $J_{HH}$ = 6.22, 2H, C*H*($CH_3$)$_2$), 1.85 (d, $J_{HH}$ = 6.04, 6H, CH(C*H*$_3$)$_2$), 1.46 (d, $J_{HH}$ = 6.03, 6H, CH(C*H*$_3$)$_2$), 1.15 (d, $J_{HH}$ = 3.72, 6H, CH(C*H*$_3$)$_2$), 1.02 (d, $J_{HH}$ = 6.34, 6H, CH(C*H*$_3$)$_2$). $^{13}$C{$^1$H} NMR (125 MHz, $CDCl_3$, 3 °C): 169.1, 126.3 (quar, $J_{CF}$ = 3.79), 117.7, 117.6, 58.5, 55.7, 30.4, 30.2, 23.3, 21.3, 21.1. $^{19}$F NMR (564 MHz, $CDCl_3$, 25 °C): −64.24. Mp: 131-132 °C. Anal. Calcd: C, 53.38; H, 7.56; N, 9.82. Found: C, 53.40; H, 7.77; N, 9.80.

**2.9.15 Synthesis of NCr(N$^i$Pr$_2$)$_2$(OC$_6$F$_5$) (17):** Under an inert atmosphere, a scintillation vial was loaded with **1** (0.15 g, 0.41 mmol, 1 equiv.), toluene (5 mL), and a stirbar. The solution was frozen in a liquid nitrogen cooled cold well, then removed to a stir plate. To the thawing solution was added $HOC_6F_5$ (0.075 g, 0.41 mmol, 1 equiv.) in toluene (5 mL) over 5 minutes. The reaction was stirred and was allowed to come to room temperature. After 1.5 h, the orange solution was dried in vacuo. The residue was extracted with pentane and filtered through Celite. The filtrate was concentrated (~5 mL) in vacuo. Cooling concentrated pentane solutions to −35

°C yielded dark orange crystals of **17** (0.16 g, 0.385 mmol, 76% yield). $^{1}$H NMR (500 MHz, $CDCl_3$, −20 °C): 5.12 (sept, $J_{HH}$ = 6.50, 2H, C*H*($CH_3$)$_2$), 3.81 (sept, $J_{HH}$ = 6.50, 2H, C*H*($CH_3$)$_2$), 1.87 (d, $J_{HH}$ = 6.50, 6H, CH(C*H*$_3$)$_2$), 1.41 (d, $J_{HH}$ = 6.00, 6H, CH(C*H*$_3$)$_2$), 1.26 (d, $J_{HH}$ = 6.50, 6H, CH(C*H*$_3$)$_2$), 1.16 (d, $J_{HH}$ = 6.00, 6H, CH(C*H*$_3$)$_2$). $^{13}$C{$^{1}$H} NMR (125 MHz, $CDCl_3$, —20 °C): 143-137, 58.7, 56.4, 30.4, 29.8, 21.6, 20.6. $^{19}$F NMR (564 MHz, $CDCl_3$, 25 °C): −161.70 (dd, $J_{FF}$ = 37.22 Hz, 13.54 Hz, 2F), −167.25 to −167.46 (m, 2F), −173.58 (tt, $J_{FF}$ = 44.56 Hz, 13.54 Hz, 1F). Mp: 129-132 °C.

**2.9.16 Synthesis of NCr(N$^{i}$Pr$_2$)$_2$(SPh)** (**18**): Under an inert atmosphere, a pressure tube was loaded with **1** (0.10 g, 0.27 mmol, 1 equiv.), toluene (5 mL), and a stirbar. To the stirring solution of **1** was added thiophenol (0.030 g, 0.27 mmol, 1 equiv.) in toluene (5 mL). The pressure tube was sealed, placed in a 65 °C oil bath, and stirred for 20 h. The reaction was taken back under an inert atmosphere, and the volatiles were removed in vacuo. The residue was extracted with pentane and filtered through Celite. The solution was concentrated to ~5 mL and placed in a −35 °C freezer yielding red-purple crystals of **19** (0.077 g, 0.21 mmol, 75% yield). $^{1}$H NMR (500 MHz, $CDCl_3$, −4 °C): 7.62-7-60 (d, 2H, Ar-*o*-C-*H*), 7.12-7.09 (t, 2H, Ar-*m*-C-*H*), 6.99-6.96 (t,1H Ar-*p*-C-*H*), 5.23-5.18 (sept, 2H, C*H*($CH_3$)$_2$), 3.72-3.67 (sept, 2H, C*H*($CH_3$)$_2$), 1.75-1.731 (d, 6H, CH(C*H*$_3$)$_2$), 1.49-1.47 (d, 6H, CH(C*H*$_3$)$_2$), 1.13-1.11 (d, 12H, CH(C*H*$_3$)$_2$). $^{13}$C{$^{1}$H} NMR (125 MHz, $CDCl_3$, −4 °C): 141.95, 132.58, 127.87, 123.94, 59.00, 55.95, 30.34, 29.91, 21.96, 20.38. Mp: 118-120 °C.

**2.9.17 Synthesis of NCr(N$^{i}$Pr$_2$)$_2$(OPth) (19):** Under an $N_2$ atmosphere a scintillation vial was loaded with *N*-(hydroxy)phthalimide (HOPth, 0.081 g, 0.494 mmol, 1 equiv), $CHCl_3$ (5 mL), and a stir bar. To this slurry was added **1** (0.181 g, 0.494 mmol, 1 equiv) in $CHCl_3$ (5 mL). The solution turned orange and stirred for 16 h at room temperature. The volatiles were removed in vacuo, and the residue was extracted with toluene (3 × 5 mL). This solution was filtered through Celite, and the filtrate was concentrated to 8 mL. Diffraction quality crystals of **18** were grown from toluene solution at −35 °C (0.110 g, 0.257 mmol, 52%). $^{1}$H NMR (500 MHz, $CDCl_3$, −2 °C): 7.68-7.67 (m, 2H, Phth), 7.59-7.57 (m, 2H, Phth), 5.13 (sept, $J_{HH}$ = 6.5 Hz, 2H, C*H*(CH$_3$)$_2$), 3.82 (sept, $J_{HH}$ = 6.5 Hz, 2H, C*H*(CH$_3$)$_2$), 1.93 (d, $J_{HH}$ = 6.5 Hz, 6H, CH(C*H*$_3$)$_2$), 1.41-1.38 (m, 12H, CH(C*H*$_3$)$_2$), 1.16 (d, $J_{HH}$ = 6.5 Hz, 6H, CH(C*H*$_3$)$_2$). $^{13}$C{$^{1}$H} NMR (125 MHz, $CDCl_3$, −2 °C): 20.38, 21.66, 56.10, 58.52, 122.32, 129.72, 133.30, 163.75. M.p. 179 °C (dec).

**2.9.18 Synthesis of NCr(N$^{i}$Pr$_2$)$_2$(OBn) (20)**: Under an inert atmosphere, a scintillation vial was loaded with **2** (0.075 g, 0.19 mmol, 1 equiv.) and hexane (10 mL). This was cooled to near frozen in a liquid nitrogen cooled cold well. In a separate vial, TlOBn (0.065 g, 0.21 mmol, 1.1 equiv.) was slurried in THF (2 mL), and a stir bar was added. The solution of **2** was then added dropwise over 5 min to the rapidly stirring slurry. The reaction was allowed to come to room temperature and stir for 16 h, during which yellow TlI precipitated. The volatiles were removed in vacuo. The residue was extracted with pentane and filtered through Celite. The filtrate was concentrated in vacuo. Cooling a concentrated pentane solution to −35 °C yielded **20** as orange

crystals (0.641 g, 0.172 mmol, 90% yield). $^{1}$H NMR (500 MHz, $CDCl_3$, −45 °C): 7.55 (d, $J_{HH}$ = 7.0, 2H, Ar-*o*-C*H*), 7.30 (app t, $J_{HH}$ = 7.5, 2H, Ar-*m*-C*H*), 7.20 (t, $J_{HH}$ = 7.5, 1H, Ar-*p*-C*H*), 5.47 (s, 2H, C$H_2$), 4.75 (sept, $J_{HH}$ = 6.0, 2H, C*H*($CH_3$)$_2$), 3.59 (sept, $J_{HH}$ = 6.0, 2H, C*H*($CH_3$)$_2$), 1.61 (d, $J_{HH}$ = 6.0, 6H, CH(C$H_3$)$_2$), 1.35 (d, $J_{HH}$ = 6.0, 6H, CH(C$H_3$)$_2$), 1.04 (br s, 12H, CH(C$H_3$)$_2$). $^{13}$C{$^{1}$H} NMR (125 MHz, $CDCl_3$, –40 °C): 143.9, 127.8, 127.3, 126.6, 80.3, 57.5, 54.1, 30.1, 29.4, 21.3, 20.7. Mp: 139-140 °C. Anal. Calcd: C, 61.09; H, 9.46; N, 11.24. Found: C, 60.87; H, 9.16; N, 11.22.

**2.9.19 Synthesis of NCr(N$^{i}$Pr$_2$)$_2$(NO$_3$)** (**21**): Under an inert atmosphere, a scintillation vial was loaded with $TlNO_3$ (0.203 g, 0.763 mmol, 3 equiv.), a stir bar, and THF (8 mL). To the slurry of $TlNO_3$ was added **2** (0.10 g, 0.25 mmol, 1 equiv.) in THF (5 mL). The reaction was stirred for 16 h at room temperature, after which time the volatiles were removed in vacuo. The residue was extracted with pentane (3 × 10 mL) and filtered through Celite. Removal of volatiles in vacuo yielded the title compound as a red-orange powder (0.063 g, 0.19 mmol, 75% yield). Diffraction quality crystals were obtained from a pentane at −35 °C. $^{1}$H NMR (600 MHz, $CDCl_3$, 25 °C): 5.54 (sept, $J_{HH}$ = 5.35, 2H, C*H*($CH_3$)$_2$), 3.92 (sept, $J_{HH}$ = 6.41, 2H, C*H*($CH_3$)$_2$), 1.95 (d, $J_{HH}$ = 6.21, 6H, CH(C$H_3$)$_2$), 1.55 (d, $J_{HH}$ = 6.23, 6H, CH(C$H_3$)$_2$), 1.22 (d, $J_{HH}$ = 6.35, 6H, CH(C$H_3$)$_2$), 1.13 (d, $J_{HH}$ = 6.32, 6H, CH(C$H_3$)$_2$). $^{13}$C{$^{1}$H} NMR (125 MHz, $CDCl_3$, 25 °C): 59.80, 58.12, 31.06, 30.00, 22.41, 22.03. Mp: 77 °C (dec).

**2.9.20 Synthesis of NCr($N^iPr_2$)$_2$(Pyrrolyl) (22):** Under an inert atmosphere, a scintillation vial was loaded with **2** (0.100 g, 0.254 mmol 1 equiv.), a stir bar, and toluene (8 mL). A slurry of freshly made thallium pyrrole (0.695 g, 0.257 mmol, 1.01 equiv.) in $Et_2O$ (5 mL) was added to the stirring solution. The reaction was allowed to stir for 20 h at room temperature, during which yellow TlI precipitated. The precipitate was removed by filatration, and the volatiles were removed in vacuo. The residue was extracted with pentane (3 × 10 mL) and concentrated in vacuo to ~5 mL. Cooling the concentrated solution to −35 °C yielded red-orange crystals of **22** (0.068 g, 0.20 mmol, 80% yield). $^1$H NMR (500 MHz, $CDCl_3$, −10 °C): 6.94-6.81 (m, 2H, pyr-C*H*), 6.26-6.17 (m, 2H, pyr-C-*H*), 5.10 (sept, $J_{HH}$ = 6.09, 2H, C*H*($CH_3$)$_2$), 3.77 (sept, $J_{HH}$ = 5.52, 2H, C*H*($CH_3$)$_2$), 1.83 (d, $J_{HH}$ = 4.64, 6H, CH(C*H*$_3$)$_2$), 1.55 (d, $J_{HH}$ = 5.03, 6H, CH(C*H*$_3$)$_2$), 1.16 (d, $J_{HH}$ = 5.16, 6H, CH(C*H*$_3$)$_2$), 1.05 (d, $J_{HH}$ = 4.30, 6H, CH(C*H*$_3$)$_2$). $^{13}$C{$^1$H} NMR (125 MHz, $CDCl_3$, −10 °C): 129.2, 107.3, 58.0, 56.0, 30.3, 30.1, 22.0, 21.3. Mp: 125-6 °C.

**2.9.21 Synthesis of NCr($N^iPr_2$)$_2$($Pyr^{C6F5}$) (23):** Under an inert atmosphere a scintillation vial was loaded with **2** (0.100 g, 0. 254 mmol 1 equiv.), a stir bar, and toluene (8 mL). A slurry of freshly made Tl($Pyr^{C6F5}$) (0.112 g, 0.257 mmol, 1.01 equiv.) in $Et_2O$ (5 mL) was added to the stirring solution. The reaction was allowed to stir for 20 h at room temperature, during which yellow TlI precipitated. The precipitate was removed by filtration, and the volatiles were removed in vacuo. The residue was extracted with pentane (3 × 10 mL) and concentrated in vacuo to ~5 mL. Cooling the concentrated solution to −35 °C yielded red-orange crystals of **23**

(0.080 g, 0.16 mmol, 63% yield). $^{1}$H NMR (500 MHz, $CDCl_3$, 0 °C): 7.35-7.32 (m, 2H, pyr-C-*H*), 6.91-6.88 (m, 2H, pyr-C-*H*), 5.15 (sept, $J_{HH}$ = 6.28, 2H, C*H*($CH_3$)$_2$), 3.82 (sept, $J_{HH}$ = 6.37, 2H, C*H*($CH_3$)$_2$), 1.87 (d, $J_{HH}$ = 6.07, 6H, CH(C*H*$_3$)$_2$), 1.57 (d, $J_{HH}$ = 6.07, 6H, CH(C*H*$_3$)$_2$), 1.18 (d, $J_{HH}$ = 6.29, 6H, CH(C*H*$_3$)$_2$), 1.11 (d, $J_{HH}$ = 6.33, 6H, CH(C*H*$_3$)$_2$). $^{13}$C{$^{1}$H} NMR (125 MHz, $CDCl_3$, 25 °C): 143.76 (dm, $J_{CF}$ = 255.75 Hz), 137.90 (dm, $J_{CF}$ = 248.5 Hz), 137.33 (dm, $J_{CF}$ = 243.13 Hz), 130.98, 130.63, 112.47, 108.97, 58.46, 56.59, 30.37, 30.24, 22.10, 21.29. $^{19}$F NMR (564 MHz, $CDCl_3$, 25 °C): −142.47 to −142.57 (m, 2F), −163.35 (t, $J_{FF}$ = 42.86 Hz, 1F), −164.77 to −164.95 (m, 2F). Mp: 169-171 °C.

**2.9.22 Synthesis of NCr(N$^{i}$Pr$_2$)$_2$(Pyr$^{C6H3(CF3)2}$) (24):** Under an inert atmosphere, a scintillation vial was loaded with **2** (0.100 g, 0. 254 mmol 1 equiv.), a stir bar, and toluene (8 mL). A slurry of freshly made Tl(Pyr$^{C6H3(CF3)2}$) (0.124 g, 0.257 mmol, 1.01 equiv.) in $Et_2O$ (5 mL) was added. The reaction was allowed to stir for 20 h at room temperature, during which yellow TlI precipitated. The precipitate was removed by filtration, and the volatiles were removed in vacuo. The residue was extracted with pentane (3 × 10 mL) and concentrated in vacuo to ~5 mL. Cooling the concentrated solution to −35 °C yielded red-orange crystals of **24** (0.098 g, 0.18 mmol, 71% yield). $^{1}$H NMR (500 MHz, $CDCl_3$, 0 °C): 7.85 (s, 2H, Ar-*o*-C*H*), 7.49 (s, 1H, Ar-*p*-C*H*), 7.29-7.28 (m, 1H, pyr-C*H*), 6.88-6.87 (m, 1H, pyr-C*H*), 6.52-6.52 (m, 1H, pyr-C*H*), 5.15 (sept, $J_{HH}$ = 6.0, 2H, C*H*($CH_3$)$_2$), 3.81 (sept, $J_{HH}$ =6.0, 2H, C*H*($CH_3$)$_2$), 1.86 (d, $J_{HH}$ = 6.0, 6H, CH(C*H*$_3$)$_2$), 1.57 (d, $J_{HH}$ = 6.0, 6H, CH(C*H*$_3$)$_2$), 1.20 (d, $J_{HH}$ = 6.0, 6H,

CH(C$H_3$)$_2$), 1.11 (d, $J_{HH}$ = 6.0, 6H, CH(C$H_3$)$_2$). $^{13}$C{$^1$H} NMR (125 MHz, $CDCl_3$, 25 °C): 138.84, 131.27 (q, $J_{CF}$ = 32.5 Hz), 130.63, 128.45, 124.26, 123.72 (q, $J_{CF}$ = 270.9 Hz), 121.84, 117.30 (s, br) 106.02, 58.28, 56.43, 30.37, 30.22, 21.99, 21.35. $^{19}$F NMR (564 MHz, $CDCl_3$, 25 °C): −62.85 (s). Mp: 116-122 °C.

**2.9.23 Synthesis of NCr(N$^i$Pr$_2$)$_2$(Indolyl) (25):** Under an inert atmosphere, a scintillation vial was loaded with **10** (0.100 g, 0.278 mmol, 1 equiv.), a stir bar, and hexanes (8 mL). This was cooled to near frozen in a liquid cooled nitrogen cold well. Freshly prepared lithium indolide (0.034 g, 0.28 mmol, 1.00 equiv.), in toluene (5 mL) was added dropwise over 5 min to the thawing solution of **10**. The reaction was allowed to stir for 20 h while warming to room temperature. The volatiles were removed in vacuo. The residue was extracted with pentane (3 × 10 mL) and filtered through Celite. The filtrate was concentrated to ~5 mL and cooled to −35 °C, which provided crystals of **25**. The crystals were redissolved in cold pentane and filtered to remove remaining lithium salts. Recrystalization at –35 °C from pentane yielded pure **25** as purple crystals (0.045 g, 0.12 mmol, 42% yield). $^1$H NMR (500 MHz, $CDCl_3$, –21 °C): 8.06 (d, $J_{HH}$ = 8.5, 1H, *H*-7 ind), 7.55 (d, $J_{HH}$ = 8, 1H, *H*-4 ind), 7.37 (d, $J_{HH}$ = 3, 1H, *H*-2 ind), 7.15 (t, $J_{HH}$ = 6.8, 1H, *H*-5 ind), 7.03 (t, $J_{HH}$ = 6.8, 1H, *H*-6 ind), 6.54 (d, $J_{HH}$ = 3, 1H, *H*-3 ind), 5.18 (sept, $J_{HH}$ = 6.50, 2H, C*H*(CH$_3$)$_2$), 3.74 (sept, $J_{HH}$ = 6.50, 2H, C*H*(CH$_3$)$_2$), 1.73 (d, $J_{HH}$ = 6.50, 6H, CH(C$H_3$)$_2$), 1.59 (d, $J_{HH}$ = 6.50, 6H, CH(C$H_3$)$_2$), 1.19 (d, $J_{HH}$ = 6.50, 6H, CH(C$H_3$)$_2$),

0.97 (d, $J_{HH}$ = 6.50, 6H, CH(C$H_3$)$_2$). $^{13}$C{$^1$H} NMR (125 MHz, $CDCl_3$, –21 °C): 144.5, 133.4, 128.8, 120.6, 119.1, 118.7, 115.9, 102.3, 58.1, 55.8, 30.6. Mp: 194-196 °C.

**2.9.24 Synthesis of NCr(N$^i$Pr$_2$)$_2$(Carbazolyl) (26):** Under an inert atmosphere a pressure tube wasloaded with **10** (0.150 g, 0.417 mmol 1 equiv.), a stir bar, and hexanes (8 mL). Freshly prepared lithium carbazolide (0.072 g, 0.42 mmol, 1.00 equiv.) in toluene (5 mL) was added to the solution of **10**. The vessel was sealed, removed from the box, and stirred in a 45 °C oil bath for 16 h. The pressure tube was taken back into the dry box, and the volatiles were removed under reduced pressure. The residue was extracted with pentane, and filtered through Celite. The filtrate was concentrated to ~5 mL and cooled to −35 °C, which provided crystals of **26**. The crystals were redissolved in cold pentane and filtered to remove remaining lithium salts. Recrystalization at –35 °C from pentane yielded pure **26** (0.063 g, 0.146 mmol, 35% yield). $^1$H NMR (500 MHz, $CDCl_3$, −20 °C): 8.02 (d, $J_{HH}$ = 7.58, 2H), 7.97 (d, $J_{HH}$ = 8.33, 2H), 7.40 (d, $J_{HH}$ = 7.71, 2H), 7.17 (d, $J_{HH}$ = 7.28, 2H), 5.30 (sept, $J_{HH}$ = 6.18, 2H, C$H$(CH$_3$)$_2$), 3.79 (sept, $J_{HH}$ = 6.21, 2H, C$H$(CH$_3$)$_2$), 1.69 (d, $J_{HH}$ = 6.07, 6H, CH(C$H_3$)$_2$), 1.62 (d, $J_{HH}$ = 6.21, 6H, CH(C$H_3$)$_2$), 1.21 (d, $J_{HH}$ = 6.08, 6H, CH(C$H_3$)$_2$), 0.96 (d, $J_{HH}$ = 6.29, 6H, CH(C$H_3$)$_2$). $^{13}$C{$^1$H} NMR (125 MHz, $CDCl_3$, −20 °C): 149.28, 125.02, 124.78, 119.15, 118.76, 114.96, 58.09, 55.81, 31.00, 29.47, 22.69, 22.26. Mp: 158-160 °C.

**2.9.25 Synthesis of NCr(N$^i$Pr$_2$)$_2$[N(Ph)Me] (27):** Under an inert atmosphere, a scintillation vial was loaded with **10** (0.150 g, 0.417 mmol 1 equiv.), a stir bar, and hexanes (8 mL). This was

cooled to near frozen in a liquid nitrogen cooled cold well. Freshly prepared lithium *N*-methyl anilide (0.047 g, 0.42 mmol, 1.0 equiv.) in toluene (5 mL) was added dropwise over 5 min. The reaction was allowed to stir for 20 h with warming to room temperature. The volatiles were removed in vacuo. The residue was extracted with pentane and filtered through Celite. The filtrate was concentrated to ~5 mL and cooled to −35 °C, which provided crystals of **27**. The crystals were recrystallized from cold pentane to obtain dark purple crystals of pure **27** (0.068 g, 0.184 mmol, 44% yield). $^{1}$H NMR (500 MHz, $CDCl_3$, –10 °C): 7.45-7.33 (m, 2H, Ar-C-*H*), 7.32-7.24 (m, 3H, Ar-C-*H*), 5.10 (sept, $J_{HH}$ = 6.09, 2H, C*H*$(CH_3)_2$), 3.77 (sept, $J_{HH}$ = 5.52, 2H, C*H*$(CH_3)_2$), 1.83 (d, $J_{HH}$ = 4.64, 6H, CH(C*H*$_3)_2$), 1.55 (d, $J_{HH}$ = 5.03, 6H, CH(C*H*$_3)_2$), 1.16 (d, $J_{HH}$ =5.16, 6H, CH(C*H*$_3)_2$), 1.05 (d, $J_{HH}$ = 4.30, 6H, CH(C*H*$_3)_2$). $^{13}$C{$^{1}$H} NMR (125 MHz, $CDCl_3$, −55 °C): 158.6, 127.9, 118.8, 115.5, 57.5, 53.2, 41.7, 29.9, 29.3, 22.0, 21.3. Mp: 194-6 °C.

**2.9.26 Synthesis of NCr(N$^{i}$Pr$_2)_2$(NCO) (28):** Under an inert atmosphere a pressure tube was loaded with sodium cyanate (0.083 g, 1.271 mmol, 5 equiv), 1,4-dioxane (8 mL), and a stir bar. To the stirring cyanate solution was added **2** (0.100 g, 0.254 mmol, 1 equiv), in acetonitrile (~8 mL). The pressure tube was sealed and placed in a 45 °C oil bath and stirred for 20 h. The tube was returned to the dry box, and the volatiles were removed in vacuo. The residue was extracted with pentane and filtered through Celite. The solution was concentrated to ~5 mL and placed in a −35 °C freezer, which yielded light orange needles of **28** (0.047 g, 0.153 mmol, 60% yield). $^{1}$H NMR (500 MHz, $CDCl_3$, 25 °C): 5.04 (sept, $J_{HH}$ = 6.34, 2H, C*H*$(CH_3)_2$), 3.81 (sept, $J_{HH}$ =

6.28, 2H, C*H*($CH_3$)$_2$), 1.90 (d, $J_{HH}$ = 6.36, 6H, CH(C*H*$_3$)$_2$), 1.47 (d, $J_{HH}$ = 6.29, 6H, CH(C*H*$_3$)$_2$), 1.23 (d, $J_{HH}$ = 6.34, 6H, CH(C*H*$_3$)$_2$), 1.10 (d, $J_{HH}$ = 6.50, 6H, CH(C*H*$_3$)$_2$). $^{13}$C{$^1$H} NMR (125 MHz, $CDCl_3$, 25 °C): 149.7, 58.8, 57.1, 30.549, 30.2, 21.5, 21.3. Mp: 115 °C (dec).

**2.9.27 Synthesis of NCr(N$^i$Pr$_2$)$_2$(NCS) (29):** Under an inert atmosphere, a scintillation vial was loaded with **2** (0.100 g, 0.254 mmol, 1 equiv.), toluene (5 mL), and a stirbar. To this solution, sodium thiocyanate (0.062 g, 0.763 mmol, 3 equiv.) in acetonitrile (10 mL) was added. The reaction stirred at room temperature for 3 d. The volatiles were removed in vacuo. The residue was extracted with pentane, and filtered through Celite. Cooling concentrated pentane solutions of the crude product to −35 °C yielded yellow-orange needles of **29** (0.043 g, 0.132 mmol, 52% yield). $^1$H NMR (500 MHz, $CDCl_3$, −13 °C): 5.10 (sept, $J_{HH}$ = 6.31, 2H, C*H*($CH_3$)$_2$), 3.86 (sept, $J_{HH}$ = 6.40, 2H, C*H*($CH_3$)$_2$), 1.92 (d, $J_{HH}$ = 6.23, 6H, CH(C*H*$_3$)$_2$), 1.45 (d, $J_{HH}$ = 6.23, 6H, CH(C*H*$_3$)$_2$), 1.28 (d, $J_{HH}$ = 6.23, 6H, CH(C*H*$_3$)$_2$), 1.11 (d, $J_{HH}$ = 6.29, 6H, CH(C*H*$_3$)$_2$). $^{13}$C{$^1$H} NMR (125 MHz, $CDCl_3$, −13 °C): 189.8, 59.3, 57.9, 30.7, 30.4, 22.0, 21.6. Mp: 138-142 °C.

**2.9.28 Synthesis of NCr(N$^i$Pr$_2$)$_2$(CN) (30):** Under an inert atmosphere, a scintillation vial was loaded with sodium cyanide (10.6 mg, 0.216 mmol, 1 equiv.) in acetonitrile (~10 mL), freshly dried 15-crown-5 (47.6 mg, 0.216 mmol, 1 equiv.), and a stir bar. After stirring for 5 min, **2** (0.085 g, 0.216 mmol, 1 equiv.) in acetonitrile (5 mL) was added. The reaction stirred at room

temperature for 6 h. The volatiles were removed in vacuo, and the residue was extracted with pentane and filtered through Celite. Cooling concentrated pentane solutions of the crude product to −35 °C yielded orange crystals of **30** (28.7 mg, 0.093 mmol, 43% yield). $^{1}$H NMR (500 MHz, $CDCl_3$, −6 °C): 5.13 (sept, $J_{HH}$ = 6.29, 2H, C*H*$(CH_3)_2$), 3.88 (sept, $J_{HH}$ = 6.04, 2H, C*H*$(CH_3)_2$), 1.89 (d, $J_{HH}$ = 5.63, 6H, CH(C*H*$_3)_2$), 1.54 (d, $J_{HH}$ = 5.63, 6H, CH(C*H*$_3)_2$), 1.36 (d, $J_{HH}$ = 5.84, 6H, CH(C*H*$_3)_2$), 1.13 (d, $J_{HH}$ = 5.84, 6H, CH(C*H*$_3)_2$). $^{13}$C{$^{1}$H} NMR (125 MHz, $CDCl_3$, −6 °C): 143.9, 58.5, 57.9, 57.7, 31.1, 31.0, 30.7, 30.5, 23.1, 22.6, 22.4, 21.9. IR: C–N stretch appears at 2172 cm$^{-1}$. M.p.: 180 °C (dec).

**2.9.29 Synthesis of NCr(N$^{i}$Pr$_2)_2$(NMe$_2$) (31):** Under an inert atmosphere, a vial was loaded with $ZnCl_2$ (0.293 g, 2.15 mmol, 4.23 equiv), a stirbar, and THF (15 mL). This was cooled in a liquid cooled nitrogen cold well for 10 min. The vial was moved to a stir plate, and a chilled solution of $LiNMe_2$ (0.220 g, 4.31 mmol, 8.47 equiv) in THF (4 mL) and DME (4 mL) was added dropwise. The reaction stirred for 1 h and was allowed to come to room temperature, during which the mixture turned cloudy white. To this suspension was added a solution of **2** (0.200 g, 0.509 mmol, 1 equiv) in THF (2 mL) dropwise. The reaction stirred at room temperature for 4 h and turned bright red. The volatiles were removed in vacuo. The residue was extracted with pentane and filtered through Celite. The pentane was removed in vacuo. The complex was recrystallized from a minimum of acetonitrile (~4 mL) and red crystals of **31** were isolated (0.110 g, 0.354 mmol, 70%). $^{1}$H NMR (500 MHz, $CDCl_3$, 25 °C): 3.89 (sept, $J_{HH}$ = 6.43, 4H, C*H*$(CH_3)_2$), 3.55 (s, 6H, N(C*H*$_3)_2$), 1.31 (d, $J_{HH}$ = 6.27, 12H, CH(C*H*$_3)_2$), 1.23 (d,

$J_{HH}$ = 6.34, 12H, CH(C$H_3$)$_2$). $^{13}$C{$^1$H} NMR (125 MHz, $CDCl_3$, 25 °C): 54.5, 53.7, 26.4, 25.1. Mp: 52-57 °C.

**2.9.30 Synthesis of [NCr(N$^i$Pr$_2$)$_2$(DMAP)]BF$_4$ (32):** Under an $N_2$ atmosphere, a scintillation vial was loaded with **2** (0.177 g, 0.450 mmol, 1 equiv), 4-dimethylaminopyridine (0.055 g, 0.450 mmol, 1 equiv), and a stir bar. To this vial, $CHCl_3$ (8 mL) was added, and the solution was stirred for 10 min. A solution of $AgBF_4$ (0.096 g, 0.495 mmol, 1.1 equiv) in acetonitrile (4 mL) was added over 5 min. The reaction stirred at room temperature for 1 h. The brown suspension was filtered through a glass frit with Celite as a filtering agent. The filtrate was dried in vacuo and washed with pentane (2 mL). The residue was extracted with $CHCl_3$ (2 × 5 mL). These extracts were filtered through Celite and dried under vacuum yielding [NCr(N$^i$Pr$_2$)$_2$(DMAP)]BF$_4$ (**32**) (0.124 g, 0.261 mmol, 58%). This was used without further purification in the synthesis of **33**. $^1$H NMR (500 MHz, $CDCl_3$, 0 °C): 8.21 (d, $J_{HH}$ = 7.0 Hz, 2H, Ar-*H*), 6.68 (d, $J_{HH}$ = 6.5 Hz, 2H, Ar-*H*), 5.50 (sept, $J_{HH}$ = 6.0 Hz, 2H, C*H*(CH$_3$)$_2$), 3.93 (sept, $J_{HH}$ = 6.0 Hz, 2H, C*H*(CH$_3$)$_2$), 3.12 (s, 6H, N(C$H_3$)$_2$) 1.86 (d, $J_{HH}$ = 6.5 Hz, 6H, CH(C$H_3$)$_2$), 1.55 (d, $J_{HH}$ = 6.5 Hz, 6H, CH(C$H_3$)$_2$), 1.23 (d, $J_{HH}$ = 6.5 Hz, 6H, CH(C$H_3$)$_2$), 1.15 (d, $J_{HH}$ = 6.5 Hz, 6H, CH(C$H_3$)$_2$). $^{19}$F NMR (564 MHz, $CDCl_3$, 25 °C): –151.9 ppm.

**2.9.31 Synthesis of NCr(N$^i$Pr$_2$)$_2$(F) (33):** Under an $N_2$ atmosphere, a scintillation vial was loaded with FSn$^n$Bu$_3$ (3.38 mg, 0.011 mmol, 10 mol%), THF (1 mL), and a stir bar. A solution of [NCr(N$^i$Pr$_2$)$_2$(DMAP)]BF$_4$ **32** (0.052 g, 0.109 mmol, 1 equiv.) from the previous step in THF

(8 mL) was added. The reaction stirred for 4 h at room temperature. The volatiles were removed in vacuo, and the residue was extracted with pentane (2 × 5 mL) and filtered through Celite. The pentane solution was concentrated to ~5 mL under vacuum, and held at −35 °C yielding **33** as red-orange crystals (0.015 g, 0.054 mmol, 49%). $^{1}$H NMR (500 MHz, $CDCl_3$, 25 °C): 5.08 (sept, $J_{HH}$ = 6.5 Hz, 2H, C*H*($CH_3$)$_2$), 3.81 (sept, $J_{HH}$ = 6.0 Hz, 2H, C*H*($CH_3$)$_2$), 1.94 (d, $J_{HH}$ = 6.5 Hz, 6H, CH(C*H*$_3$)$_2$), 1.44 (d, $J_{HH}$ = 6.5 Hz, 6H, CH(C*H*$_3$)$_2$), 1.23 (d, $J_{HH}$ = 6.0 Hz, 6H, CH(C*H*$_3$)$_2$), 1.12 (d, $J_{HH}$ = 6.5 Hz, 6H, CH(C*H*$_3$)$_2$). $^{13}$C{$^{1}$H} NMR (125 MHz, $CDCl_3$, 25 °C): 21.21, 21.45, 30.15, 30.22, 56.63, 58.65. $^{19}$F NMR (564 MHz, $CDCl_3$, 25 °C): −145.24. M.p. 100-102 °C.

**2.9.32 Synthesis of [NCr(N$^{i}$Pr$_2$)$_2$(HMPA)]PF$_6$ (34):** In a 20 mL scintillation vial equipped with a stir bar was loaded with **2** (0.050 g, 0.14 mmol, 1 equiv.), HMPA (0.025 g, 0.14 mmol, 1 equiv.) and 3.0 mL of $CHCl_3$. This was allowed to stir for ten minutes. A solution of $AgPF_6$ (XX g, XX mmol, 1 equiv.) in 3.0 mL of acetonitrile was added over five minutes. The reaction stirred for one hour at room temperature. The solution was filtered through a glass frit with Celite as a filtering agent. The filtrate was dried in vacuo and washed with pentane (2 mL). The residue was extracted with $CHCl_3$ (2 × 5 mL). These extracts were filtered through Celite and dried under vacuum yielding [NCr(N$^{i}$Pr$_2$)$_2$(HMPA)]PF$_6$ (**34**). $^{1}$H NMR (500 MHz, $CDCl_3$, 25 °C): 5.24 (sept, $J_{HH}$ = 6.5 Hz, 2H, C*H*($CH_3$)$_2$), 3.93 (sept, $J_{HH}$ = 6.5 Hz, 2H, C*H*($CH_3$)$_2$), 2.68 (d, $J_{HH}$ = 10 Hz, 18H, N(C*H*$_3$)$_2$), 1.94 (d, $J_{HH}$ = 6.0 Hz, 6H, CH(C*H*$_3$)$_2$), 1.43 (d, $J_{HH}$ = 6.5 Hz,

6H, CH(C$H_3$)$_2$), 1.25 (d, $J_{HH}$ = 6.5 Hz, 6H, CH(C$H_3$)$_2$), 1.20 (d, $J_{HH}$ = 6.5 Hz, 6 H, CH(C$H_3$)$_2$).

**2.9.33 Synthesis of NCr(N$^i$Pr$_2$)$_2$(CH$_2$SiMe$_3$) (35):** In a 20 mL scintillation vial equipped with a stir bar was loaded with **10** (0.050 g, 0.140 mmol, 1.0 equiv.) and 8 mL of pentane. This solution was placed into a liquid nitrogen cooled cold well to cool for 5 min. To this cold, stirring solution was added 0.139 mL of 1.0 M LiCH$_2$SiMe$_3$ dropwise. The solution was allowed to warm up to room temperature and stir for 1 h. The solution turned from orange-red to a yellow-brown color. The pentane solution was cooled and then filtered through Celite to remove LiOPh. The solution was concentrated *in vacuo* and placed in a freezer yielding yellow-orange crystals (0.036 g, 0.10 mmol, 73%). $^1$H NMR (500 MHz, CDCl$_3$, 1.67 $^o$C): 4.93 (sept, $J_{HH}$ = 6.0 Hz, 2H, C$H$(CH$_3$)$_2$), 3.52 (sept, $J_{HH}$ = 6.0 Hz, 2H, C$H$(CH$_3$)$_2$), 1.60 (d, $J_{HH}$ = 6.5 Hz, 6H, CH(C$H_3$)$_2$), 1.41 (d, $J_{HH}$ = 6.0 Hz, 6H, CH(C$H_3$)$_2$), 1.14 (d, $J_{HH}$ = 6.5 Hz, 6H, CH(C$H_3$)$_2$), 1.12 (d, $J_{HH}$ = 6.5 Hz, 6H, CH(C$H_3$)$_2$), 0.056 (s, 9H, Si(C$H_3$)$_3$), -0.033 (s, 2H, C$H_2$Si(CH$_3$)$_3$). $^{13}$C{$^1$H}NMR (125 MHz, CDCl$_3$, 10 $^o$C): 56.1, 53.5, 30.8, 29.4, 29.0, 22.4, 20.1, 1.6. $^{29}$Si NMR (119.16 MHz, CDCl$_3$, 25 $^o$C): 2.078 (s, CH$_2$*Si*(CH$_3$)$_3$). Mp: 90-92 $^o$C.

**2.9.34 Synthesis of NCr(N$^i$Pr$_2$)$_2$(CH$_2$C(Me)$_2$Ph) (37):** A 20 mL scintillation vial equipped with a stir bar was loaded with **2** (0.020 g, 0.10 mmol, 1 equiv.) and 2 mL of ether. This solution was placed into a liquid nitrogen cooled cold well to cool for 5 min. To this cold stirring solution was added a cold solution of Mg(CH$_2$C(Me)$_2$Ph)$_2$ (0.011 g, 0.04 mmol, 0.7 equiv.) in 2 mL of

ether dropwise. This was allowed to warm to room temperature and stir for 1.5 h. A white solid precipitated, and the solution turned yellow-brown. The solvent was removed *in vacuo* and the brown solid dissolved in hexane. The solution was cooled to –35 $^{o}$C and filtered through Celite to remove $MgI_2$. The solution was concentrated *in vacuo* and placed in a freezer yielding yellow-orange crystals (0.019 g, 0.048 mmol, 95% yield). $^{1}$H NMR (500 MHz, $CDCl_3$, 25 $^{o}$C): 7.33 (d, $J_{HH}$ = 7.5 Hz, 2H, *ortho*), 7.13 (app t, $J_{HH}$ = 8.0 Hz, 2H, *meta*), 6.98 (app t, $J_{HH}$ = 7.0 Hz, 1H, *para*), 4.74 (sept, $J_{HH}$ = 6.5, 2H, C*H*$(CH_3)_2$), 3.40 (sept, $J_{HH}$ = 6.5 Hz, 2H, C*H*$(CH_3)_2$), 1.49 (s, 6H, C(C*H*$_3)_2$Ph), 1.47 (s, 2H, C*H*$_2$C$(CH_3)_2$Ph), 1.45 (d, $J_{HH}$ = 6.0 Hz, 6H, CH(C*H*$_3)_2$), 1.32 (d, $J_{HH}$ = 6.0 Hz, 6H, CH(C*H*$_3)_2$), 1.05 (d, $J_{HH}$ = 6.0 Hz, 6H, CH(C*H*$_3)_2$), 1.01 (d, $J_{HH}$ = 6.0 Hz, 6H, CH(C*H*$_3)_2$). $^{13}$C{$^{1}$H} NMR (125 MHz, $CDCl_3$, 25 $^{o}$C): 154.7, 127.7, 125.5, 124.5, 64.7, 55.8, 53.3, 39.6, 32.0, 31.0, 28.9, 22.7, 19.7. Mp: 71-73 $^{o}$C.

**2.9.35 Synthesis of NCr(N$^{i}$Pr$_2$)$_2$(CH$_2$CMe$_3$) (38):** A 20 mL scintillation vial equipped with a stir bar was loaded with **6** (0.027g, 0.065 mmol, 1.0 equiv.) and 4 mL of pentane. This was placed into a liquid nitrogen cold well to cool for five min. To this cold stirring solution was added $LiCH_2CMe_3$ (0.005 g, 0.065 mmol, 1.0 equiv.) in 3 mL of cold ether dropwise. Over a period of one h a white solid precipitated. The solution was pumped dry, and the product was dissolved in pentane. The pentane solution was cooled to –35 $^{o}$C and filtered through Celite to remove LiOAd. The solution was concentrated in vacuo and stored in the freezer yielding crystals ( % yield).$^{1}$H NMR (500 MHz, $CDCl_3$, 2 $^{o}$C): 4.85 (sept, $J_{HH}$ = 6.5 Hz, 2H,

C*H*($CH_3$)$_2$), 3.49 (sept, $J_{HH}$ = 6.5 Hz, 2H, C*H*($CH_3$)$_2$), 1.58 (d, $J_{HH}$ = 6.0 Hz, 6H, CH(C*H*$_3$)$_2$), 1.41 (d, $J_{HH}$ = 6.0 Hz, 6H, CH(C*H*$_3$)$_2$), 1.26 (s, 2H, C*H*$_2$C($CH_3$)$_3$), 1.14 (d, $J_{HH}$ = 6.5 Hz, 6H, CH(C*H*$_3$)$_2$), 1.11 (d, $J_{HH}$ = 6.0 Hz, 6H, CH(C*H*$_3$)$_2$), 1.09 (s, 9H, $CH_2$C(C*H*$_3$)$_3$). $^{13}$C{$^1$H} NMR (125 MHz, $CDCl_3$, $^o$C): Mp:

**2.9.36 Synthesis of NCr(N$^i$Pr$_2$)$_2$(CCSi$^i$Pr$_3$) (39):** A 20 mL scintillation vial equipped with a stir bar was loaded with **10** (0.050 g, 0.140 mmol, 1.0 equiv.) and 5 mL of hexane. This was placed in a liquid nitrogen cooled cold well to cool for 5 min. To this cold stirring solution was added a cold solution of LiCCSi$^i$Pr$_3$ (0.026 g, 0.140 mmol, 1.0 equiv.) in 5 mL of hexane. The reaction was allowed to warm up to room temperature and stir for 1.5 h. The solution was cooled to –35 $^o$C and filtered through Celite to remove LiOPh. This solution was concentrated in vacuo and then placed in the freezer yielding orange crystals (0.052, 0.115 mmol, 83% yield). $^1$H NMR (500 MHz, $CDCl_3$, –18 $^o$C): 5.05 (sept, $J_{HH}$ = 6.0 Hz, 2H, C*H*($CH_3$)$_2$), 3.72 (sept, $J_{HH}$ = 6.5 Hz, 2H, C*H*($CH_3$)$_2$), 1.80 (d, $J_{HH}$ = 6.0 Hz, 6H, CH(C*H*$_3$)$_2$), 1.48 (d, $J_{HH}$ = 6.5 Hz, 6H, CH(C*H*$_3$)$_2$), 1.25 (d, $J_{HH}$ = 6.5 Hz, 6H, CH(C*H*$_3$)$_2$), 1.10 (d, $J_{HH}$ = 6.5 Hz, 6H, CH(C*H*$_3$)$_2$), 1.00 (br s, 21H, Si(C*H*($CH_3$)$_2$)$_3$. $^{13}$C{$^1$H} NMR (125 MHz, $CDCl_3$, –20 $^o$C): 150.4, 119.0, 57.5, 55.8, 30.6, 30.4, 21.9, 21.4, 18.8, 11.4. $^{29}$Si NMR (119.16 MHz, $CDCl_3$, 25 $^o$C): –6.108 (s, CC*Si*$^i$Pr$_3$). Mp: 109-110 $^o$C.

**2.9.37 Synthesis of NCr($N^iPr_2$)$_2$($CC^tBu$) (40):** In a 20 mL scintillation vial equipped with a stir bar was loaded **10** (0.037 g, 0.102 mmol, 1.0 equiv.) and 7 mL of hexanes. This was placed in a liquid nitrogen filled cold well to cool for five min. To this cold stirring solution was added a cold solution of Li$CC^tBu$ (0.009 g, 0.1 mmol, 1.0 equiv.) in 2 mL of ether. The reaction was allowed to warm to room temperature and stir for 1 h. Over this period, the solution turned from dark-red to light orange-red. Then the solvent was removed *in vacuo*. The product was dissolved in pentane, chilled, and filtered through Celite to remove LiOPh. The cold solution was concentrated and placed in a freezer at –35 $^oC$ yielding bright red-orange crystals (0.035 g, 0.101 mmol, 98% yield). $^1H$ NMR (500 MHz, $CDCl_3$, 1 $^oC$): 5.07 (sept, $J_{HH}$ = 6.5 Hz, 2H, C*H*($CH_3$)$_2$), 3.69 (sept, $J_{HH}$ = 6.0 Hz, 2H, C*H*($CH_3$)$_2$), 1.80 (d, $J_{HH}$ = 6.5 Hz, 6H, CH(C*H*$_3$)$_2$), 1.46 (d, $J_{HH}$ = 6.5 Hz, 6H, CH(C*H*$_3$)$_2$), 1.25 (d, $J_{HH}$ = 6.5 Hz, 6H, CH(C*H*$_3$)$_2$), 1.17 (s, 9H, C(C*H*$_3$)$_3$), 1.10 (d, $J_{HH}$ = 6.0 Hz, 6H, CH(C*H*$_3$)$_2$). $^{13}C\{^1H\}$ NMR (125 MHz, $CDCl_3$, 25 $^oC$): 127.0, 114.7, 57.4, 55.6, 31.7, 30.6, 30.3, 28.9, 21.7, 21.1. Mp: 110-112 $^oC$.

**Synthesis of Reagents:**

**TlOBn:** In the dry box, a scintillation vial was loaded with benzyl alcohol (0.150 g, 1.39 mmol, 1 equiv), pentane (3 mL), and a stirbar. The solution was cooled to near frozen in a liquid nitrogen cooled cold well. The vial was moved to a stir plate, and freshly filtered TlOEt (0.349 g, 1.40 mmol, 1.01 equiv) in pentane (3 mL) was added dropwise. The reaction was allowed to come to room temperature with stirring. After 2 h, the volatiles were removed in vacuo yielding TlOBn as a white powder (0.415 g, 1.33 mmol, 96%).

$^{1}$H NMR (500 MHz, $C_6D_6$, 25 °C): 4.92 (s, 2H, PhC$H_2$O), 7.06-7.09 (m, 1H, *p*-Ar-*H*), 7.19-7.21(m, 2H, *m*-Ar-*H*), 7.23-7.25 (m, 2H, *o*-Ar-*H*). $^{13}$C{$^{1}$H} NMR (125 MHz, $C_6D_6$, 25 °C): 66.58, 127.07, 127.81, 128.86, 146.53. M.p. 74-76 °C (Lit.[18e] 74-78 °C).

**LiCCSi($^{i}$Pr)$_3$:** In a 20 mL scintillation vial equipped with a stir bar was loaded tri(*iso*propyl)silylacetylene (0.20 g, 1.1 mmol, 1 equiv.) and 8 mL of hexane. The solution was placed in a liquid nitrogen cooled cold well. To this cold stirring solution was added 1.6 M *n*-butyl lithium in hexanes (0.625 mL, 1.10 mmol, 1.0 equiv.) by syringe. The solution was allowed to warm to room temperature and stir for 1 h. The solvent was removed *in vacuo* leaving a sticky oil. This was used directly in the next reaction. (0.181 g, 0.9 mmol, 87.4% yield). This is a slight modification of the literature procedure.[33]

**LiCC$^{t}$Bu:** In a 20 mL scintillation vial equipped with a stir bar was loaded 3,3-dimethyl-1-butyne (0.100 g, 1.21 mmol, 1 equiv.) and 5 mL of hexane. This solution was cooled for 5 min in a liquid nitrogen cooled cold well. To this cold stirring solution was added 1.6 M *n*-butyl lithium in hexanes (0.760 mL, 1.21 mmol, 1.0 equiv.) and was allowed to warm to room temperature and stir for 1 h. Over this period the solution turned cloudy and a white precipitate formed. The solvent was removed *in vacuo* leaving a white solid. (0.101 g, 1.1 mmol, 96% yield). The melting point matched the reported literature value.[34]

# REFERENCES

REFERENCES


1) For a few prominent examples: (a) Wiedner, E. S.; Gallagher, K. J.; Johnson, M. J. A.; Kampf, J. W. *Inorg. Chem.* **2011**, *50*, 5936-5945 (b) Heppekausen, J.; Stade R.; Goddard, R.; Fürstner, A. *J. Am. Chem. Soc.* **2010**, *132*, 11045-11057 (c) Geyer, A. M.; Wiedner, E. S.; Gary, J. B.; Gdula, R. L.; Kuhlmann, N. C.; Johnson, M. J. A.; Dunietz, B. D.; Kampf, J. W. *J. Am. Chem. Soc.* **2008**, *130*, 8984-8999 (d) Gdula, R. L.; Johnson, M. J. A. *J. Am. Chem. Soc.* **2006**, *128*, 9614-9615 (e) Chisholm, M. H.; Delbridge, E. E.; Kidwell, A. R.; Quinlan, K. B. *Chem. Commun.* **2003**, 126-127

2) (a) Schrock, R. R. *Chem. Commun.* **2003,** *19*, 2389-2391 (b) Shaver, M. P.; Fyzuk, M. D. *Adv. Synth. Catal.* **2003**, *345*, 1061-1076 (c) Yandulov, D. V.; Schrock, R. R. *Science* **2003**, *301*, 76-78 (d) Birk, T.; Bendix, J. *Inorg. Chem.* **2003**, *42*, 7608-7615 (e) Leung, S. K. Y.; Haung, J. S.; Liang, J. L.; Che, C. M. Zhou, Z. Y. *Angew. Chem., Int. Ed.* **2003**, *42*, 340-343

3) (a) Chang, C. J.; Low, D. W.; Gray, H. B. *Inorg. Chem.* **1997**, *36*, 270-270 (b) Laplaza, C. E.; Johnson, A. R.; Cummins, C. C. *J. Am. Chem. Soc.* **1996**, *118*, 709 (c) Kol, M.; Schrock, R. R.; Kempe, R.; Davis, W. M. *J. Am. Chem. Soc*. **1994**, *116*, 4382-4390 (d) Woo, L. K. *Chem. Rev.* **1993**, *93*, 1125-1136 (e) Woo, L. K.; Goll, J. G.; Czapla, D. J.; Hays, J. A. *J. Am. Chem. Soc.* **1991**, *113*, 8478-8484 (f) Woo, L. K.; Goll, J. G. *J. Am. Chem. Soc.* **1989**, *111*, 3755-3757

4) Ozawa, H. T.; Yoshida, H.; Imori, Y.; Kuribayashi, Y.; Nankano, E.; Azuma, N. *Inorg. Chim. Acta* **1998**, *281*, 207-212

5) (a) Meyer, K; Bendix, J.; Bill, E.; Weyhermuller, K.; Wieghardt, K.; Nuber, B. Inorg. Chem. 1998, 37, 5180-5188 (b) Niemann, A.; Bossek, U.; Haselhorst, G.; Wieghardt, K.; Nuber, B. *Inorg. Chem.* **1996**, *35*, 906-915

6) Odom, A. L.; Cummins, C. C.; Protasiewicz, J. D. *J. Am. Chem. Soc.* **1995**, *117*, 6613-6614

7) Alyea, E. C.; Basi, J. S.; Bradley, D. C.; Chisholm, M. H.; *Chem. Commun.* **1968**, 495

8) Chiu, H. T.; Chen, Y. P.; Chuang, S. H.; Jen, J. S.; Lee, G. H.; Peng, S. M.; *Chem. Commun.* **1996**, 139-140

9) Takahashi, T. PhD Dissertation, University of Michigan **1985**

10) Neely, F. L.; Bottomley, L. A. *Inorg. Chem.* **1997**, *36*, 5432-5434

11) Bottomley, L. A.; Neely, F. L. *Inorg. Chem.* **1997**, *36*, 5435-5439

12) Dorough, G. D.; Miller, J. R.; Huennekens, F. M. *J. Org. Chem.* **1951**, *73*, 4315-4320

13) Buchler, J. W.; Dreher, C.; Lay, K. L.; Raap, A.; Gersonde, K. *Inorg. Chem*. **1983**, *22*, 879-884

14) Chen, S.; Chisholm, M. H.; Davidson, E. R.; English, J. B.; Lichtenberger, D. L. *Inorg. Chem.* **2009**, *48*, 828-837

15) Odom, A. L.; Cummins, C. C. *Organometallics* **1996**, *16*, 898-900

16) Odom, A. L.; Cummins, C. C. *Polyhedron* **1998**, *17*,675-688

17) (a) Stuhl, L. S.; Carter, S. J. *Organometallics* **1988**, *7*, 1909-1918 (b) Liesegang, G. W.; Farrow, M. M; Vazquez, F. A.; Purdie, N.; Eyring, E. M. *J. Am. Chem. Soc.* **1977**, *99*, 3240-3243 (c) Izatt, R. M.; Terry, R. E.; Haymore, B. L.; Hansen, L. D.; Dalley, N. K.; Ayondett, A. G.; Christensen, J. J. *J. Am. Chem. Soc.* **1976**, *98*, 762-767 (d) Frensdorf, H. K. *J. Am. Chem. Soc.* **1971**, *93*, 600-606

18) (a) Buzzeo, M. C.; Iqbal, A. H.; Long, C. M.; Millar, D.; Patel, S.; Pellow, M. A.; Saddoughi, S. A.; Smenton, A. L.; Turner, J. F. C.; Wadhawan, J. D.; Compton, R. G.; Golen, J. A.; Rheingold, A. L.; Doerrer, L. H. *Inorg. Chem.* **2004**, *43*, 7709-7725 (b) Burke, P. J.; Matthews, R. W.; Gillies, D. G. *Dalton Trans.* **1980**, 1439-1442 (c) Candy, C. F.; Jones, R. A.; Wright, P. H. *J. Chem. Soc. C* **1970**, 2563-2567. (d) Candy, C. F.; Jones, R. A. *J. Org. Chem.* **1971**, *36*, 3993-3994 (e) Sidgwick, N. V.; Sutton, L. E. *J. Chem. Soc.* **1930**, 1461-1473

19) Swartz, D. S. II; Staples, R. J.; Odom, A. L. *Dalton Trans.* **2011**, *40*, 7762-7768

20) Rose, T. L.; Kon, A. B. *Inorg. Chem.* **1993**, *32*, 781-782

21) Krygowski, T. M.; Cyrański, M. K. *Chem. Rev.* **2001**, *101*, 1385-1419

22) (a) Anderson, H. J.; Bauer, L. *J. Chem. Educ.* **1999**, *76*, 1151 (b) Katrizky, A. R.; Karelson, M.; Sild, S.; Krygowski, T. M.; Jug, K. *J. Org. Chem.* **1998**, *63*, 5228-5231

23) Fleckenstein, J. E.; Koszinowski, K. *Organometallics* **2011**, *30*, 5018-5026

24) Anderson, R. A.; Wilkinson, G. *J. Chem. Soc. Dalton* **1977**, 809-811

25) Song, J. I.; Berno, P.; Gambarotta, S. *J. Am. Chem. Soc.* **1994**, *116*, 6927-6928

26) Seyferth, D.; Rochow, E. G. *J. Org. Chem.* **1955**, *20*, 250-256

27) Hollingworth, G. J.; Perkins, G.; Sweeney, J. J. *Chem. Soc., Perkin Trans.* **1996**, *1*, 1913-1919

28) (a) Rasmussen, K. G.; Juhl, K.; Hazell, R. G.; Jorgensen, K. A. *J. Chem. Soc. Perkin Trans. II* **1998**, 1347-1350 (b) Doolan, P. C.; Gore, P. H.; Hollingsworth, R.; Waters, D. N.; Al-Ka'bi, J.; Farooqi, J. A. *J. Chem. Soc. Perkin Trans II* **1986**, 501-506

29) Butcher, E.; Rhodes, C. J.; Standing, M.; Davidson, R. S.; Browser, R. *J. Chem. Soc. Perkin Trans. II* **1992**, 1469-1474

30) Tolman, C. A. *Chem. Rev.* **1977**, *77*, 313-348

31) Collier, M. R., Lappert, M. F.; Pearce, R. *J. Chem. Soc. Dalton Trans.* **1973**, 445

32) Schrock, R. R.; Fellmann, J. D. *J. Am. Chem. Soc.* **1978**, *100*, 3359-3370

33) Li, J.; Zhang, K.; Zhang, X.; Chi, C.; Wu, J.; Huang, K. W. *J. Org. Chem.* **2010**, *75*, 856-863

34) Miller, M. J.; Lyttle, M. H.; Streitwieser, A. *J. Org. Chem.* **1981**, *46*, 1977-1984

35) http://home.cc.umanitoba.ca/~budzelaa/gNMR/gNMR.html, 8/23/2010

## Chapter 3: Kinetic Experiments and Discussion of the Results

### 3.1: Overview of Kinetics Experiments

The kinetics for this project concern the dynamic rotation of the amido ligands on the chromium nitrido complexes. Measuring the barrier of amido rotation using NMR is a developed science. For example, the measured barrier of rotation of *N*,*N*-dimethylacetamide (DMA) by various NMR techniques, such as SSMT,[1] CLSA,[2] and EXSY[3] is 73 ± 5 kcal/mol.[4,5] The use of these techniques is dependent on the rate of exchange. Shown in Figure 3.1, slow exchange on the NMR timescale[6] for two site exchange in a simulated spectrum[5] appears as two separate peaks. Fast exchange causes the two peaks to coalesce into one peak.

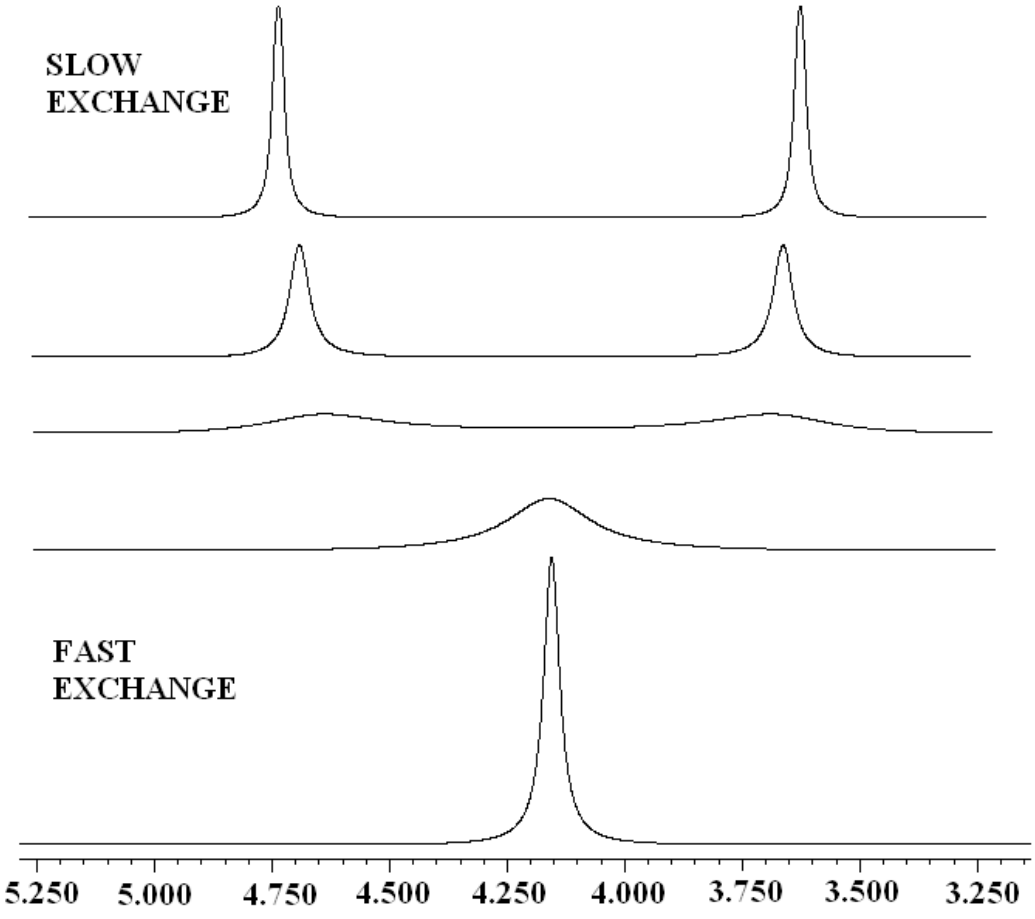


**Figure 3.1:** Simulated NMR spectra[5] of two sites exchanging at different rates

The majority of our chromium nitrido complexes fall in the slow exchange regime at room temperature. Due to this phenomenon, the technique most suited for our compounds to measure the exchange on the amido ligands is SSMT, with one expection. CLSA was used on $NCr(N^{i}Pr_2)_2NMe_2$ (**31**) because the exchange limit was too fast to measure using SSMT on our current instrumentation.

But before the experiment can be performed a few parameters for the experiment must be determined to allow for reliable data collection. An accurate 90° pulse width[7] of the exchanging peaks is needed because this will give better signal for our peaks, which results in a more reliable $T_1$. Using the 90° degree pulse width, $T_1$ is then determined by the inversion-recovery experiment.[8] Once these have been determined, the spin saturation experiment can begin. Below is a description on preparation of the sample, a detailed discussion on $T_1$, and a description of the SSMT experiment.

### 3.1.1 Preparation of the Sample

The sample was weighed out so the concentration is between 0.0222 M and 0.0333 M. Then 0.075 mL of $CDCl_3$, *d*-toluene or *d*-benzene was added to the weighed sample and loaded into a JY tube. The sample was taken out of the glovebox and freeze-pump-thawed to remove any dissolved oxygen or gases. This is important because the presence of dissolved gases such as oxygen can shorten $T_1$s, which may affect our measurements.[9]

### 3.2 Measuring $T_1$s and apparent $T_1$s of exchanging resonances.

In spin saturation magnetization experiments involving exchange between two sites, the rate is determined by the ratio of the fractional decrease in integration of one site in the presence of saturation of the other to its $T_1$. In a system experiencing two site exchange (Figure 3.2), the relaxation of spins for peak A is dependent on the rate of decay from the excited state $A^*$ to the ground state A; the same is true for peak B. When $T_{1A} = T_{1B}$, the source of relaxation is the same. In this case, the $T_1$ of the peak experiencing exchange is measured without saturation.[1a,c] But if $T_{1A}$ and $T_{1B}$ differ by more than 30% or if more than two peaks are experiencing exchange, the $T_1$ of the peak experiencing exchange in the presence of saturation is measured and is known as the apparent $T_1$.[10]

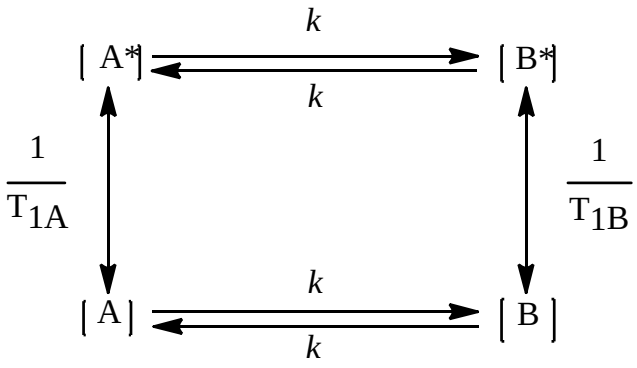


**Figure 3.2:** Kinetic scheme for two site exchange

In our chromium nitrido system, both $T_1$ and apparent $T_1$ of the septet corresponding to the isopropyl methyne hydrogens were measured. For example, in $NCr(N^iPr_2)_2I$ (**2**) these septets appear at 5.32 and 3.78 ppm (Figure 3.3). The deshielded peak was chosen for saturation.

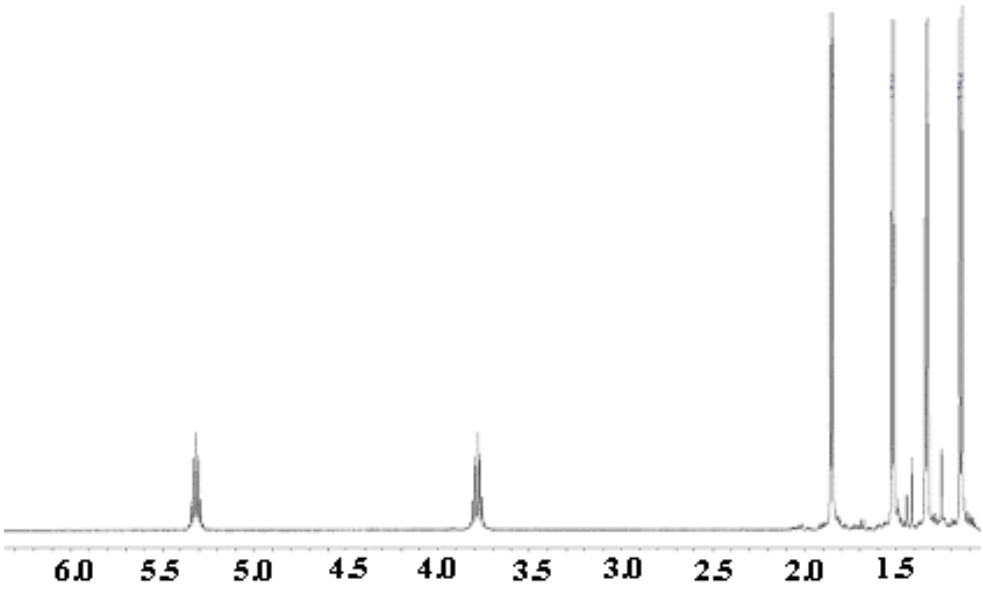


**Figure 3.3:** $^{1}$H NMR spectrum of NCr(N$^{i}$Pr$_2$)$_2$I (**2**) at 25 °C

This peak was chosen because the control experiment that compensates for decoupling sidebands would not saturate other peaks that could affect exchange. Data for both the $T_1$ and apparent $T_1$ of the peak at 5.32 ppm are shown below for **2**. The relationship between $T_1$ and apparent $T_1$ ($T_{1app}$) is:

$$T_{1app} = \frac{M_z^A(\infty)}{M_z^A(0)} T_1 \quad \text{Eqn. 1}$$

where $M_Z(\infty)$ is the intensity (or integrated area) of the resonance upon saturation (applied for, at least, 5 × $T_1$) of the exchanging site and $M_Z(0)$ is the intensity of the resonance with no saturation.

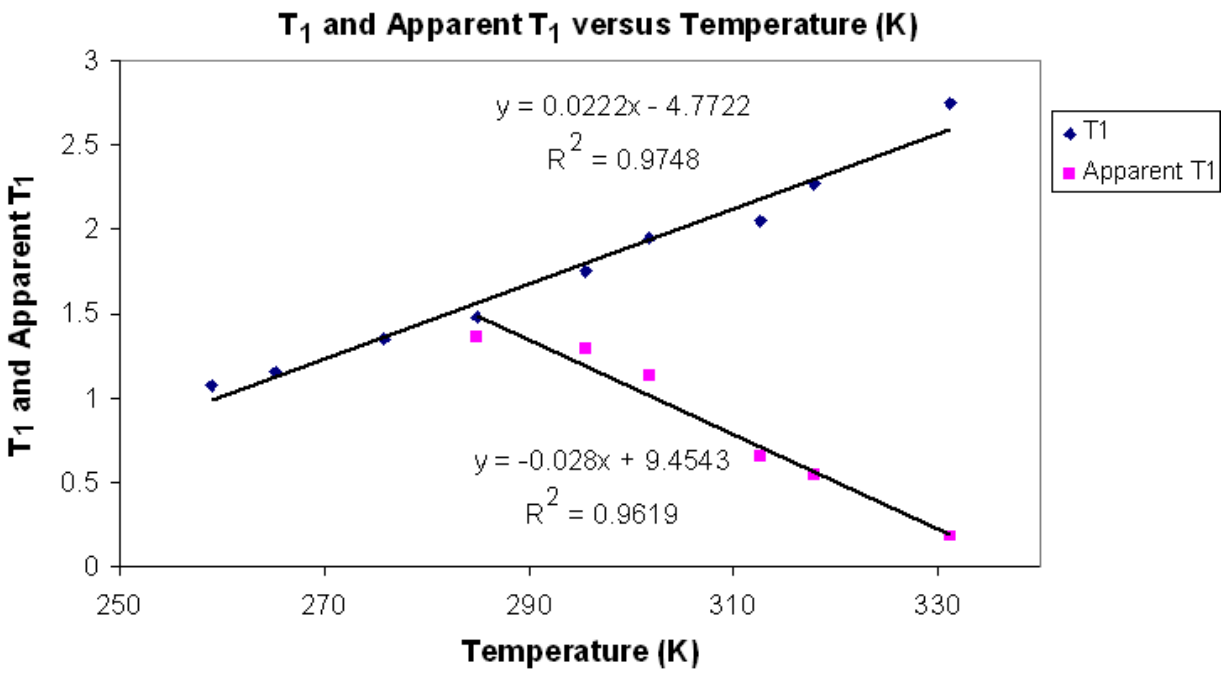


**Figure 3.4:** $T_1$ and apparent $T_1$ of **2** at different temperatures

At 285 K and below, **2** does not experience exchange of the isopropyl groups on the NMR timescale as seen by the lack of change in chemical shifts and linewidths of the exchanging sites. At this extreme, Equation 1 simplifies to $T_{1app} = T_1$. This was observed in our experiments. Above 335 K, exchange is fast on the NMR timescale ($k >> \delta_a - \delta_b$) and individual peaks are not observable. In the temperature regime where the exchange can be measured, $T_1$ increases with temperature. The opposite is observed for $T_{1app}$, as expected from Equation 1. This data tells us that only the measurement of the $T_1$ and not $T_{1app}$ is required for the kinetic study. $T_{1app}$ is only measured when the two exchanging peaks have $T_1$s that differ by more than 30%.[10]

For all of the chromium nitrido compounds, their NMR spectra show two septets that represent the methyne protons on the isopropyl groups.

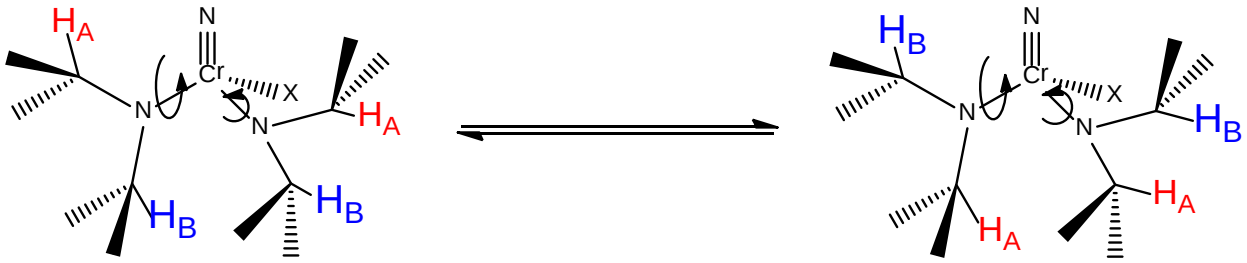


**Figure 3.5:** Amido rotation and exchange of equivalent methyne peaks

Protons $H_A$ and $H_B$ shown in Figure 3.5, are in two different chemical environments. For the chromium complex on the left, $H_A$ is syn to the nitrido and $H_B$ is anti to the nitrido. As the diisopropyl amido ligands rotate about the chromium-nitrogen bond, protons $H_A$ and $H_B$ exchange positions. The $^1$H NMR spectrum of $NCr(N^iPr_2)_2I$[12] in Figure 3.3 has two septets and four doublets. Since these peaks are inherent in all of our series, understanding the orientation of the diisopropyl amido peaks will help us make sure we are doing the correct measurements and know what we are doing in our kinetics experiments.

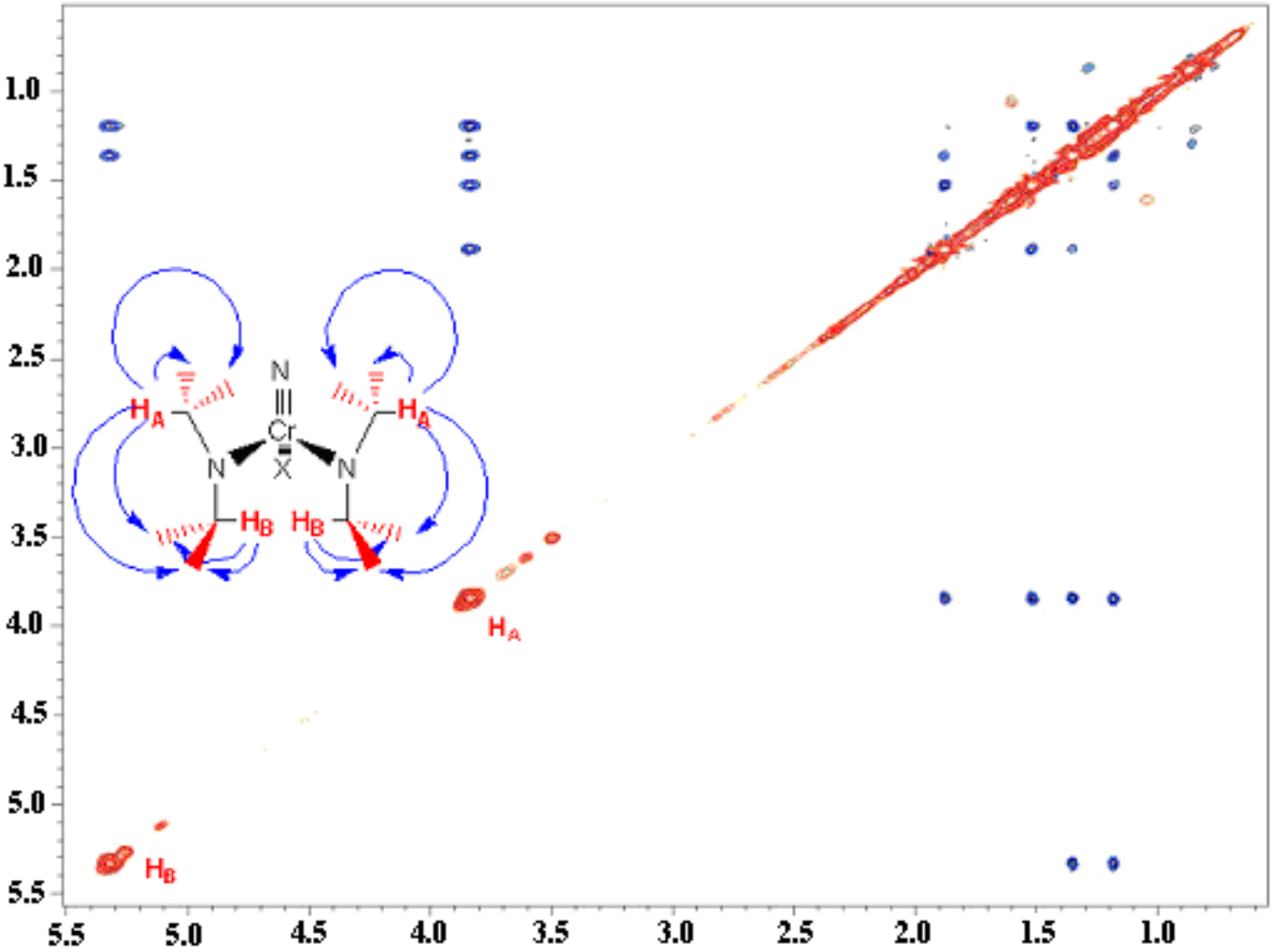


**Figure 3.6:** 2D NOESY spectrum of **2** at –60 $^{o}$C

Assignment of the chemical shifts for $H_A$ and $H_B$ of **2** are based upon the 2D NOESY spectrum (Figure 3.6). In the spectrum, positive resonances are in red, while negative are in blue. Thus, for this small molecule, red cross peaks represent exchange and blue cross peaks represent NOE's.[11] The blue arrows on the structure show observed NOE interactions between the methyne and methyl protons. The resonance at 3.83 ppm is assigned to $H_A$ since it shows NOE interactions with all four methyl resonances. $H_B$ is assigned to 5.35 ppm and has two NOE interations. The spectrum in Figure 3.6 is of **2** at –60 $^{o}$C, where no exchange between the methyne peaks occurs. There is free rotatation about the N—C bond bearing $H_A$ allowing interaction with all methyl groups. $H_B$ cannot rotate as freely and does not come within the NOE limit of 5 Å. Furthermore, it is plausible that since $H_B$ spends more time closer to the metal center, it experiences a greater downfield shift due to the deshielding zone of the metal center. A homo decoupling experiment also confirms assignment as shown in Figure 3.7.

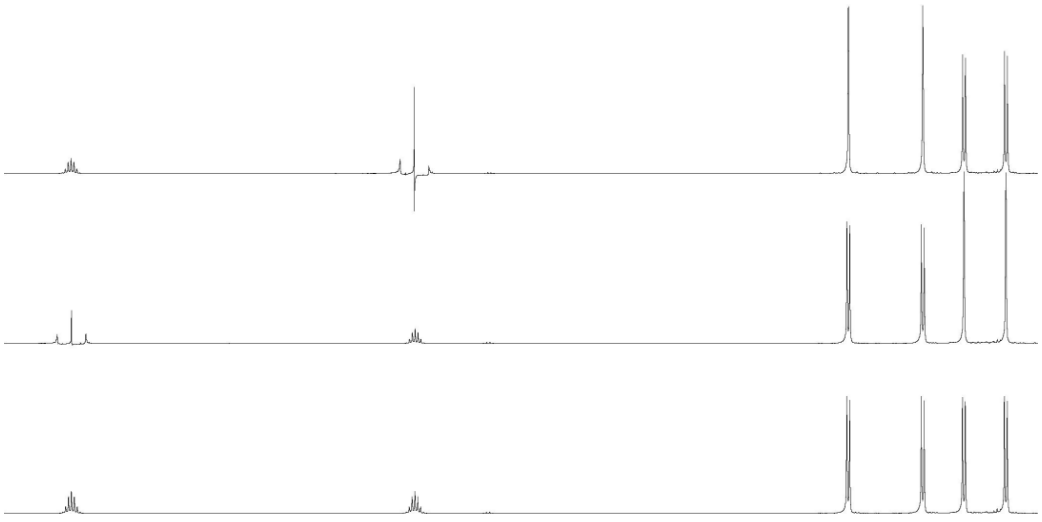

**Figure 3.7:** Homo-decoupling experiment of **2** at 25 $^{o}$C

### 3.3 Spin Saturation Magnetization Experiment

In the spin saturation magnetization transfer experiment, the more shielded methyne is saturated with a radio frequency pulse, while the change in the integration in the more deshielded peak is observed. To account for spill over, an offsite point equidistant from the exchanging peak is saturated. The reason for choosing the right peak for irradiation is because the offsite point cannot be on or near a peak that is experiencing exchange with the observed peak. As shown in Figure 3.7, the septet at 3.53 ppm and the doublet at 1.85 ppm are coupled, and if the doublet was irradiated it could transfer some of its magnetization over to the septet giving erroneous results. In Figure 3.8, the spectrum on the bottom is the end result of saturation; the height and area of the observed peak experiencing exchange will depend on how much exchange is occurring.

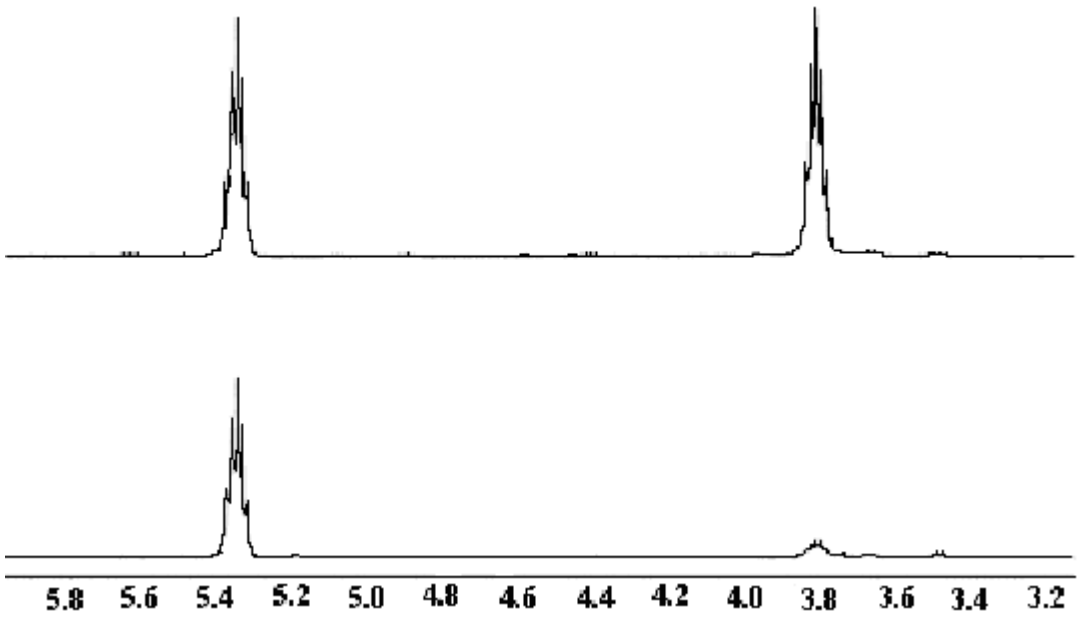


**Figure 3.8:** The top $^{1}$H spectrum is of **2** before irradiation and the bottom $^{1}$H spectrum is after irradiation.

The saturation pulse sequence shown in Figure 3.9 illustrates why an accurate $T_1$ is required for the experiment. The saturation delay (satdly) is set to $5 \times T_1$. If satdly is too short, $T_1$ will have time to relax, resulting in a larger peak, and give unreliable data.

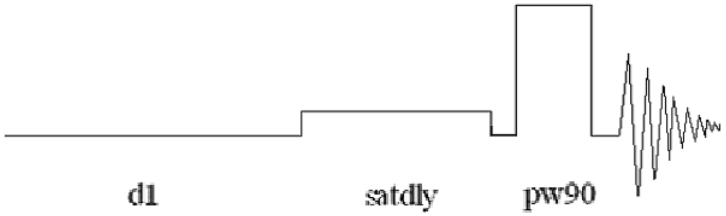


**Figure 3.9:** Presat pulse sequence

In Figure 3.2, [A] and [A*] are the ground and excited spin-state populations for site A (or peak), and [B] and [B*] are the ground and excited spin-state populations for site B (or peak) for a site experiencing two site exchange.[13] $T_{1A}$ and $T_{1B}$ are the spin lattice relaxation times and *k* is the rate constant for exchange between site A and B.

$$\frac{d[A]}{dt} = -k[A] + k[B] = -\frac{d[B]}{dt} \quad \text{Eqn. 2}$$

$$\frac{d[A^*]}{dt} = -k[A^*] + k[B^*] = -\frac{d[B^*]}{dt} \quad \text{Eqn. 3}$$

Equations 2 and 3 are the rate equations for ground and excited spin states without spin-lattice relaxations.

$$\frac{dM_A}{dt} = \frac{M_{OA} - M_A}{T_{1A}} \qquad \frac{dM_B}{dt} = \frac{M_{OA} - M_A}{T_{1B}} \quad \text{Eqn. 4 and 5}$$

In Equations 4 and 5, $M_A = [A] - [A^*]$ and $M_B = [B] - [B^*]$ are the net-magnetizations between exchanging sites A and B. And $M_{OA}$ and $M_{OB}$ are net magnetization at equilibrium.

$$\frac{dM_A}{dt} = -k(M_A - M_B) + \frac{M_{OA} - M_A}{T_{1A}} \quad \text{Eqn. 6}$$

$$\frac{dM_B}{dt} = k(M_A - M_B) + \frac{M_{OB} - M_B}{T_{1B}} \quad \text{Eqn. 7}$$

Combining Equations 2, 3, 4, and 5 gives Equations 6 and 7, which are the rate equations for net magnetization in the presence of chemical exchange and with spin lattice relaxation processes. When $T_{1A}$ and $T_{1B}$ are close in value, then $T_{1A} = T_{1B} = T_1$. The rate of exchange is the same for both exchanging sites.

If site B is selectively irradiated without affecting the nearby exchanging peak, the population difference between the ground and excited spin states will be equal to 0. $M_B = [B] - [B^*] = 0$ and the signal will be absent from the NMR spectrum (see Figure 3.8) giving Equation 8.

$$\frac{dM_A}{dt} = -k(M_A - 0) + \frac{M_{OA} - M_A}{T_{1A}} \quad \text{Eqn. 8}$$

The saturated spin-state in site B will transfer to site A through internal rotation or exchange and result in a reduced signal of site A, or peak in our experiment. The intensity of signal will vary depending on rate of exchange. The faster the exchange the smaller the peak and the slower it rotates, the larger the peak. If the sample is cooled to the point where the rotation is frozen out, an NOE will occur instead of exchange.[14] If saturation is long enough to reach steady state, then $dM_A/dt = 0$ giving Equation 9.

Once all of the data has been collected the $\Delta G^{\ddagger}$ barrier of rotation can be calculated using the Eyring Equation.[15] Integration of the observed peak with ($M_A$) and without ($M_{OA}$)

saturation was performed and used to determine the rate of exchange between the methynes using Equation 9.

$$k = \frac{1}{T_{1A}}\left(\frac{M_{OA}}{M_A} - 1\right) \qquad \text{Eqn. 9}$$

Where $M_{OA}$ is integration before spin saturation magnetization transfer and $M_A$ is after integration after exchange. Then the $T_1$ of the exchanging peak was determined using the inversion recovery method. By knowing the temperature of the experiment, the barrier of rotation of the amido can be determined using the Eyring Equation shown in Equation 10.

$$k = \kappa\left(\frac{k_b T}{h}\right) \exp^{-\Delta G/RT} \qquad \text{Eqn. 10}$$

Where $k_b$ is the Bolztmann constant, T is temperature (K), $h$ is Planck's constant, κ is the transmission coefficient and in this case it equals 1, $k$ is the rate of exchange determined using Equation 9 and R is the gas constant ($1.987\times10^{-3}$ kcal·mol$^{-1}$·K$^{-1}$).

In the SSMT experiment, 3 runs were collected at one temperature, or as close as possible to one temperature allowed by the instrumentation. Unfortunately, the temperature deviated ±1 $^{o}$C, while in a few cases by as a much as 5 $^{o}$C. Temperature was measured by a methanol standard.[16]

## 3.4 CONTROL EXPERIMENTS:

### 3.4.1 Investigation of Solvent Effects on $T_1$ and $\Delta G^{\ddagger}$

A series of control experiments were performed to investigate the techniques for sources of error. To see if the solvent had an effect on the $T_1$ values, four different SSMT experiments were run using *d*-toluene, *d*-benzene, and $CDCl_3$ solvents and gave similar energy barrier numbers that fell within the error bars. Comparison of our SSMT value of 16.1 kcal/mol for **9** with literature is in good agreement, 16.0 kcal/mol.[18] Our value was determined in $CDCl_3$, while the one in the literature was determined in *d*-benzene. Compound **1** was studied in $CDCl_3$ and *d*-toluene, because the compound, **31,** had to be cooled to –80 $^{o}$C where $CDCl_3$ would freeze. For **31**, the solvent chosen was *d*-toluene. The $\Delta G^{\ddagger}$ values 13.1 and 12.8 kcal/mol in $CDCl_3$ and *d*-toluene, respectively, were determined for **1**. Although, these results suggest that solvent interactions play little to no role in the experiment; a more polar deuterated solvent was not tested, which may coordinate to the chromium center and affect the barrirer of rotation or affect the transition state of rotation of the amido ligands.[17]

### 3.4.2 Investigation of Magnetic Field on $T_1$ and $\Delta G^{\ddagger}$

To see if the field had an effect on the barrier of rotation, SSMT on **2** was performed on both a 500 MHz and a 300 MHz Varian NMR instrument. The results showed similar values: 18.2 and 18.3 kcal/mol, respectively.

### 3.4.3 Investigation of Paramagnetic Materials on $T_1$ and $\Delta G^{\ddagger}$

Paramagnetic materials in solution are known to hasten the spin lattice relaxation $T_1$.[18] Since the rate is very sensitive to the $T_1$ value, the barrier of rotation calculated could give misleading results. In one experiment, we ran SSMT on **2**, and in another experiment doped the sample with $Cr(acac)_3$, a paramagnetic compound often used to speed up relaxation times.[19]

**Table 1:** Data from paramagnetic doped experiment of **2**

| Run | $M_{OA}$ | $M_A$ | $T_1$ | $\Delta G^{\ddagger}$ (kcal/mol) | Temperature |
|---|---|---|---|---|---|
| Pure Sample | 100 | 76.1 | 1.082 | 18.3 | 27.5 $^{o}$C |
| Doped Sample | 100 | 89.8 | 0.4393 | 18.5 | 28.4 $^{o}$C |

As indicated in Table 1, the $T_1$ for the pure sample is 1.082 and $\Delta G^{\ddagger}$ is 18.3 kcal/mol. The $T_1$ for the doped sample was about twice as fast, 0.4393, but $\Delta G^{\ddagger}$ was 18.5 kcal/mol. Essentially, the paramagnetic dopant affected the $T_1$ and exchange relaxation equally. So, if there were samples that contained even a small percentage of paramagnetic materials the $\Delta G^{\ddagger}$ values obtained are well within the error of the experiment.

### 3.5: CLSA and Eyring Plots of $NCr(N^{i}Pr_2)_2NMe_2$ (31) and $NCr(N^{i}Pr_2)_2OAd$ (6)

Due to the temperature limit of –80 $^{o}$C on current NMR instrumentation, we could not obtain the two well resolved septets required for the SSMT experiment for **31**. In this case

CLSA[2] was used, and a barrier of 9 kcal/mol was obtained. A sample of spectra from the CLSA experiment is shown in Figure 3.10 for compounds **31** and **6**.

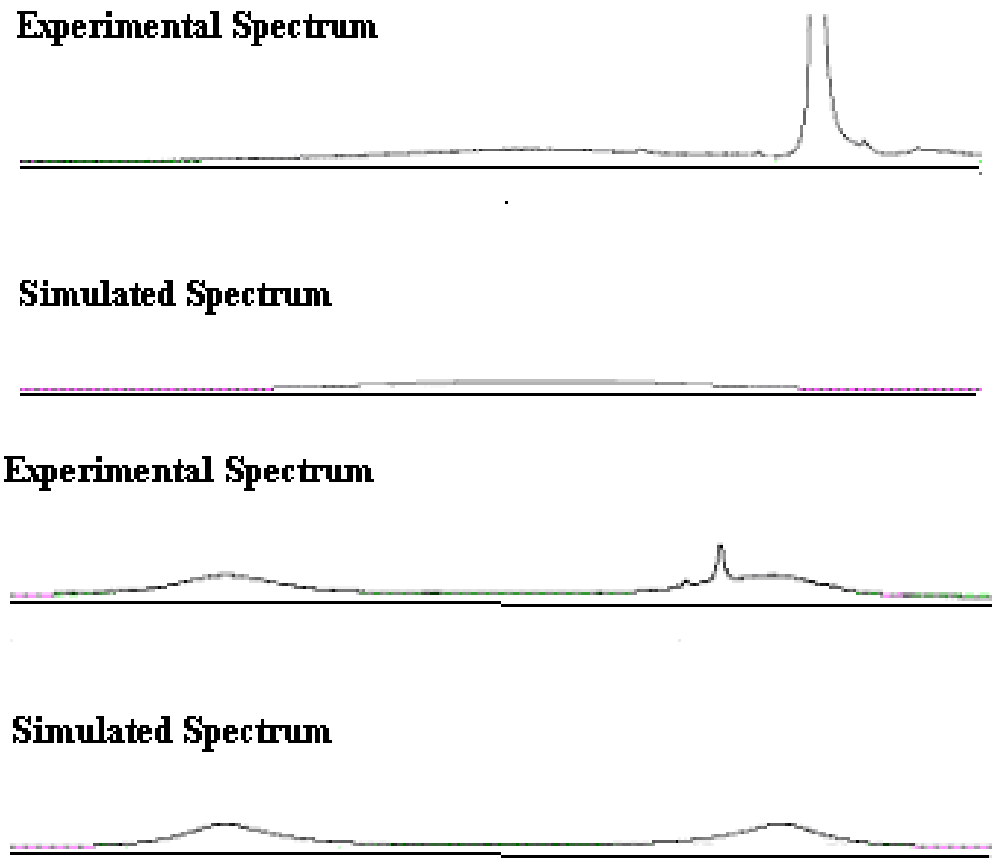


**Figure 3.10:** Simulated and experimental spectrum of **31** (top) and **6** (bottom)

To determine if numbers from complete line shape analysis agree with spin saturation transfer experiments, complete line shape was performed on **6**. The barrier to rotation determined by CLSA was 12.7 kcal/mol, and the value found using SSMT was 12.8 kcal/mol.

### 3.6 Discussion of $\Delta G^{\ddagger}$, $\Delta H^{\ddagger}$, and $\Delta S^{\ddagger}$ and Ligand Donating Parameter

The $\Delta G^{\ddagger}$ barrier to rotation is the amount of energy in the system that has to be overcome for the diisopropylamido ligand to rotate. Rotation about the diisopropylamido ligands is dependent on temperature due to the entropy factor.Thus, six different compounds spread over the series were investigated to extract $\Delta S^{\ddagger}$ from Eyring plots. Chosen were $NCr(N^{i}Pr_2)_2I$ **2**, $NCr(N^{i}Pr_2)_2CN$ (**30**), $NCr(N^{i}Pr_2)_2O$-*p*-$(SMe)C_6H_4$ (**12**), $NCr(N^{i}Pr_2)_2OBn$ (**20**), $NCr(N^{i}Pr_2)_2OAd$ (**6**), and $NCr(N^{i}Pr_2)_3$ (**1**) to see the effect of sterics and temperature on $\Delta S^{\ddagger}$.

**Table 2:** Data from Eyring plots for selected chromium compounds in $CDCl_3$

| Compound | $\Delta G^{\ddagger}$ (kcal/mol) | $\Delta H^{\ddagger}$ (kcal/mol) | $\Delta S^{\ddagger}$ (cal/mol·K) | Temp. (K) | Temp Range[a] |
|---|---|---|---|---|---|
| **2** | 18.6 ± 0.3 | 15.8 ± 0.3 | -9.4 | 302 | 47 |
| **30** | 16.9 ± 0.6 | 12.4 ± 0.4 | -16.4 | 274 | 37 |
| **12** | 14.5 ± 0.6 | 13.6 ± 0.3 | -3.3 | 245 | 43 |
| **20** | 13.2 ± 0.8 | 11.9 ± 0.3 | -6 | 217 | 36 |
| **6** | 12.8 ± 0.4 | 10.5 ± 0.3 | -10 | 233 | 30 |
| **1** | 13.1 ± 0.8 | 11.6 ± 0.3 | -5.1 | 226 | 27 |
| **1**[b] | 12.8 ± 0.6 | 12.4 ± 0.3 | -1.6 | 229 | 30 |

[a] The temperature range of the data points for the Eyring plots

[b] Thermodynamic data extracted from experiment performed in *d*-toluene

Table 2 shows thermodynamic terms for each compound in $CDCl_3$. Caution must be taken as the temperature ranges are quite narrow for both runs and since $\Delta S^{\ddagger}$ is extrapolated from the fit the errors are quite large.[21] Eyring plots for the selected compounds are in the selected text and figures section B1. The value -9.0 cal/mol·K was chosen for $\Delta S^{\ddagger}$ for all of the compounds because that number from Iodide is the largest temperature range and had the least

amount of error. The only exception was **31**, where the $\Delta S^{\ddagger}$ = –4.1 cal/ mol·K came from the LSA data.

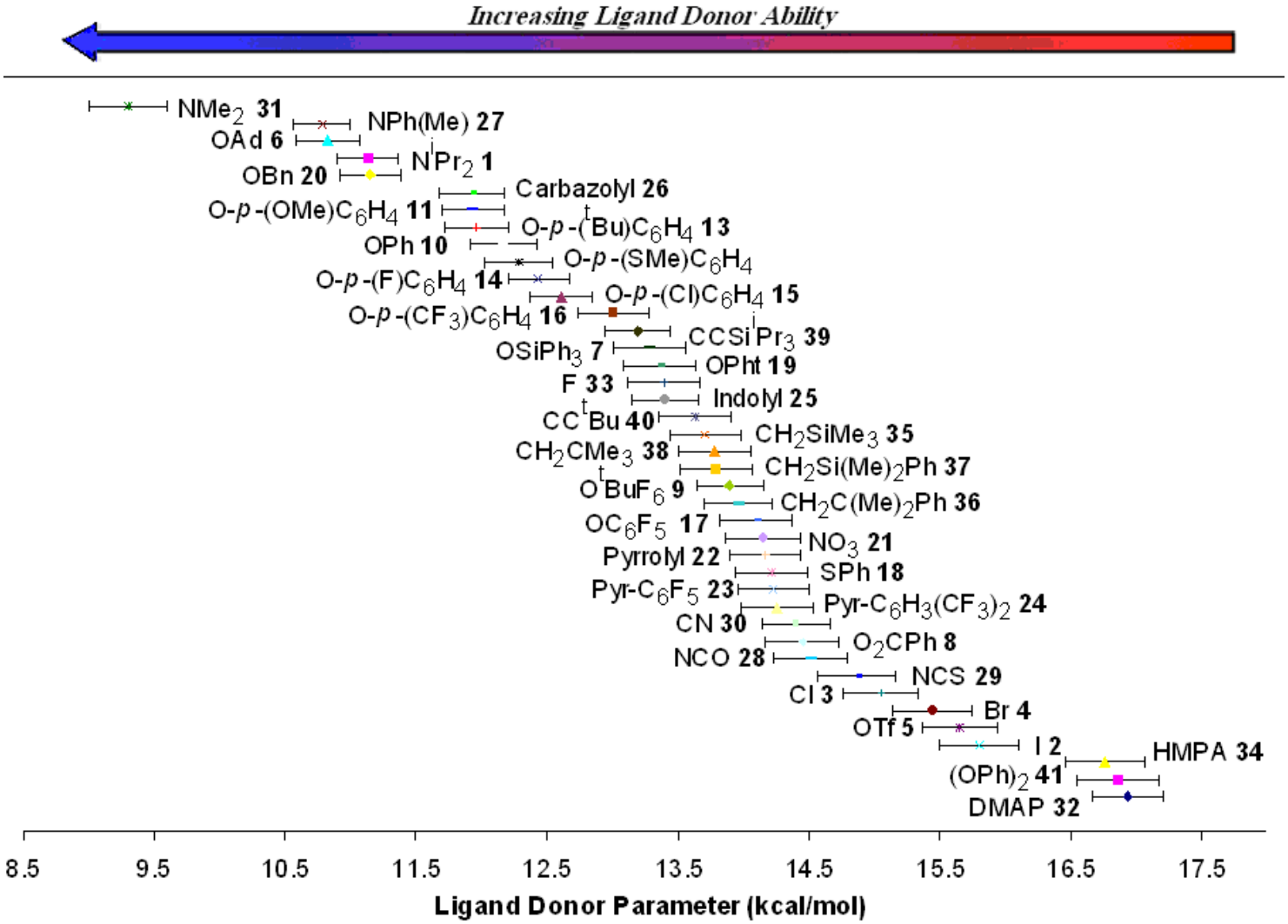


**Figure 3.11:** LDP (kcal/mol) values of $NCr(N^{i}Pr_2)_2X$ and the associated error

**Table 3:** Values for LDP (kcal/mol) for **1-41**

| X = | LDP |
|---|---|
| $NMe_2$ (**31**) | 9.34 ± 0.32[a] |
| OAd (**6**) | 10.83 ± 0.24 |
| N(Me)Ph (**27**) | 10.86 ± 0.23 |
| $NPr^i_2$ (**1**) | 11.12 ± 0.23 |
| OBn (**20**) | 11.15 ± 0.23 |
| Carbazolyl (**26**) | 12.04 ± 0.25 |
| O-*p*-$(OMe)C_6H_4$ (**11**) | 12.14 ± 0.24 |
| O-*p*-$(^tBu)C_6H_4$ (**13**) | 12.18 ± 0.25 |
| OPh (**10**) | 12.38 ± 0.25 |
| O-*p*-$(SMe)C_6H_4$ (**12**) | 12.51 ± 0.26 |
| O-*p*-$(F)C_6H_4$ (**14**) | 12.64 ± 0.23 |
| O-*p*-$(Cl)C_6H_4$ (**15**) | 12.81 ± 0.23 |
| O-*p*-$(CF_3)C_6H_4$ (**16**) | 13.00 ± 0.28 |
| $CCSi^iPr_3$ (**39**) | 13.19 ± 0.25 |
| $OSiPh_3$ (**7**) | 13.28 ± 0.27 |
| OPht (**18**) | 13.35 ± 0.23 |
| F (**33**) | 13.39 ± 0.27 |
| Indolyl (**25**) | 13.40 ± 0.25 |
| $CC^tBu$ (**40**) | 13.62 ± 0.27 |
| $CH_2SiMe_3$ (**35**) | 13.71 ± 0.27 |
| $CH_2CMe_3$ (**38**) | 13.78 ± 0.27 |
| $CH_2Si(Me)_2Ph$ (**37**) | 13.79 ± 0.28 |
| $O^tBuF_6$ (**9**) | 13.89 ± 0.26 |
| $CH_2C(Me)_2Ph$ (**36**) | 13.96 ± 0.26 |
| $NO_3$ (**21**) | 14.15 ± 0.29 |
| Pyr (**22**) | 14.16 ± 0.28 |
| SPh (**19**) | 14.22 ± 0.27 |
| $OC_6F_5$ (**17**) | 14.32 ± 0.28 |
| $Pyr^{C6F5}$ (**23**) | 14.33 ± 0.28 |
| $Pyr^{C6H3(CF3)2}$ (**24**) | 14.36 ± 0.28 |
| CN (**30**) | 14.40 ± 0.27 |
| $O_2CPh$ (**8**) | 14.45 ± 0.28 |
| NCO (**28**) | 14.51 ± 0.29 |
| NCS (**29**) | 14.86 ± 0.30 |
| Cl (**3**) | 15.05 ± 0.29 |
| Br (**4**) | 15.45 ± 0.30 |

**Table 3** (cont'd)

| | |
|---|---|
| OTf (**5**) | 15.75 ± 0.29 |
| I (**2**) | 15.80 ± 0.30 |
| HMPA[b] (**34**) | 16.76 ± 0.30 |
| $(OPh)_2$ (**41**) | 16.86 ± 0.32 |
| DMAP[b] (**32**) | 16.94 ± 0.27 |

[a]value determined in *d*-toluene

[b]counter ions

Foremost, compounds **2**, **3**, **4**, **21**, **28**, **29**, **30**, and **33** descend in order of donating ability, which follows the same trend seen in the spectrochemical series[22] of the same compounds. Unfortunately, it is not known whether $\sigma$ or $\pi$ donations dominate in bonding.

Looking at the carbon bound donors, the LDPs are within error of each other, have a narrow range, and follows the general trend of going from $sp^3$ to $sp$ agrees with stronger M—C bonds with increasing s-orbital participation. The bond distance between carbon and chromium for the alkynyls **39** and **40** is 1.996 and 1.978 Å respectively, much shorter than the $sp^3$-bound carbons which range from 2.041 to 2.085 Å. It is not known why $NCr(N^iPr_2)_2CCSi^iPr_3$ (**39**) is significantly different from the alkyls but not $NCr(N^iPr_2)_2CC^tBu$ (**40**). Unfortunately, no $sp^2$-bound carbon donors could be synthesized at this point in time. All routes led to decomposition, and $^1$H NMR showed products of $\beta$-hydride elimination.[12]

The pyrrolyl complex (**22**) and its derivatives show interesting and broader range of donor properties. For all cases, both $^1$H NMR and x-ray diffraction confirm that pyrrole is bound

$\eta^1$ through the nitrogen. Pyrrolyl was a far poorer donor than indolyl, which was a poorer donor than carbazolyl. This is consistent with the expected availability of the nitrogen lone pair for donation in these particular heterocycles. The pyrrolyl ring's aromaticity depends upon the nitrogen lone pair to reach the 6 $\pi$-electrons required by the Hückel rule for aromaticity. As a consequence, the aromatic stabilization energy of pyrrole directly competes with $\pi$-donation, which leads to pyrrole being a poorer $\pi$-donor.[23] For indolyl and even more so for carbazolyl, the aromaticity of the 5-membered heterocycles must compete with the 6-membered carbocycle(s) in resonance form contributions to the aromaticity.[24] As a result, the nitrogens in indolyl and carbazolyl seem to donate more strongly to the metal center than pyrrolyl because of the greater availability of their nitrogen-based lone pairs.

As for the substituted pyrrolyl ligands **23** and **24**, the LDP numbers are within error of pyrrolyl **22**. A recent study demonstrated that electron withdrawing groups on pyrrole ligands bound to a titanium center had faster rates of hydroamination that were significantly different.[25] This suggests that our system isn't sensitive enough to small differences of LDP between very similar ligands.

Small differences in donor ability can also be seen with the *para*-substituted phenoxide series. Only two phenoxides have LDPs significantly different, O-*p*-$(CF_3)C_6H_4$ (**16**) and O-*p*-$(OMe)C_6H_4$ (**11**), whereas the rest overlap in between. Looking at the series, the trend indicates that more electron-withdrawing groups in the *para* position the worse of a donor the phenoxide becomes. The effect of having more electron-withdrawing groups on the phenyl ring is more pronounced in the pentafluorophenoxide ligand (**17**), where the LDP is 14.32 kcal/mol.

The strongest donors appear to be the alkoxides and amides. Changes in the electron-withdrawing groups bound to the $\beta$-carbon can cause the oxygen of alkoxides to become a very poor donor as in the case of $O^tBuF_6$ (**9**). Change in the $\beta$-element from carbon to silicon, as in going from adamantoxide (**6**) to triphenylsiloxide (**7**), also results in a higher LDP. Silicon is known to be Lewis acidic and could be $\pi$ accepting from the oxygen lone pairs.[26] In the case of the amides, differences in the LDP may be more likely due to steric interactions. This difference will be discussed in more detail in Section 3.7.

Of interest to our group is how our system compares anionic to neutral donors. Neutral donors especially DMAP and HMPA have higher LPDs than most of ligands, although it is not yet known what affect the presence of a counter ion has on our measurements. More studies are on their way to follow up these questions.

In an attempt to place a tin alkyl onto the phenoxide, a ligand swap occurred and formed a bis(phenoxide) chromium nitrido complex **41**. Although, this complex has been synthesized and structurally characterized,[18] it was of interest to compare it with the rest of the series. With an LDP of 16.86 kcal/mol, it appears to be a worse donor. Replacing the second diisopropylamido ligand with a worse donor should cause the remaining diisoproplyamido to donate more strongly, hence a higher barrier of rotation.

As an interesting note, the $T_1$ values for the two peaks corresponding to the methynes differed by 36% requiring the use of the apparent $T_1$. Caution must be taken for this number because only one run was performed and the entropy for this compound may differ from the

current system with two amido ligands. Further study is needed, but this demonstrates that mono-diisopropylamido complexes can be studied with our system.

### 3.7 Sterics Investigation using Percent Buried Volume and Solid G

As one can imagine, the donor ability of a ligand can be affected by its size and shape. Investigation of sterics by Tolman's cone angle[27] provided researchers with valuable information for optimization of catalysts. Although the cone angle is useful for comparing steric interactions for phosphines, it fails when applied to more encompassing ligands such as NHCs[28] or pincer ligands.[29] In our study, sterics was investigated using two different parameters: Percent Buried Volume (%$V_{bur}$)[30] and Solid G.[31]

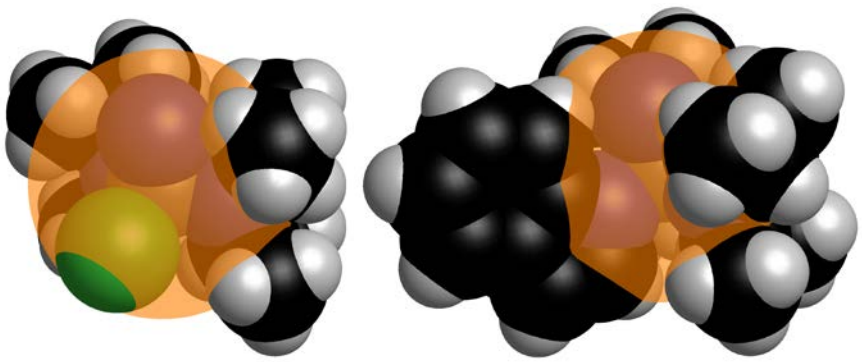

**Figure 3.12:** Space filling model of chloro **3** (left) and indolyl **25** (right) inscribed in a sphere that shows a radius of 3.5 Å

To determine %$V_{bur}$ of the ligands, crystallographic bond distances and angles were entered into Sam*V*ca, a web-based utility developed by Cavallo and co-workers.[30] A sphere encompasses the molecule starting from the metal center with a radius of 3.5 Å, which is the default radius set by the program, shown in Figure3.1.

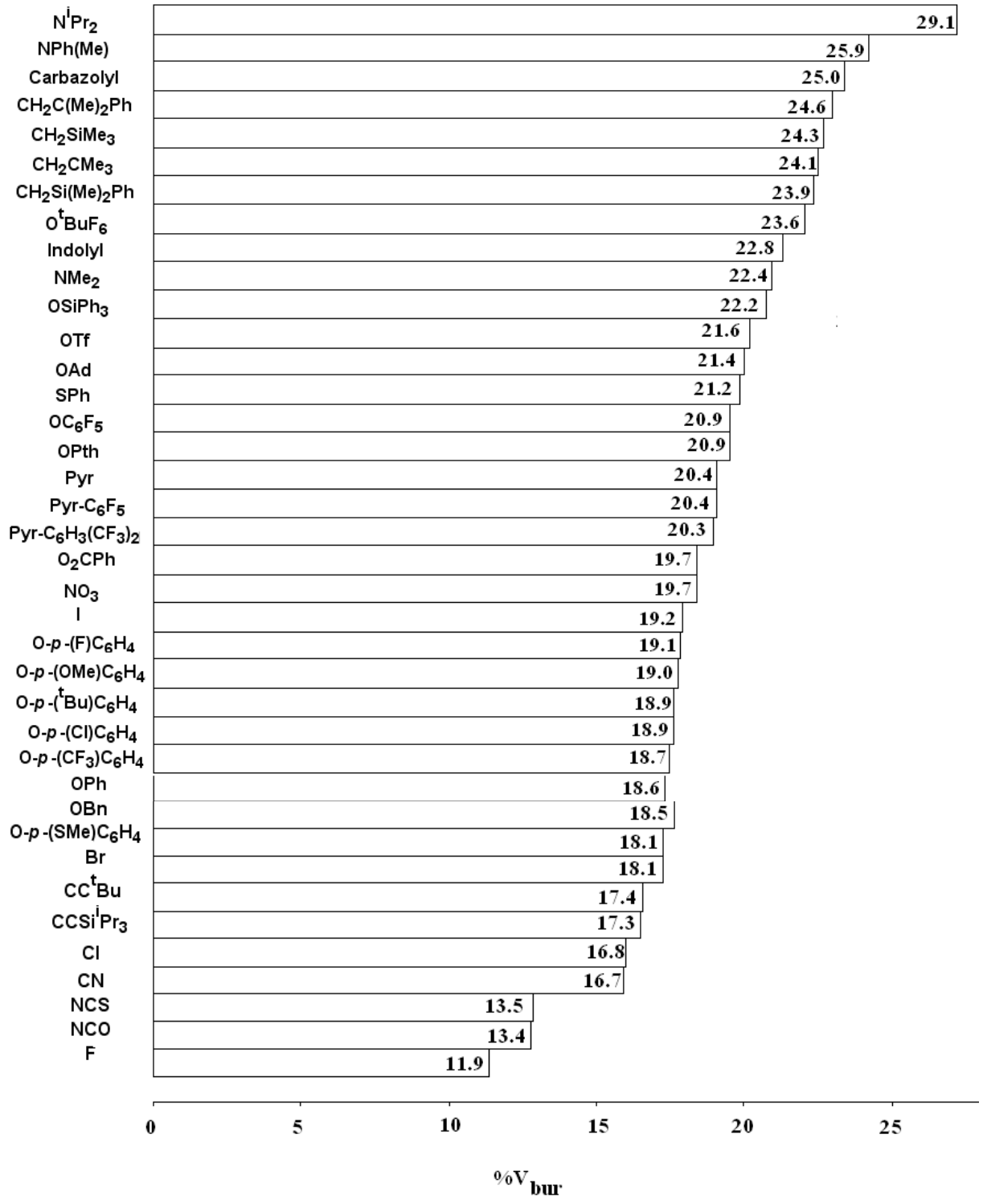


**Figure 3.13:** The %$V_{bur}$ for the ligands in this study. Values are for the percentage volume occupied by the ligand in a sphere of radius 3.5 Å from the chromium center.

Solid G treats the metal center as a point source of light and projects the shadows of the ligands onto a sphere larger than the molecule.[31] An example of the Solid Angle Model is shown in Figure 3.14 for indolyl **25**, where the molecule is in a similar orientation as in the right of Figure 3.12. The Solid Angle Parameters for the series of X ligands are shown in Figure 3.15. The *x*-axis values are in percentage of the sphere occupied by the X ligand.

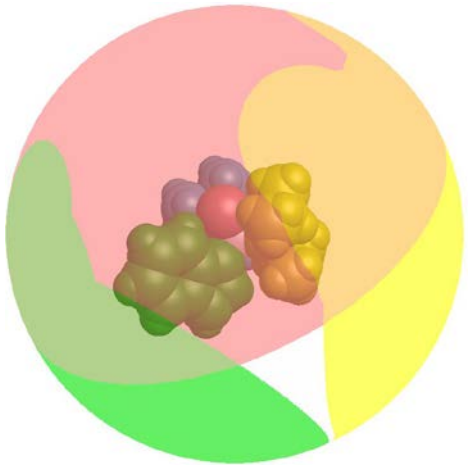

**Figure 3.14:** The Solid Angle Model from the Solid G program for **25** with indolyl (green), diisopropylamido (yellow and blue), and nitrido (red)

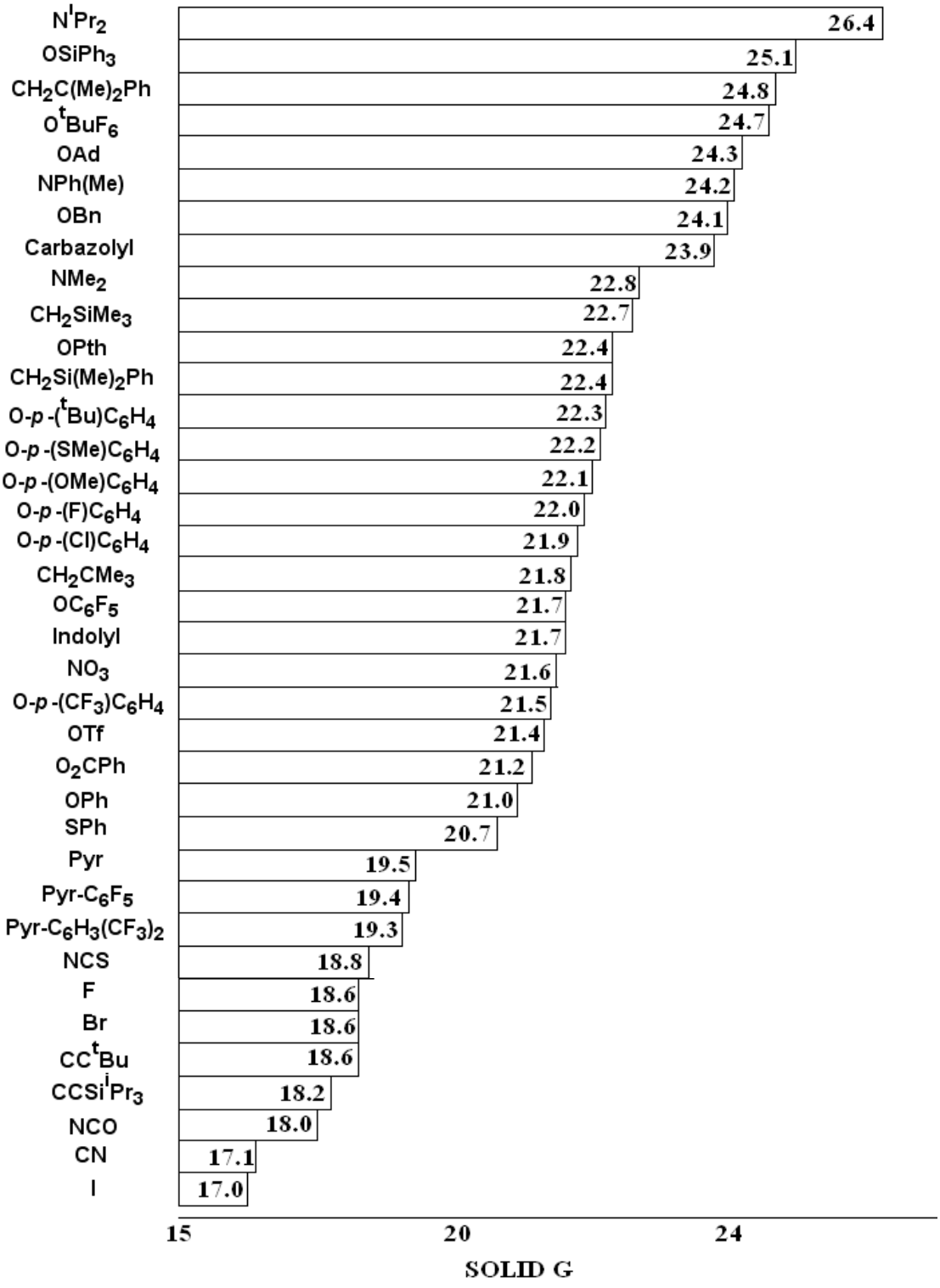


**Figure 3.15:** The percentage of the chromium coordination sphere shielded, $G_M(L)$, from the Solid G program for the ligands used in this study.

There are obvious differences in how the two methods, $\%V_{bur}$ and Solid Angle, describe the sterics in the chromium system. For example, the phenoxides and halides change order within the series between the two methods. The pyrrolyl ligands go from being very large in $\%V_{bur}$ to less sterically encumbering in Solid Angle. The perspective changes depending on the method used, but the amido ligands show the same trend in both methods. Smaller sterics may explain why the dimethyl amido is a much better donor than the bulkier di*iso*propylamido ligands.

Likewise, there is no obvious correlation between the donor abilities of the donor ligands with bond distances. For the chromium nitrido distance, the distance is similar for all of the complexes measured so far. For example, the nitrido distances in the poorly donating triflate **5**, strongly donating and relatively small benzyloxy **20**, and the large diisoproplyamido **1** were found to be 1.543(3), 1.543(2), and 1.544(3) Å, respectively. The Cr—N (nitrido) values range from 1.524(3) in nitrate (**21**) to 1.553(4) in O-*p*-$(CF_3)C_6H_4$ **16** for the whole series.

Steric factors seem evident in the tris(diisopropylamido) complex **1** according to other data (vide infra), but it is difficult to discern this from the X-ray diffraction studies alone. The average Cr—N (amido) distance in the published structure for **1** is 1.842(3) Å. This distance in **1** is somewhat larger than many of the derivatives prepared. For example, the average Cr–N(diisopropylamido) distances for a few derivatives are: Cl **3** 1.813(2), OBn **20** 1.823(1), OAd **6** 1.822(7), N(Me)Ph **27** 1.830(2), and OTf **5** 1.805(3) Å. However, the average diisopropylamido distance in **1** is very much in line with the sterically less encumbered $NMe_2$ **31** with average Cr–N distances of 1.842(4) Å; incidentally, **31** was one of the compounds examined that displayed full molecule disorder in the X-ray diffraction experiments. The disorder was fully modeled.

### 3.8 Comparison with the Literature

#### 3.8.1: LDP versus pKa Values of HX Compounds

How does our LDP compare with the literature? Many organometallic chemists gauge donor ability by checking the $pK_a$ of the free ligand. This quick check is reasonable in that a stronger acid, lower $pK_a$, will lose a proton better because the electrons in the conjugate base are more stable and donate less electron density. Whereas, a weaker acid, higher $pK_a$, has a stronger conjugate base that is less stable, therefore, has more electron density to donate.[32] Comparison of $pK_a$ in water[33] with LDP of the ligands is shown in Figure 3.16.

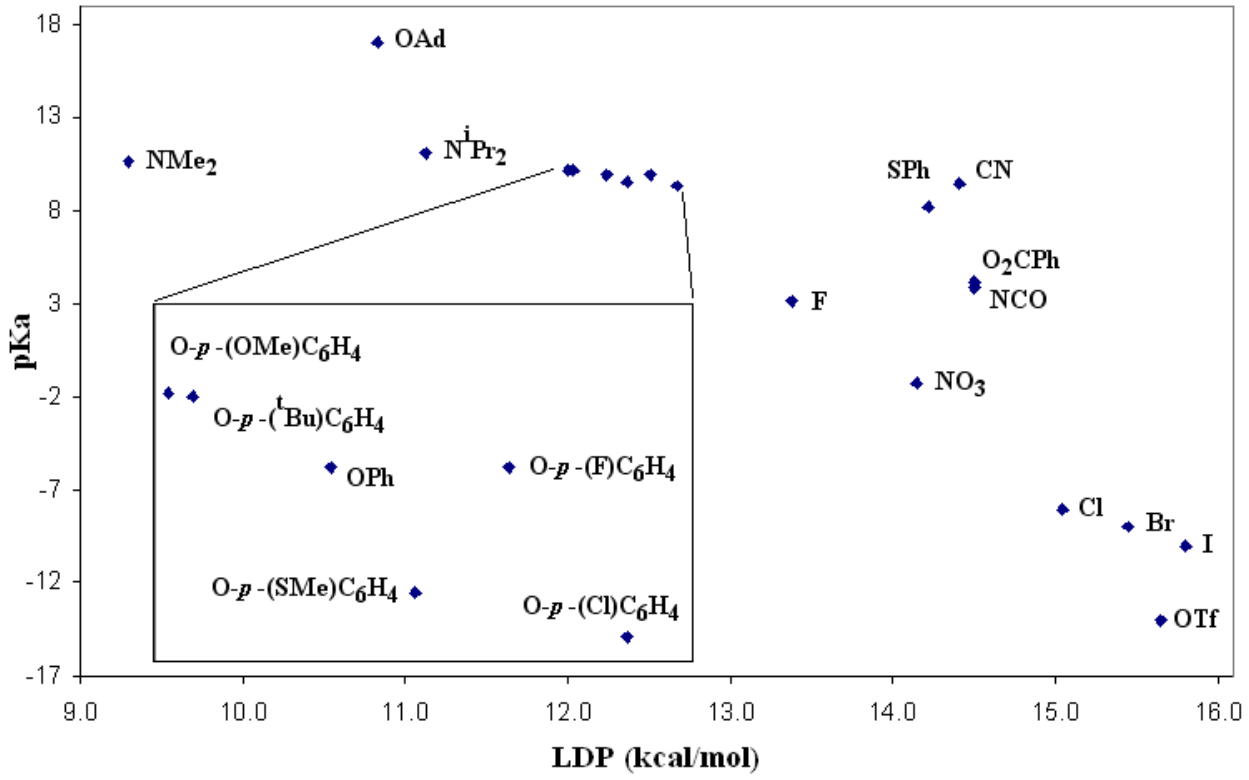


**Figure 3.16:** Plot of $pK_a$ in water versus LDP

As seen in Figure 16, $pK_a$ is at best a rough estimate for donor ability. Contributing resonance forms of a ligand that affect the $pK_a$ also affect donor ability. An explanation for why $pK_a$ does not correlate very well with LDP is that a proton bound to the ligand doesn't have $\pi$-orbitals to accept electron density from the lone pairs on the ligand, while chromium does.

### 3.8.2: LDP of Phenoxides versus Hammett Parameters

Hammett parameters are a proven method for evaluating electronic effects in aromatic systems. By studying the reaction rates and equilibrium constants of *para* and *meta*-substituted benzoic acid derivatives, the donating effect of the group in the *para* and *meta* position can be determined.[34] We were interested in seeing how the $\sigma_p$ of *para*-substitution would correlate with the substituted phenoxides.

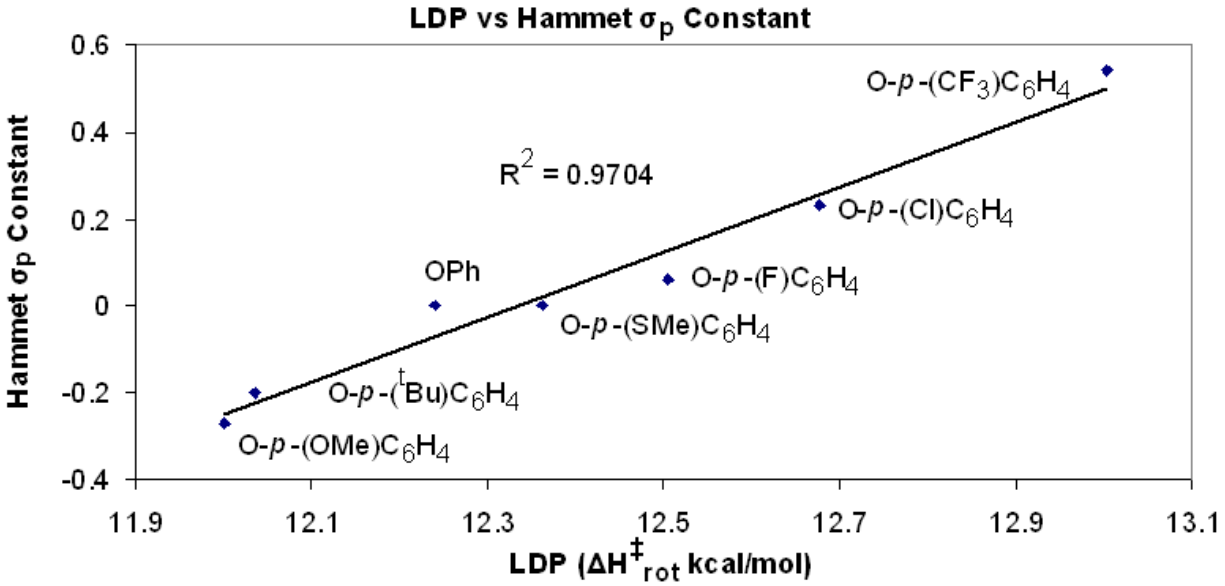


**Figure 3.17:** LDP versus Hammet parameters of the *para*-substituted phenoxides

In Figure 3.17, LDP is compared to the Hammett $\sigma$ parameter for para-substituted phenoxides. With the exception of **11** and **16**, phenoxides have LDP parameters that are within error of each other. The series of LDP versus the Hammett Parameters ($\sigma_p$) for the substituents reveals a linear correlation. This suggests our system has the ability to determine electronic effects on ligands.

### 3.8.3: LDP versus $^{13}$C NMR Chemical Shifts in Tungsten Metallacycles

In the past our group published a paper where a tungsten metallacycle was prepared to investigate carbonyl olefination.[35] It was observed that the W—C bond would range between double bond and single bond depending on the X ligand bound to tungsten. Changes in the X ligand directly affected the $^{13}$C NMR chemical shift of $C_1$, suggesting two contributing resonance forms occurring in the metallacycle (see Figure 3.18).

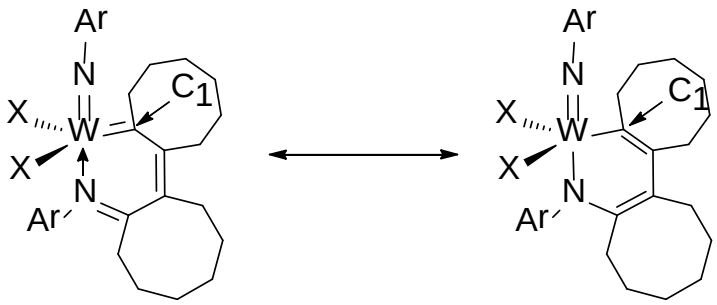


Ar = 2,6-di(*iso*-propyl)phenyl

X = OEt, O-*p*-(OMe)$C_6H_4$, $OC_6F_5$, Cl, OTf/Cl

**Figure 3.18:** Alkylidene-imine (left) and alkyl-amido (right) resonance forms

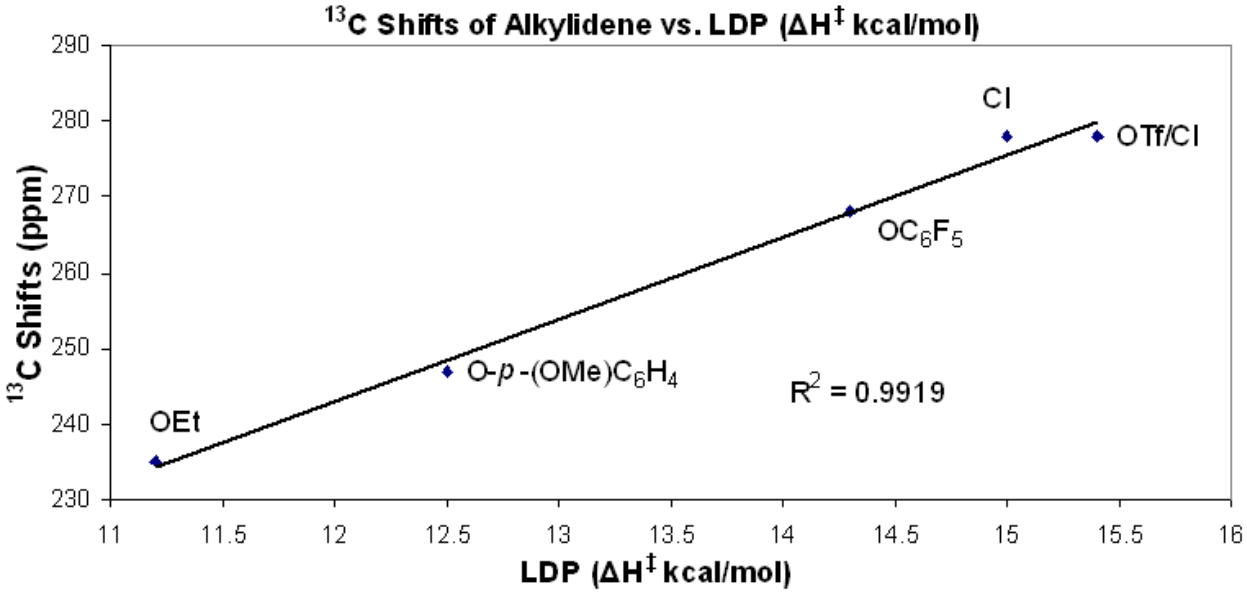


**Figure 3.19:** Alkylidene shifts of $C_1$ carbon versus LDP

Unfortunately, the paper only covered the synthesis and investigation of five compounds. But, there is good correlation between the X ligands studied using the $^{13}C$ NMR chemical shifts in the tungsten system and the LDP values of our chromium system. Although, we did not study a ligand containing an ethoxy group, we substituted the LDP value from OBn (**20**). Also, one tungsten metallacycle contained a mixture of Cl and OTf as ligands. In this case, we averaged the LDP values for Cl (**3**) and OTf (**5**).

### 3.8.4: LDP versus AOM Parameters of Cr(III) Complexes

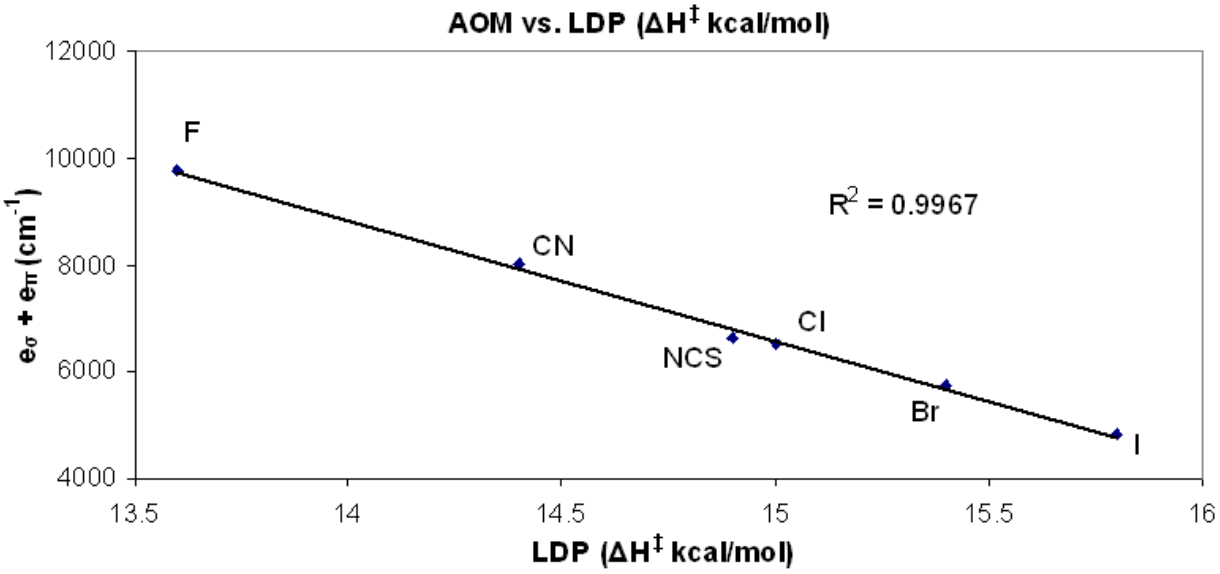


**Figure 3.20:** Plot of experimentally determined $e_\sigma + e_\pi$ values for Cr(III) complexes versus LDP

Donor properties of ligands can be determined using visible absorption spectroscopy to assign energy transitions. These values can be parameterized as $\sigma$ and $\pi$ donor energies, $e_\sigma$ and $e_\pi$ respectively, using the Angular Overlap Model (AOM).[36] There is a strong correlation shown in Figure 3.20 of AOM parameters versus LDP, but only when combining both $\sigma$- and $\pi$- effects.

### 3.8.5: LDP versus Values from Electronic Spectra of $Cp^*_2TiX$ Complexes

In 1996, Lukens, Smith, and Andersen[37] reported a "$\pi$-donor spectrochemical series for X" in $Cp^*_2TiX$ titanium-(III) compounds with a large number of X ligands. The study employed EPR and absorption spectroscopy to elucidate the electronic structure of $d^1$ titanium complexes. Of specific interest in the context of this paper, Andersen and coworkers reported a singly

occupied $a_1$ to $b_2$ energy gap, which "depends directly upon the $\pi$-donor ability of X". Mach and coworkers have since extended the system to include additional alkoxide ligands.[38]

A plot of the energy gap, $a_1$ (approximately nonbonding)[38] and the $b_2$ $\pi$-antibonding orbital ($\Delta E_{xz}$) in $Cp^*_2TiX$ Andersen complexes versus LDP for all X in common between the two studies is shown in Figure 3.21 (blue and red circles). In the case of X = OMe, the value for $\Delta E_{xz}$ was correlated with the LDP value for **20** in the plot (blue line). The obvious outlier is X = N(Me)Ph (red circle), which is well away from what seems to be a linear correlation between the $Cp^*_2TiX$ spectroscopic data and LDP. Andersen and coworkers centered much of their discussion on the differences between X = N(Me)Ph and the other compounds, and this is quite obvious in Figure 3.21 as well. Also plotted in Figure 3.21 are Mach's data (green squares) on $Cp^*_2TiX$, where we used our X = OAd data for their X = O$^t$Bu example.

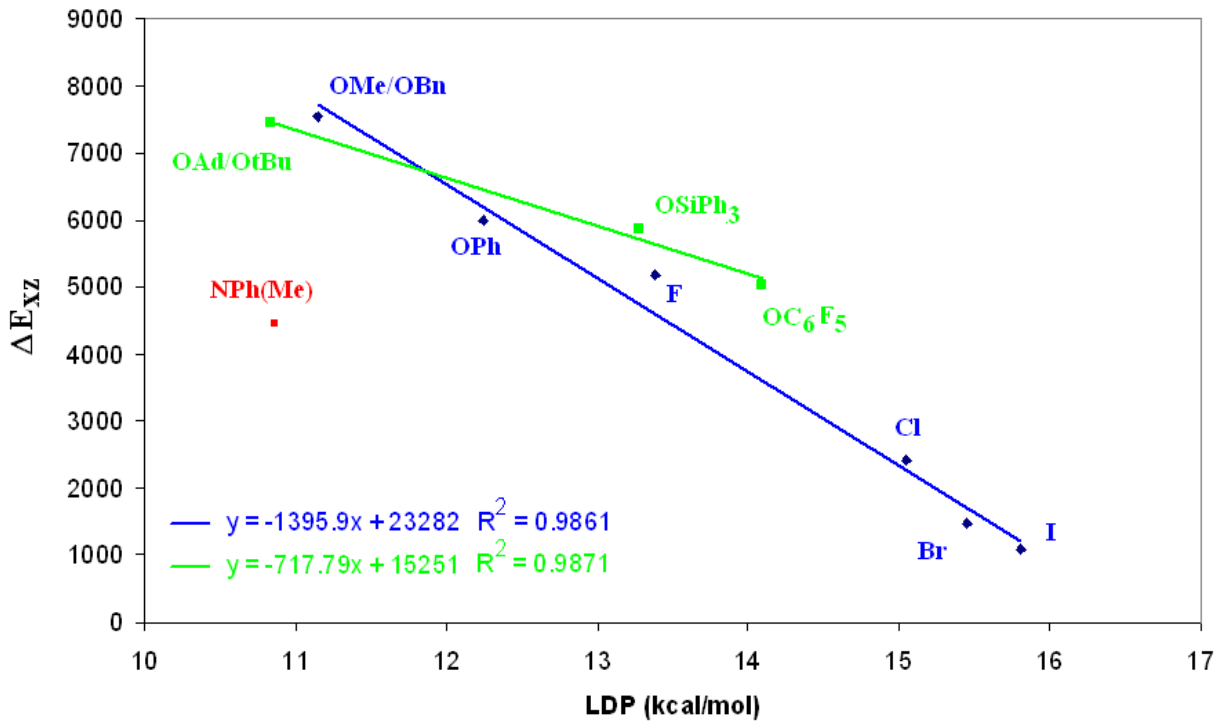


**Figure 3.21**. Plot of $\Delta E_{xz}$ in wavenumbers ($cm^{-1}$) [Andersen data[37] (red and blue squares), Mach's data[38] (green squares)] versus LDP (kcal/mol) for X. For the data represented by circles, methylcyclohexane was the solvent. The data represented by green squares were taken in either hexane or toluene. The data for X = NPh(Me) was not used in determining the linear fit to the Andersen data (blue line)

There are indications that the X = N(Me)Ph in $Cp^*_2TiX$ has little or no $\pi$-effects to the nitrogen; although there are indications of agostic effects to the methyl.[41] In the structure from X-ray diffraction, the $Cp^*$(centroid)–Ti–N–Me average dihedral in the X = N(Me)Ph complex is 86.9°. In other words, the large N(Me)Ph ligand rests in the plane bisecting the $Cp^*$-Ti-$Cp^*$ unit, and the nitrogen lone pair is orthogonal to the empty orbital of appropriate symmetry to act

as an acceptor. Consequently, the experimental Ti–N bond distance is quite long at 2.054(2) Å. This is similar to Ti–N(pyrrolyl) distances,[30] usually a much weaker donor than N(Me)Ph (vide supra). This distance is also much closer to the Ti–N single bond distance of 2.07 Å than the Ti=N distance of 1.77 Å using Pyykkö's radii.[39] In contrast, Ti–$NMe_2$ distances, where there is a strong dative $\pi$-bond, are typically ~1.90 Å.[40]

It can be concluded that the lack of correlation for X = N(Me)Ph is due to a deficiency of $\pi$-bonding in the $Cp^*_2TiX$ system due to steric effects that do not allow the amido to reach the electronically preferred geometry, as readily seen in both the X-ray diffraction study and in correlations with LDP.

The exact cause for the two different slopes of the Andersen and Mach data is unknown; however, there are several small differences in the data sets, solvents, slightly different instrumentation, and possible differences in concentration. In addition, the Andersen data are relative to $Cp^*_2TiH$ as $\Delta E_{xz} = 0$, and we did not adjust the baseline in the Mach data similarly. If the data from the two groups are taken all together and linearly fit, the line obtained is y = 20761 – 1205x with a much worse $R^2$ of 0.93 versus the $R^2$ = ~0.99 obtained fitting the data from the two groups independently. This fit for Mach's data is for only four points from the four new alkoxides in common between our study and Mach's reports. In addition, one of the four points was done with a substitution in the LDP value, *tert*-butoxide for 1-adamantoxide.

Overall, the LDP correlate fairly well with the $Cp^*_2TiX$ spectroscopic data in cases where steric effects are not apparent, i.e., all X ligands in common between the two studies except for where the X ligand is an amido derivative.

### 3.9 Conclusion

We have shown the versatility of our system. We can look at the donor properties of ligands that are anionic donors with and without lone pairs and neutral donors. Such a broad scope allowed us to compare ligands within a series, such as amides or phenoxides, and different ligands, such as halides versus alkoxides. These types of single parameter studies should not replace full mechanistic and computational studies for systems; instead this is a quick technique that will hopefully be useful for the discussion of properties and mechanisms for metal complexes in low *d*-electron counts.

We have demonstrated that there is good correlation with AOM, Anderson's data, and Hammett parameters. Although, there was poor overlap with pKa, our series appears to give insight into the donor properties of ligands and perhaps will be useful to research groups interested in catalyst design. Using steric parameterization, such as $\%V_{bur}$ and Solid G, may be required to gain a good understanding of the sterics in a system and they may impact donor ability. If another system under study does not correlate at all with LDP, there is any number of possible explanations ranging from differences in ligand donor properties, differences in metal acceptor properties, steric interactions, or simply a lack of correlation of the property being measured with ligand donor ability.

There are many avenues to explore with this system. The synthetic method used to synthesize the two neutral donors, DMAP and HMPA, should also work for placing phosphines and NHCs onto the chromium center. If that is possible, then we could see how the LDP of our ligands compare with the Tolman Electron Donating parameter.[27] But understanding the effect of the counter ion in the SSMT experiment is still under investigation. It would also be of interest

to see how the change in the metal affects the LDP of the ligands. Changes in orbital overlap may have a pronounced effect on the donor properties of the ligands.

The synthesis and study of **41** demonstrates the potential for studying the donor properties of bidentate or two different mono-anionic ligands with our chromium system. It would be of interest to see how sterics, ring strain, and conjugation on the metallacycle formed by the bidentate ligand affect LDP. Of special interest would be investigation of bidentate ligands that have a neutral and anionic donor component.

Parameterizations similar to ours have been successful in explaining reaction mechanisms and trends in activity. For example, Basolo, Pearson, Burdett, and many others used AOM to explain reactivity of later transition metal systems. Hopefully, LDP will be useful in ongoing catalytic studies in our group and on high valent metal complexes.

# REFERENCES

REFERENCES


1) (a) Jarek, R. L.; Flesher, R. J.; Shin, S. K. *J. Chem. Educ.* **1997,** *74*, 976-982 (b) Mann, B. E. *J. Magn. Reson.* **1977**, *25*, 91-94 (c) Dahlquist, F. W.; Longmuir, K. J.; Du Vernet, R. B. *J. Magn. Reson.* **1975**, *17*, 406-410 (d) Forsén, S. *J. Chem. Phys.* **1963**, *31*, 2892-2901

2) (a) Binsch, G. *J. Am. Chem. Soc.* **1969**, *96*, 1304-1309 (b) Allerhand, A.; Gutowsky, S. H.; Jonas, J.; Meinzer, R. A. *J. Am. Chem. Soc.* **1966**, *88*, 3185-3194 (c) McConnell, H. M. *J. Chem. Phys.* **1958**, *28*, 430-431

3) Vassilev, N. G.; Dimitrov, V. S. *Magn. Reson. Chem.* **2001**, *39*, 607-614 (b) Kessler, H.; Oschkinat, H. Griesinger, C. Bermel, W. *J. Magn. Reson.* **1986**, *70*, 106-133 (c) Bauer, C. J.; Freeman, R.; Frenkiel, T.; Keeler, J. Shaka, A. J. *J. Magn. Reson.* **1984**, *58*, 442-457

4) Drakenberg, T.; Dahlqvist, K.-I.; Forsén, S. *J. Phys. Chem.* **1972**, *72*, 2178-2183

5) Gaede, H. C. NMR Exchange Spectroscopy *Modern NMR Spectroscopy in Education*, Chapter 13, **2007**, 176-189

6) Bryant, R. G. *J. Chem. Educ.* **1983**, *60*, 933-935

7) (a) Hull, L. A. *J. Chem. Educ.* **1990**, *67*, 782-783 (b) Harris, Robin. Nuclear Magnetic Resonance Spectroscopy. London: Pitman Books Limited, 1983.

8) (a ) Lorigan, G. A.; Minto, R. E.; Zhang, W. *J. Chem. Educ.* **2001**, *78*, 956 (b) Jackman, L. M.; Cotton, F. A. Dynamic Nuclear Magnetic Resonance Spectroscopy; Academic Press: New York, 1975

9) Although, our samples were prepared in a dry box under $N_2$ atmosphere we took extreme precaution to obtain accurate data that had a limited number of reasons for introducing error into our experiment.

10) (a) Perrin, C. L., Johnston, E. R. *J. Magn. Reson.* **1979**, *33*, 619-626 (b) Mann, B. E. *J. Magn. Reson*. **1977**, *25*, 91-94

11) Yan, J.-L.; Mao, X.-A.; Shen, L.-F. *Chem. Phys. Lett*. **1997**, *272*, 278-283

12) Odom, A. L.; Cummins, C. C. *Organometallics* **1996**, *15*, 898-900

13) Forsén, S.; Hoffman, R. A. *J. Chem. Phys.* **1963**, *39*, 2892-2901

14) Klochkov, V. V.; Shaikhutdinov, R. A.; Khairutdinov, B. I.; Klimovitskii, E. N.; Findeisen, M.; Berger, S. *Appl. Magn. Reson.* **2003**, *24*, 97-103

15) (a) Laidler, K. J. *J. Chem. Educ.* **1984**, *61*, 494-498 (b) Laidler, K. J.; King, M. C. *J. Phys. Chem.* **1983**, *87*, 2657-2664 (c) Eyring, H. *J. Chem. Phys.* **1935**, *3*, 107-115

16) (a) Drakensberg, T.; Dahlqvist, K.-I.; Forsén, S. *Acta Chem. Scand.* **1970**, *24*, 694 (b) Van Geet, A. L. *Anal. Chem.* **1968**, *40*, 2227-2229

17) (a) Rablen, P. R.; Miller, D. A.; Bullock, V. R.; Hutchinson, P. H.; Gorman, J. A. *J. Am. Chem. Soc.* **1999**, *121*, 218-226 (b) Drakensburg, T.; Dahlqvist, K.-I.; Forsén, S. *J. Phys. Chem.* **1972**, *76*, 2178-2183

18) Odom, A. L.; Cummins, C. C. *Polyhedron* **1998**, *17*, 675-688

19) Drago, R. S.; Zink, J. I.; Richman, R. M.; Perry, W. D. *J. Chem. Educ.* **1974**, *51*, 371-376 (b) Drago, R. S.; Zink, J. I.; Richman, R. M.; Perry, W. D *J. Chem. Educ.* **1974**, *51*, 464-467

20) Harris, Robin. Nuclear Magnetic Resonance Spectroscopy. London: Pitman Books Limited, 1983

21) Isbrandt, L.; Tung, W. C.-T.; Rogers, M. T. *J. Magn. Reson.* **1973**, *9*, 461-466

22) Atkins, P.; Overton, T.; Rourke, J.; Welle, M.; Armstrong, F. Shriver and Atkins Inorganic Chemistry 4th Ed. New York: Freeman and Company, **2006**

23) Harris, S. A.; Ciszewski, J. T.; Odom, A. L. *Inorg. Chem.* **2001**, *40*, 1987-1988

24) (a) Hou, D.-R.; Wang, M.-S.; Chung, M.-W.; Hsieh, Y.-D.; Tsai, H.-H. G. *J. Org. Chem.* **2007**, *72*, 9231-9239 (b) Balaban, A. T.; Oniciu, D. C.; Katritzky, A. R. *Chem. Rev.* **2004**, *104*, 2777-2812

25) Swartz II, D. L.; Odom, A. L. *Organometallics* **2006**, *25*, 6125-6133

26) (a) Varga, V.; Císařová, I.; Gyepes, R.; Horáček, M.; Kubišta, J.; Mach, K. *Organometallics* **2009**, *28*, 1748-1757 (b) Damoun, S.; Langenaeker, W.; Van de Woude, G.; Geerlings, P. *J. Phys. Chem.* **1995**, *99*, 12151-12157

27) Tolman, C. A. *Chem. Rev.* **1977**, *77*, 313-348

28) Arduengo III, A. J.; Krafczyk, R.; Schmutzler, R. *Tetrahedron* **1999**, *55*, 14523-14534

29) (a) Azerraf, C.; Gelman, D. *Organometallics* **2009**, *28*, 6578- 6584 (b) Benito-Garagorii, D.; Kirchner, K. *Acc. Chem. Res.* **2008**, *41*, 201-213 (c) Yoon, M. S.; Ryu, D.; Kim, J.; Ahn, K. H. *Organometallics* **2006**, *25*, 2409-2411 (d) van der Boom, M. E.; Milstein, D. *Chem. Rev.* **2003**, *103*, 1757-1792 (e) Moulton, C. J.; Shaw, B. L. *J. Chem. Soc., Dalton Trans.* **1976**, 1020-1024

30) Clavier, H.; Nolan, S. P. *Chem. Commun.* **2010**, *46*, 841-861

31) Guzei, I. A.; Wendt, M. *Dalton Trans.* **2006**, 3991-3999

32) (a) Rahman, M. M.; Liu, H.-Y.; Prock, A.; Giering, W. P. *Organometallics* **1989**, *8*, 1-7 (b) Canty, A. J.; Lee, C. V. *Organometallics* **1982**, *1*, 1063-1066

33) (a) Fickling, M.M; Fischer, A.; Mann, B.R.; Packer, J.; Vaughan, J. *J. Am. Chem. Soc.* **1959**, *81*, 4226-4230 (b) R. D. Howells, J. D. Mc Cown *Chem. Rev.*, **1977**, *77*, 69–92 (c) Hall, H.K., Jr. *J. A.m. Chem. Soc*. **1957**, *79*, 5441 (d) Brownstein, S.; Stillman, A.E. *J. Phy. Chem*. **1959**, *63*, 2061-2062

34) Hansch, C.; Leo, A; Taft, R. W. Chem. Rev. 1991, 91, 165-195

35) Lokare, K. S.; Odom, A. L. *Inorg. Chem.* **2008**, *47*, 11191-11196

36) Hoggard, P. E. *Structure and Bonding* **2004**, *106*, 37-57

37) Lukens, W. W. Jr.; Smith III, M. R.; Andersen, R. A. *J. Am. Chem. Soc.* **1996**, *118*, 1719-1728

38) (a) Gyepes, R.; Varga, V.; Horacek, M.; Kubista, J.; Pinkas, J.; Mach, K. *Organometallics* **2010**, *29*, 3780-3789 (b) Varga, V.; Cisarova, I.; Gyepes, R.; Horacek, M.; Kubista, J.; Mach, K. *Organometallics* **2009**, *28*, 1748-1757

39) (a) http://www.chem.helsinki.fi/~pyykko/, 5/23/2011 (b) Pyykkö, P.; Atsumi, M. *Chem. Eur. J.* **2009**, *15*, 12770-12779

40) For example, amidobis[1,3-bis(trimethylsilyl)cyclopentadienyl]titanium(III) has a Ti–$NH_2$ distance of 1.933(3) Å. (a) Sofield, C. D.; Walter, M. D.; Andersen, R. A. *Acta Cryst. C* **2004**, *60*, 465-466. The compound $H_2NTiCp^*_2$ has a Ti–N distance of 1.944(2) Å. (b) Brady, E.; Telford, J. R.; Mitchell, G.; Lukens, W. *Acta Cryst C* **1995**, *51*, 558-591. Neither of these $NH_2$ complexes has a statistically significant difference in the Ti–N distance from the value in $Me(H)NTiCp^*_2$, however.

## Chapter 4: Hydroamination on a Solid Support

### 4.1: Hydroamination and Rationale for Surface Chemistry

Traditionally, imines are synthesized by condensation of an aldehyde or ketone with a primary amine.[1] Even in the presence of an acid or heat the scope of the reaction is limited. Generation of imines can be accomplished in an atom-efficient way through hydroamination of alkynes and primary amines using transition metal catalysts.[2] With this new methodology, we gain access to a variety of imines with specific frameworks and functional groups not accessible using traditional methods.[3] Many imines produced using transition metals can be used to generate new heterocycles found in pharmaceuticals and natural product synthesis.[4]

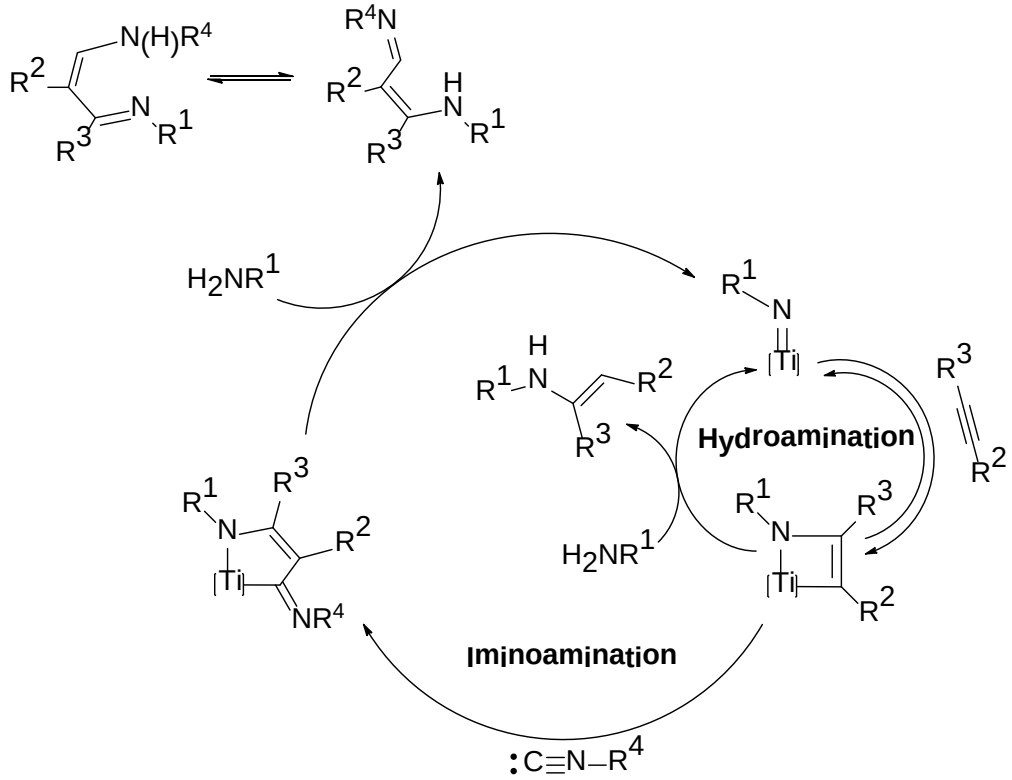


**Scheme 4.1:** Proposed mechanistic pathway for hydroamination and iminoamination

We believe that our catalytic cycle follows a similar mechanistic cycle as elucidated by Bergman.[5] Shown in Scheme 4.1, one equivalent of a primary amine will deprotonate 2 dimethylamido ligands and generate the imido titanium complex, the active catalyst. In the presence of an alkyne, [2 + 2]-cycloaddition occurs forming a 4-membered metallacycle that can be protolytically cleaved by another primary amine to generate an enamine with catalyst reformation.

Depending on other compounds present in solution the catalytic cycle may take a different route, and Iminoamination[2b] will occur with the addition of isonitrile. This 1,1-insertion of the isonitrile into the titanium-carbon bond forming a 5-membered metallacycle. In the presence of excess primary amine, the metallacycle is protolytically cleaved, regenerating the imido titanium catalyst and a tautormer of a 1,3-diimine. In some cases,[2b] excess isonitrile will result in 4-component coupling (4CC) products that can cyclize to form 2,3-diaminopyrroles.

A more recent study investigated the activity of a titanium hydroamination catalyst with ligand modification.[6] Evaluation of the 2-aryl substituted dmpm ligand was based on the rates of hydroamination. The results suggest that adding electron withdrawing substituents to the pyrroles made the titanium catalyst more active. Unfortunately, these active ligands are expensive to make, and it would be advantageous to make them reusable. This is one of the main driving forces for placing our catalyst on a surface.

Our approach to binding the titanium catalyst to the surface is to attach the selected ancillary ligand to a surface that will hold onto titanium. This method is commonly found in the literature.[7] The surface of choice for our titanium catalyst is polystyrene beads because of their

ease of use and the absence of functional groups, such as carbonyls, that could interfere with the activity of our catalyst.

This approach has many potential benefits; the current workup for hydroamination reactions involve removal of solvent through vacuum, distillation of product or column chromatography, and discarding of the catalyst. The last step is problematic, especially since the synthesis of the ligand was time intensive and expensive. By binding the elaborate ligand to a surface, it will be easily recovered and simplify the workup to removal of the catalyst by filtration and removal of solvent *in vacuo* to isolate the product. Not only is recovering the catalyst more efficient, but reduces the amount of waste produced.

Another issue with our catalyst is the lack of reactivity after cooling incomplete reactions. When the temperature of a reaction is cooled down to room temperature to check the progress of a reaction, the catalyst can not be reactivated by heating the reaction mixture. One explanation is that the titanium imido catalyst cannot re-enter the catalytic cycle when its cooled, because it forms stable dimers. These dimers are known to form throughout group 4 transition metals and could be very stable.[8] By binding the catalyst to a surface, the titanium will avoid dimerization, as in solution, and, hopefully, remain active after being cooled to room temperature.

**4.2: Synthesis of dmpm Ligand and Attachment to Polystyrene Beads**

We chose the dmpm ligand because it demonstrates some of the highest activity for hydroamination with titanium,[6] and the synthesis and workup is straightforward. The dmpm ligand is synthesized by reaction of pyrrole and acetone with 10 mol% TFA.[9] The condensation reaction needs to be covered if the experimental conditions require long reaction times because

pyrrole is known to polymerize and form mixtures of porphyrins in the presence of light and oxygen.[10]

After many attempts to place the dmpm ligand onto the surface, the most successful route was using Suzuki-Miyaura conditions to couple the dmpm ligand to polystyrene.[11] To accomplish this, the dmpm fragment needed to contain a halide. Therefore, we selected 4-bromoacetophenone as a ketone in our synthesis of $H_2$dmpmPhBr because Suzuki-Miaurya Coupling works better if the coupling partner is iodide or iromide and on an aromatic ring.[12]

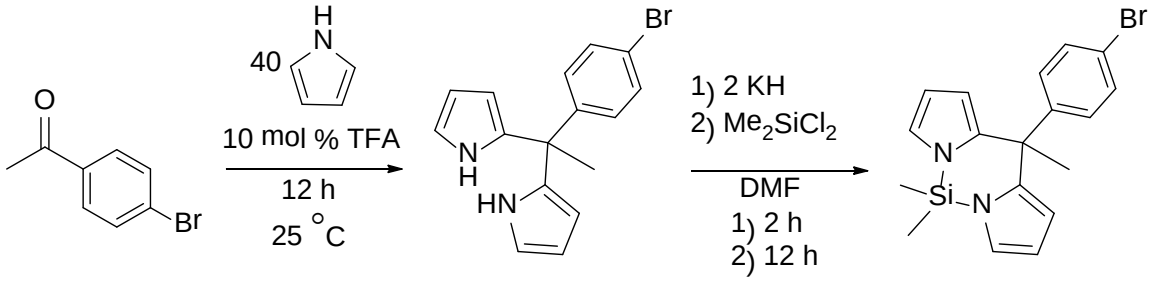


**Scheme 4.2:** Synthesis and protection of $H_2$dmpmPhBr

In control experiments it was found that the nitrogens on the dmpm ligand needed to be protected or else it will react with the palladium catalyst during the coupling reaction. Using a BOC group resulted in the formation of a very stable bridging carbonyl that could not be deprotected, even using TBAF at higher temperatures. Instead, pyrroles were protected with a bridging dimethyl silane using conditions found in the literature.[13] THF was investigated as a solvent for placing the $Me_2Si$ group on dmpm because it is more volatile and makes the workup easier than using DMF as the solvent. Unfortunately, this resulted in low yields, even when heated.

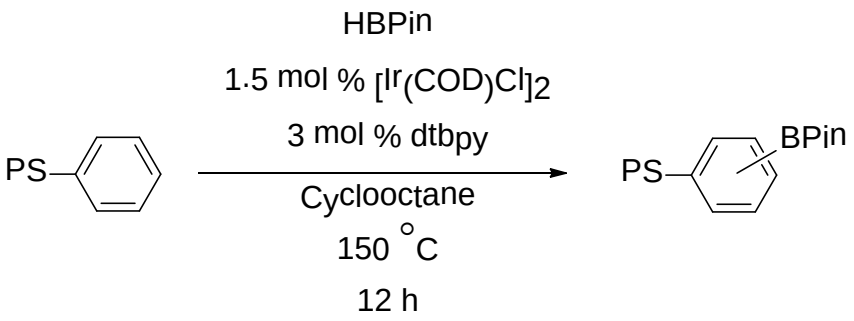


**Scheme 4.3:** Borylation of polystyrene resin

The coupling partner is the borylated polystyrene[14] beads made by adding iridium catalyst and HBPin at 150 $^{o}$C in cyclooctane. To get good borylation, the PS beads had to swell in cyclooctane for 12 hours.[15] Collection of the beads on a frit yielded grey beads that showed characteristic B—C and B—O stretches in the IR. To certify that the BPin group was bound to styrene and not free HBPin physisorbed in the polystyrene resin, the borylated beads were placed in a Soxhlet extractor and washed with dichloromethane overnight. No change in weight or in IR spectrum was observed after drying, indicating that the BPin was on the surface.

The optimum coupling conditions were determined to be refluxing the borylated beads with catalyst and OCdmpmPhBr under $N_2$ atmosphere in acetonitrile.[16] Again, better yields are obtained when the beads swell in the solvent for long periods of time, such as 6 h. As with the workup for the borylation, the beads were placed in a Soxhlet extractor and washed with dichloromethane to remove any starting materials. After drying under vacuum, the light-brown beads changed in weight. The absence of B—C and B—O stretches and the presence of N—C and C—O stretches in the IR suggests that the OCdmpmPh fragment was bound to the surface.

## 4.3: Experimental

### 4.3.1 General Procedure:

All reactions and manipulations were carried out in an MBraun glovebox under nitrogen atmosphere and/or using standard Schlenk techniques. Ethereal solvents, pentane, hexanes, toluene, acetonitrile, and benzene were purchased from Aldrich Chemical Co. and purified using alumina columns to remove water after sparging with dinitrogen to remove oxygen. 4-bromoacetophenone and dicyclobiphenylphophine were purchased from Sigma Aldrich and stored under $N_2$. *N*,*N*-dimethylformamide (DMF), dimethyldichlorosilane, and cyclooctane were purchased from Sigma Aldrich and distilled from $MgSO_4$ under $N_2$ atmosphere and stored under $N_2$. $[Ir(COD)Cl]_2$ and $Pd(OAc)_2$ were purchased from Strem Chemicals and stored under $N_2$ atmosphere before use. $K_2CO_3$, was purchased from Jade Scientific and used as received. HBPin was purchased from BASF and stored under $N_2$ atmosphere before use. The polystyrene resin was purchased from ChemPep, dried under vacuum, and stored under $N_2$ atmosphere before use. Trifluoroacetic acid (TFA) was purchased from EMD Chemicals and used as received. Spectra were taken on Varian instruments located in the Max T. Rogers Instrumentation Facility at Michigan State University. These include a UNITYplus 500 spectrometer equipped with a 5 mm Pulsed-Field-Gradient (PFG) switchable broadband probe and operating at 499.955 MHz ($^{1}H$) and 125.77 MHz ($^{13}C$), and a UNITYplus 300 spectrometer operating at 299.976 MHz ($^{1}H$). Samples for IR were prepared in Nujol form and collected on a Nicolet IR-42 Mid-IR spectrometer.

### 4.3.2 Synthesis of $H_2$dmpmPhBr

To a 250 mL Schlenk flask equipped with a stir bar was loaded with 4-bromo-acetophenone (3.0 g, 15 mmol, 1 equiv) and pyrrole (42 mL, 603 mmol, 40 equiv). The flask was covered and trifluoroacetic acid (0.12 mL, 1.5 mmol, 0.1 equiv) was added by syringe. After stirring for 12 h at room temperature, $Na_2CO_3$ (1.6 g, 15 mmol, 1 equiv) was added in 10 mL of water and stirred for 10 min until bubbling stopped. Both water and pyrrole were distilled off under vacuum leaving an oily brown solid. This oily solid was titrated with toluene and placed under vacuum 5 times to give an off-white solid. The product further purified by column chromatography [Alumina: $CH_2Cl_2$]. $^1$H NMR (500 MHz, $CDCl_3$, 25 $^o$C): 7.76 (br s, 2H), 7.37 (d, $J_{HH}$ = 9.0 Hz, 2H), 6.97 (d, $J_{HH}$ = 9.0 Hz, 2H), 6.67-6.65 (m, 2H), 6.17-6.15 (m, 2H), 5.94-5.92 (m, 2H), 2.01 (s, 3H). $^{13}$C NMR (127 MHz, $CDCl_3$, 25 $^o$C): 146.5, 136.8, 131.2, 129.3, 120.7, 117.2, 108.4, 106.5, 44.5, 28.7. MS *m/z* 316.

### 4.3.3: Synthesis of OCdmpmPhBr

Under a nitrogen atmosphere, a 250 mL Schlenk flask equipped with a stir bar was loaded with $H_2$dmpmPhBr (6.20 g, 19.7 mmol, 1.0 equiv.) and 50 mL of $CH_2Cl_2$. To this stirring solution was added $BOC_2O$ (10.7 g, 49.2 mmol, 2.5 equiv.) and DMAP (0.361 g, 2.96 mmol, 0.15 equiv.) as solids. Then triethylamine (2.75 mL, 18.7 mmol, 1.0 equiv.) was added and the flask was sealed and stirred for 16 h. The reaction was stopped and the solvent was removed *in vacuo* leaving behind an off-white solid. The solid product was dissolved in a minimum amount of ether (~7 mL) and was layered with pentane (~20 mL). This was placed in the fridge at –10 $^o$C to crystallize out over night resulting in a white solid. $^1$H NMR (300 MHz, $CDCl_3$, 25 $^o$C): 7.47

(m, 2H), 7.33 (d, $J_{HH}$ = 8.40 Hz, 2H), 6.98 (d, $J_{HH}$ = 8.7 Hz, 2H), 6.33-6.31 (m, 2H), 6.15-6.13 (m, 2H), 1.98 (s, 3H). MS m/z: 340.

### 4.3.4 Synthesis of ($Me_2Si$)dmpmPhBr

In a glove box, a 25 mL scintillation vial equipped with a stir bar was loaded with $H_2$dmpmPhBr (0.5 g, 1.6 mmol, 1 equiv) and DMF. The solution was chilled in a liquid nitrogen filled cold well. To this cold stirring solution was added KH (0.13 g, 3.2 mmol, 2 equiv). The mixture was allowed to warm to room temperature and stir for 2 h. This solution was cooled in a cold well, and to this cold stirring solution was added $Me_2SiCl_2$ (0.20 mL, 1.6 mmol, 1 equiv) in 2 mL of cold ether. The solution was allowed to warm to room temperature and stir for 12 h. The solution was pumped down, leaving a yellowish oil. $^1$H NMR (500 MHz, $CDCl_3$, 25 $^o$C): 7.25 (d, $J_{HH}$ = 14 Hz, 2H), 6.80-6.78 (m, 2H), 6.70 (d, $J_{HH}$ = 14 Hz, 2H), 6.44-6.42 (m, 2H), 6.35-6.32 (m, 2H), 1.95 (s, 3H), 0.082 (s, 6H). MS *m/z* 372.

### 4.3.5 Borylation of Polystyrene

In a dry box, a 500 mL 3-neck flask equipped with a stir bar was loaded polystyrene resin (3.00 g, 3.4 mmol, 1 equiv.) and 60 mL of cyclooctane. This was allowed to stir over night. To this stirring solution was added $[Ir(COD)Cl]_2$ (0.030 g, 0.45 mmol, 1.5 mol %) and di-*tert*-butylbipyridine (0.24 g 0.89 mmol, 3 mol %). The mixture stirred for 5 min. Then a solution of HBPin (3.12 g, 29.8 mmol, 1.0 equiv.) in 10 mL of cyclooctane was added. This was sealed, taken out of the dry box, and placed under a nitrogen atmosphere on the Schlenk line. A reflux condenser was attached to flask, and the solution was refluxed for 12 h at 150 $^o$C. The reaction mixture was cooled to room temperature and the beads were collected by filtration on a fritted

funnel. 10 mL aliquots of dichloromethane were added to the 3-neck flask and poured into the frit to remove any residual catalyst. The beige-colored resin was washed with 10 mL of deionized water followed by 20 mL of dichloromethane. The resin was then moved to a Soxhlet thimble and continuously rinsed with dichloromethane for 16 h to remove any traces of the iridium catalyst. The resin was carefully moved to a 10 mL round bottom flask and placed under a vacuum over night to remove any traces of solvent. (4.21 g, 9.52 mmol, 39% yield). IR: (Nujol, $cm^{-1}$) 1361.4 (B—O), 1140.9 (B—C).

### 4.3.6 Coupling of OCdmpmPhBr to BPin Resin

In a dry box, a 150 mL Schlenk flask equipped with a stir bar was loaded with BPin Resin (0.100 g, 0.787 mmol, 1.0 equiv.) and 20 mL of acetonitrile. The solution was allowed to stir for 4 h. To the stirring suspension was added $Pd(OAc)_2$ (0.009 g, 0.0394 mmol, 5 mol%), $PCy_2$Biphenyl (0.028 g, 0.0787 mmol, 10 mol%), OCdmpmPhBr (0.230 g, 0.787 mmol, 1.0 equiv.) and $K_2CO_3$ (0.115 g, 0.787 mmol, 1.0 equiv.). The flask was covered with a septum, taken out of the dry box, and placed under an $N_2$ atmosphere. A reflux condenser was attached that was connected to the Schlenk line. The suspension refluxed at 100 $^oC$ for 16 h. The reaction was cooled to room temperature. To the reaction was added water (~10 mL), and it was stirred for 10 min. The heterogeneous mixture was poured into a frit to collect the grayish-brown beads, which were washed with water (3 × 10 mL) and dichloromethane (3 × 10 mL). The beads were collected into a vial and dried under vacuum overnight. (0.1139 g, 0.340 mmol, 47% yield) IR: (Nujol, $cm^{-1}$) 1743 (C—O).

## 4.4: Conclusion and Future Work

Modifying the beads to couple a dmpm derivative to the surface has been shown to work. The groundwork has been laid for attaching a dmpm ligand to a surface. All that remains to be tested is adding the titanium catalyst and studying the catalyst under hydroamination reactions. These experiments are sure to reveal interesting aspects of hydroamination and answer some of the questions put forth in Section 4.1.

# REFERENCES

REFERENCES


1) (a) McMurry, J. Organic Chemistry 6th Ed. Brooks Cole, **2003** (b) Panunzio, M.; Zarantonello, P. *Org. Proc. Res. Dev.* **1998**, *2*, 49-59 (c) McNaught, A. D.; Wilkinson, A. *IUPAC Compendium of Chemical Terminology*, 2nd Ed. Oxford: Blackwell Scientific Publications, **1997**

2) (a) Reyes-Sánchez, A.; Cañavera-Buelvas, F.; Barrios-Francisco, R.; Vifeuentes-Vaca, O. L.; Flores-Alamo, M.; García, J. J. *Organometallics* **2011**, *30*, 3340-3345 (b) Barnea, E.; Majumder, S.; Staples, R. J.; Odom, A. L. *Organometallics* **2009**, *28*, 3876-3881 (c) Swartz, D. L.; Odom, A. L. *Organometallics* **2006**, *25*, 6125-6133 (d) Odom, A. L. *Dalton Trans.* **2005**, 225-233 (e) Cao, C.; Ciszewski, J. T.; Odom, A. L. *Organometallics*, **2001**, *20*, 5011-5013 (f) Johnson, J. S.; Bergman, R. G. *J. Am. Chem. Soc.* **2001**, *123*, 2923-2924 (g) Kim, Y. K.; Livinghouse, T.; Bercaw, J. E. *Tetrahedron Lett.* **2001**, *42*, 2933-2935 (h) Beller, M.; Thiel, O. R.; Trauthwein, H.; Hartung, C. G. *Chem. Eur. J.* **2000**, *6*, 2513-2522 (i) Kawatsura, M.; Hartwig, J. F. *J. Am. Chem. Soc.* **2000**, *122*, 9546-9547 (j) Weber, L.; Barlmeyer, M.; Quasdorff, J. M.; Sievers, H. L.; Stammier, H. G.; Neumann, B. *Organometallics* **1999**, *18*, 2497-2504 (k) Walsh, P. J.; Baranger, A. M.; Bergman, R. G. *J. Am. Chem. Soc.* **1992**, *114*, 1708-1719

3) (a) Nugent, T. C.; El-Shazly, M. *Adv. Synth. Catal.* **2010**, *352*, 753-819 (b) Ngai, M.-Y.; Barchuk, A.; Krische, M. J. *J. Am. Chem. Soc.* **2007**, *129*, 12644-12645 (c) Krska, S. W.; Zuckerman, R. L.; Bergman, R. G. *J. Am. Chem. Soc.* **1998**, *120*, 11828-11829 (d) Cantrell, G. K.; Meyer, T. Y. *J. Am. Chem. Soc.* **1998**, *120*, 8035-8042 (e) Cantrell, G. K.; Meyer, T. Y. *Organometallics* **1997**, *16*, 5381-5383

4) (a) Fustero, S.; Sánchez-Roselló, M.; Barrio, P.; Simón-Fuentes, A. *Chem. Rev.* **2011**, *111*, 6984-7034 (b) Chen, F-E.; Huang, J. *Chem. Rev.* **2005**, *105*, 4671-4706 (c) Kitajima, M.; Misawa, K.; Said, N. K. I. M.; Horie, S.; Hatori, Y.; Murayama, T.; Takayama, H. *J. Nat. Med.* **2006**, *60*, 28-35 (d) Sáéndez, C.; Salas, J. A. *Nat. Prod. Rep.* **2006**, *23*, 1007-1045 (e) Kitajima, M. *J. Nat. Med.* **2007**, *61*, 14-23

5) (a) Baranger, A. M.; Walsh, P. J.; Bergman, R. G. *J. Am. Chem. Soc.* **1993**, *115*, 2753-2763 (b) Walsh, P. J.; Baranger, A. M.; Bergman, R. G. *J. Am. Chem. Soc.* **1992**, *114*, 1708-1719

6) Swartz II, D. L.; Odom, A. L. *Organometallics*, **2006**, *25*, 6125-6133

7) (a) Guinó, M.; Hii, K. K. *Chem. Soc. Rev.* **2007**, *36*, 608-617 (b) Shin, J.; Jensen, S. M.; Ju, J.; Lee, S.; Xue, Z.; Noh, S. K.; Bae, C. *Macromolecules* **2007**, *40*, 8600-8608 (c) Lenaerts, P.;

Driesen, K.; Deun, R. V.; Binnemaus, K. *Chem. Mater.* **2005**, *17*, 2148-2154 (d) Benaglia, M.; Puglisi, A.; Cozzi, F. *Chem. Rev.* **2003**, *103*, 3401-3429 (e) Leadbeater, N. E.; Marco, M. *Chem. Rev.* **2002**, *102*, 3217-3274 (f) McNamara, C. A.; Dixon, M. J.; Bradley, M. *Chem. Rev.* **2002**, *102*, 3275-3300 (g) Iiskola, E. I.; Timonen, S.; Pakkanen, T. T.; Härkki, O.; Lehmus, P.; Seppälä, J. V. *Macromolecules* **1997**, *30*, 2853-2859 (h) Bonds Jr., W. D.; Brubaker Jr., C. H.; Chandrasekaran, E. S.; Gibbons, C.; Grubbs, R. H.; Kroll, L. C. *J. Am. Chem. Soc.* **1975**, *97*, 2128-2137 (i) Collman, J. P.; Hegedus, L. S.; Cooke, M. P.; Norton, J. R.; Dolcetti, G.; Marquardt, D. N. *J. Am. Chem. Soc.* **1972**, *94*, 1789-1790

8) (a) Lober, C.; Vendier, L.; *Inorg. Chem.* **2011**, *50*, 9927-9929 (b) DeKock, R. L.; Peterson, M. A.; Reynolds, L. E. L.; Chen, L-H.; Baerends, E. J.; Vernooijs, P. *Organometallics* **1993**, *12*, 2794-2805 (c) Walsh, P. J.; Hollander, F. J.; Bergman, R. G. *Organometallics* **1993**, *12*, 3705-3723 (d) Arney, D. J.; Bruck, M. A.; Huber, S. R.; Wigley, D. E. *Inorg. Chem.* **1992**, *31*, 3749-3755 (e) Thorn, D. L.; Nugent, W. A.; Harlow, R. L. *J. Am. Chem. Soc.* **1981**, *103*, 357-363

9) Lindsey, J. S.; Boyle, P. D.; O'Shea, D. R.; Wagner, R. W.; Hung, C. H.; Miller, M. A.; Littler, B. J. *J. Org. Chem.* **1999**, **64**, 1391-1396

10) (a) Zhang, X.; Zhang, J.; Song, W.; Liu, Z. *J. Phys. Chem. B* **2006**, *110*, 1158-1165 (b) Zhou, M.; Heinze, J. *J. Phys. Chem. B* **1999**, *103*, 8451-8457 (c) Baltazzi, E.; Krimen, L. I. *Chem. Rev.* **1963**, *63*, 511-556

11) Miyaura, N.; Suzuki, A. *Chem. Rev.* **1995**, *95*, 2457-2483

12) (a) LeBlond, C. R.; Andrews, A. T.; Sun, Y.; Sowa Jr., J. R. *Org. Lett.* **2001**, *3*, 1555-1557 (b) Suzuki, A. *J. Organomet. Chem.* **1999**, *576*, 147-168

13) Jolicoeur, B.; Chapman, E. E.; Thompson, A.; Lubell, W. D. *Tetrahedron* **2006**, *62*, 11531-11563

14) Shin, J.; Jensen, S. M.; Ju, J.; Lee, S.; Xue, Z.; Noh, S. K.; Bae, C. *Macromolecules* **2007**, *40*, 8600-8608

15) (a) Walsh, D. P.; Pang, C.; Parikh, P. B.; Kim, Y. S.; Chang, Y. T. *J. Comb. Chem.* **2002**, *4*, 204 (b) Sarin, V. K.; Kent, S. B. H.; Merrifield, R. B. *J. Am. Chem. Soc.* **1980**, *102*, 5463-5470

16) Billingsley, K. L.; Anderson, K. W.; Buchwald, S. L. *Angew. Chem. Int. Ed.* **2006**, *45*, 3484-3488

# APPENDICIES

APPENDICIES

## A1: Instructions for pw90 using Varian

The maximum signal produced from a length of a pulse described in microseconds is called the 90° pulse-width (pw90). The pw90 value is dependent on many factors including the type of nucleus, pulse power, preparation of research sample, NMR tube, and probe tuning. In most cases the default pw90 is sufficient to obtain data, but in the case of more advance experiments such as kinetics, it is crucial to get accurate data. The maximum signal where the signal to noise ratio is favorable is at the 90° pulse. Finding the 90° pulse is time consuming but a much easier method is finding a null point (360° pulse) in the spectrum of the peak of interest. Dividing this pulse number by 4 will give the desired 90° pulse.

1) Acquire a clean and well shimmed spectrum of your compound. If shimming is an issue, then tuning of the $^{1}H$ channel may be required.

2) Type **pw90?** (This reports the 90° pulse-width currently used as default. Remember this number.)

3) Type **array** (Allows you to set up an arrayed experiment.)

Then you will need to answer the following questions (highlighted in blue).

*Parameter to be arrayed:* **pw** (pw = pulse width)

*Enter number of steps in array:* **10** (this is the number of points to check for 360° pulse)

*Enter starting value =* **(4*pw90) – 1** (The pw90 is the number from step 2. In this case if your pw90 was 11, then the starting value you would be entering is 43. If you don't see a null point, pick a number smaller than the pw90 reported in step 2 and start over.)

*Enter array increment:* **0.5** (This is the point that a spectrum is taken of the sample. Although, larger increments can ballpark where the pw90 is located, smaller increments are required for obtaining accurate pw90.)

4) Type **pw[1]=1** (This will replace the first array with 1 $\mu$s pulse. This way the phasing will start off positive and the rest of the spectra should be inverted and slowly becoming positive with time.)

5) Type **da** (displays the array)

6) Type **ds** (display spectrum. Expand around the peak or peaks of interest.)

7) Type **gain='y'** (Turns automatic gain off which is not allowed in arrayed experiments.)

8) Type **d1=3** (Sets d1 to 3 seconds. This is the recycle delay that is seen in a pulse. See figure below. It is the time before the sample is pulsed. The d1 should be set to at least 1.5 times your $T_1$. If you don't have a feel for what the $T_1$ might be for your peak of interest you may have to play around with the $T_1$ determination to get an idea.)

9) Type **nt=2 time** (nt is the number of scans, which for most cases 2 or 4 scans should be fine. Typing time will tell you how long the run will take.)

10) Type **go**

Once the experiment is finished….

11) Type **ai** (absolute intensity, meaning is scales the peaks correctly)

12) Type **wft** (weighted Fourier transform)

13) Type **dssh** (display stacked plots horizontally You should get something that looks like what is shown in Figure A1.1.)

**Figure A1.1:** pw90 of **2** at 25 °C

14) Type **dssl** (Look for the spectrum with the lowest peak intensities that is close to a null where the peaks are going from negative to positive. This is your determined value.)

15) Type **pw90=your determined value/4** (for example, if the null point in the arrayed was associated with 44 then pw90=44/4.)

16) Type **pw=pw90** (resets the pw to the new pw90)

17) Type **pw?** (Checks to see what the current pw90 is set to)

18) Type **gain='n'** (Turns autogain on.)

19) Type **ga** (Obtain a new spectrum with the best signal to noise ration using the new pw90.)

**Trouble Shooting:**

Sometimes, when you search for a pw90 doing the arrayed experiment the peaks appear to relax back but then get inverted as shown in Figure 2.

**Figure A1.2:** Bad pw90 due to poorly tuned $^{1}$H channel

If this happens, it means that the $^{1}H$ channel was not properly tuned. Tuning the probe should fix this problem. Even when this doesn't happen it might be a good idea to check the instrument before doing the experiment.)

**A2: Instructions for $T_1$ Determination using Varian**

The Longitudinal or Spin Lattice Relaxation Time ($T_1$) is a time constant for the return of excited spins back to equilibrium. Knowledge of the $T_1$ of a signal of interest is important for the setup of some 1D and 2D NMR experiments. Determination of the $T_1$ will be done by the inversion recovery method. A 180° pulse will be applied to the sample and time between the 180° pulse and the 90° pulse (read pulse) will be incremented. The signals will be inverted and will begin to recover as the time between the 180° and 90° pulses are increased. Once signals are positive and the spins have reached their equilibrium magnetization then you can determine the $T_1$ value of the peak(s) of interest.

1) Obtain a clean and well shimmed spectrum of your sample using your pw90.
2) Type **gain='y'** (Turns off autogain for arrayed experiment.)
3) Type **fn=2*np** (Includes zero-filling to improve the spectrum.)
4) Type **ga**
5) Type **dot1** (Command to set up a $T_1$ experiment. You will be prompted to answer the questions highlighted in blue.)

*Enter the minimum $T_1$ expected (sec):* **0.5** (0.1 to 1 sec would be an okay starting point.)

*Enter the maximum $T_1$ expected (sec):* **3** (It might be a good idea to choose as large a range as possible the first time you do the experiment. Setting the minimum to 0.1 and maximum to 10 will give you an idea but the experiment might take a while.)

*Enter the number of transients:* **0.15** (The time the experiment will take. You can also set the time by typing **nt=the number of scans you want** and typing **go**.)

6) Type **dg** (Display parameters)

7) Type **ga**

8) After the experiment finishes, type **wft dssh**. (This Fourier Transforms your spectra and displays them horizontally. Your screen should look like what is shown in Figure A2.1. What you are seeing is the spins relaxing back to equilibrium as the increment of time (d2) between 180° pulse and the 90° pulse increases.)

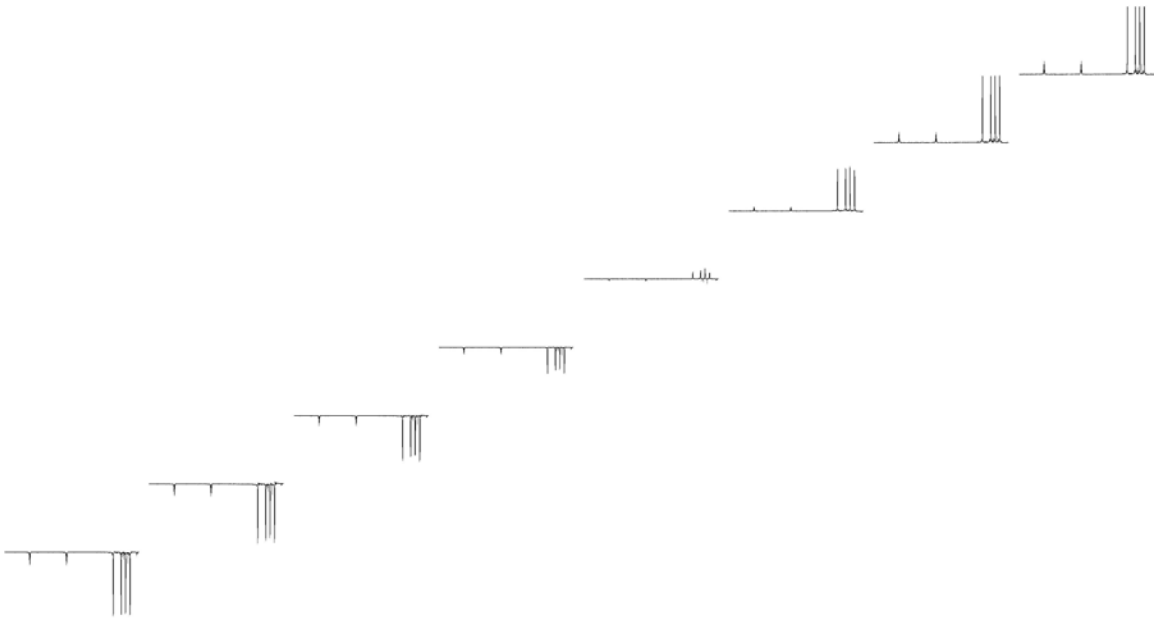

**Figure A2.1:** Spectra from $T_1$ experiment of $NCr(N^iPr_2)_2I$ (**2**)

9) Type **dssl** (This displays the numbered experiments. Look for the very last spectrum. In this spectrum the spins will have relaxed back to equilibrium.)

10) Type **ds(# of last spectrum)** (Displays the last spectrum in the arrayed experiment.)

11) Expand in on the peak(s) of interest and chose the threshold of the most middle of the peak. Therefore, if you have a septet, then set the threshold to include the middle and highest peak.)

12) Type **dll** (Displays the listed line frequencies and intensities.)

13) Type **fp** (Measure the intensity of each line in dll listing in arrayed spectra.)

14) Type **t1** (Performs a $T_1$ determination using exponential curve fitting. If you type **expl(# of selected line)**, you will see a graph similar to the one shown in Figure A2.2. The $T_1$ is determined from the equation of the line from plotting the intensity of the peaks (magnetization/intensity) versus time.

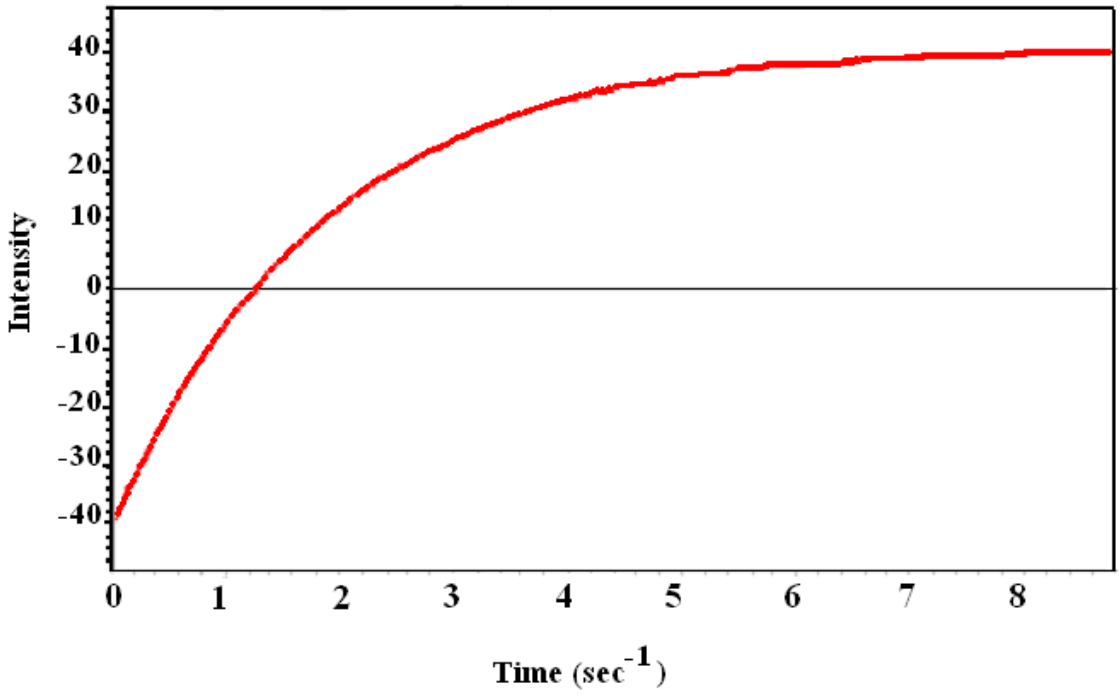


**Figure A2.2:** $T_1$ determination from magnetization versus time plot of **2**

15) Type **printon t1 printoff** (This will print the $T_1$ values of the peaks selected along with the error in the $T_1$ values based on the fit of the curve.)

**A3: Instructions for SSMT Experiment using Varian**

Spin saturation magnetization transfer is an NMR technique used to determine the exchange rate between nuclei that have two distinct chemical shifts that still experience exchange in the slow regime on the NMR timescale. Two experiments will be performed: first, one of the exchanging peaks will be irradiated and second, it will not be irradiated. The difference in height of the observed peak experiencing exchange will be recorded. Combining the $T_1$ and the change in magnetization (peak integration) rate for the exchange can be determined. Since the rate of exchange is very dependent on temperature it is required that the sample equilibrates to the desired temperature for at least ten minutes before beginning the experiment.

First, turn the spinning off and acquire a quality $^1$H spectrum of the sample. It is important to turn the spinning off because NOE can contribute to the transfer of magnetization.

1) Choose the option **Presat** from the menu.
2) Type **satdly= #** (set satdly equal to at least $5 \times T_1$)
3) Type **satpwr=-4** (satpwr is the amount of energy going into the sample to irradiate the peak; if satpwr is too high it will saturate the other peak)
4) Type **pw90= #** (set pw90 to the value determined in the first experiment)
5) Type **dps** (dps is display pulse sequence to make sure everything is set up correctly for experiment)

6) Type **ds** (ds is display spectrum)

7) Type **aph vsadj** (to see the whole spectrum and expand upon the region of exchange)

***A special note:** When expanding around two peaks experiencing exchange, it is important to give enough room on both sides of the peaks that is greater than the distance between the two peaks experiencing exchange. The reason for this is that if the window is too small and the offsite peak is set by the computer it will choose the left most position the cursor sees on the screen, which is the end of the screen. If the offsite point is not equally distant from the peak experiencing exchange then the irradiation will be offset and contribute to error in the peak integration.

8) Place the cursor on the right peak. Type **sd** (sd = set decoupler frequency)

9) Place the left cursor on the left peak and the right cursor on the right peak that are experiencing exchange. See Figure A3.1.

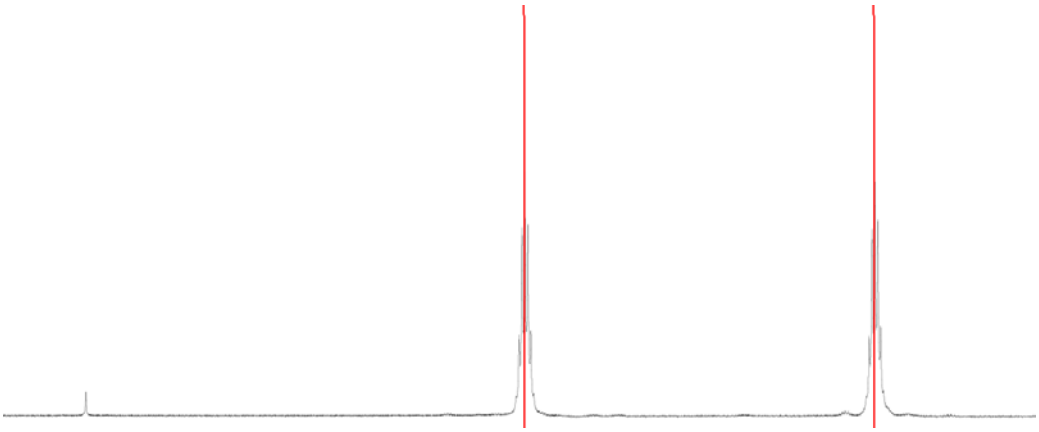

**Figure A3.1:** Placing right and left cursors on septets belonging to **2**

10) Type **cr=cr+delta** (This moves the cursors to the left of the left most peak that is equal to the distance between the two exchanging peaks. This is done to account for decoupler spillover. See Figure A3.2.)

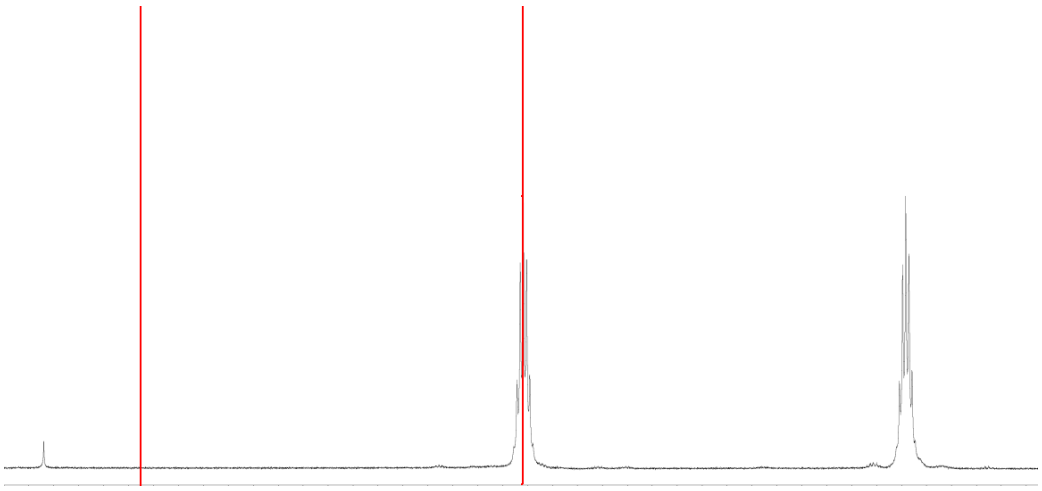

**Figure A3.2:** Setting offsite point equidistant from the septet for saturation

11) Type **sda** (Sets the decoupler to the new offsite saturation frequency.)

12) Type **gain='y'**

13) Type **da** (Displays saturation frequencies set for the peaks.)

14) Type **satfrq=value,value** (Enter the two saturation frequencies listed from typing da.)

15) Type **dof=0** (Sets decoupler to a single frequency, but not be used during experiment.)

16) Type **ss=-2** (ss=steadystate, allows for relaxation back to equilibrium before making scans.)

17) Type **nt= #**

18) Type **go** or **ga**

**B1: Eyring Plots for Selected Chromium Nitrido Complexes**

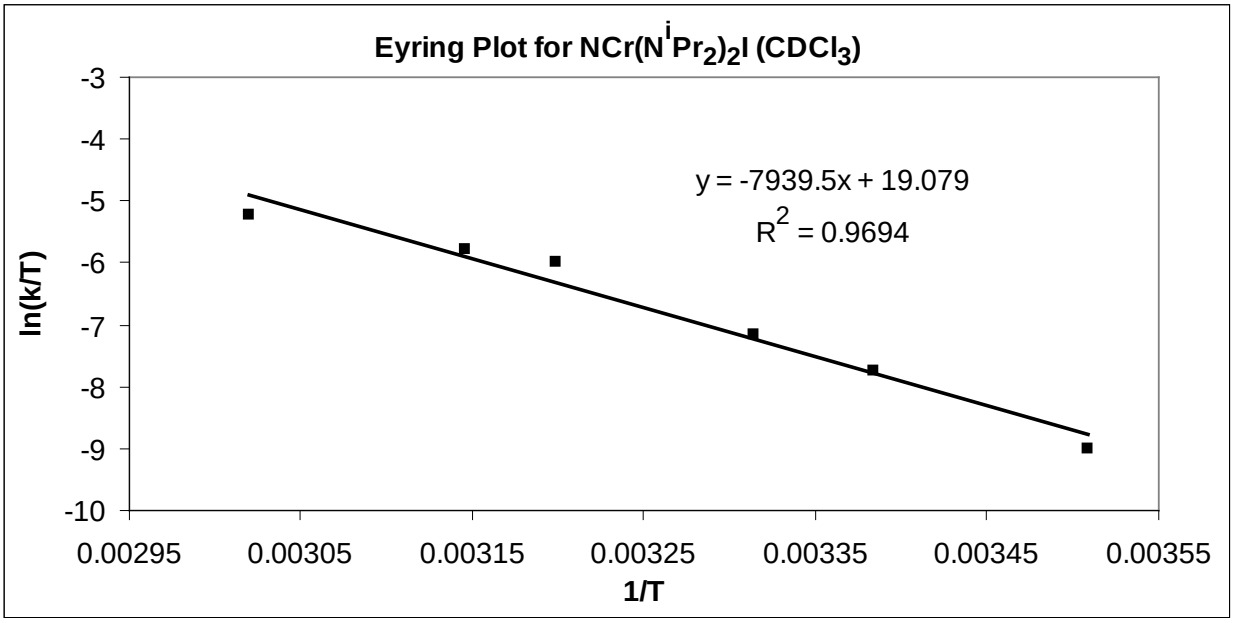


**Figure B1.1:** Eyring Plot of **2**

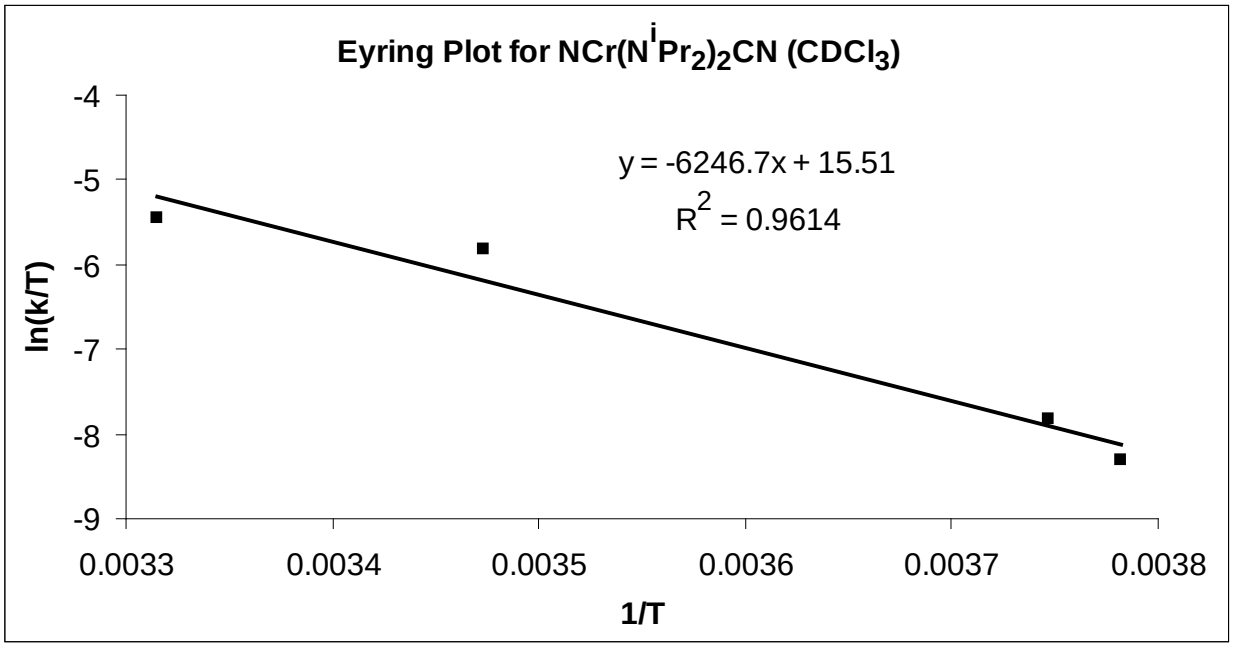


**Figure B1.2:** Eyring Plot of **30**

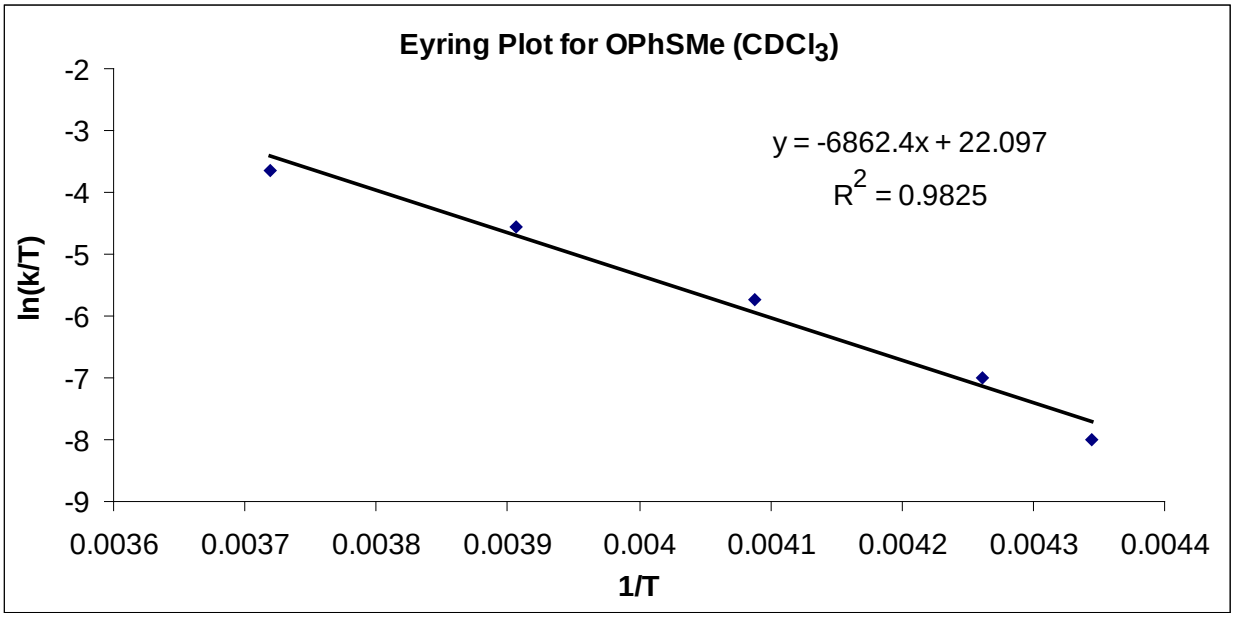


**Figure B1.3:** Eyring Plot of **12**

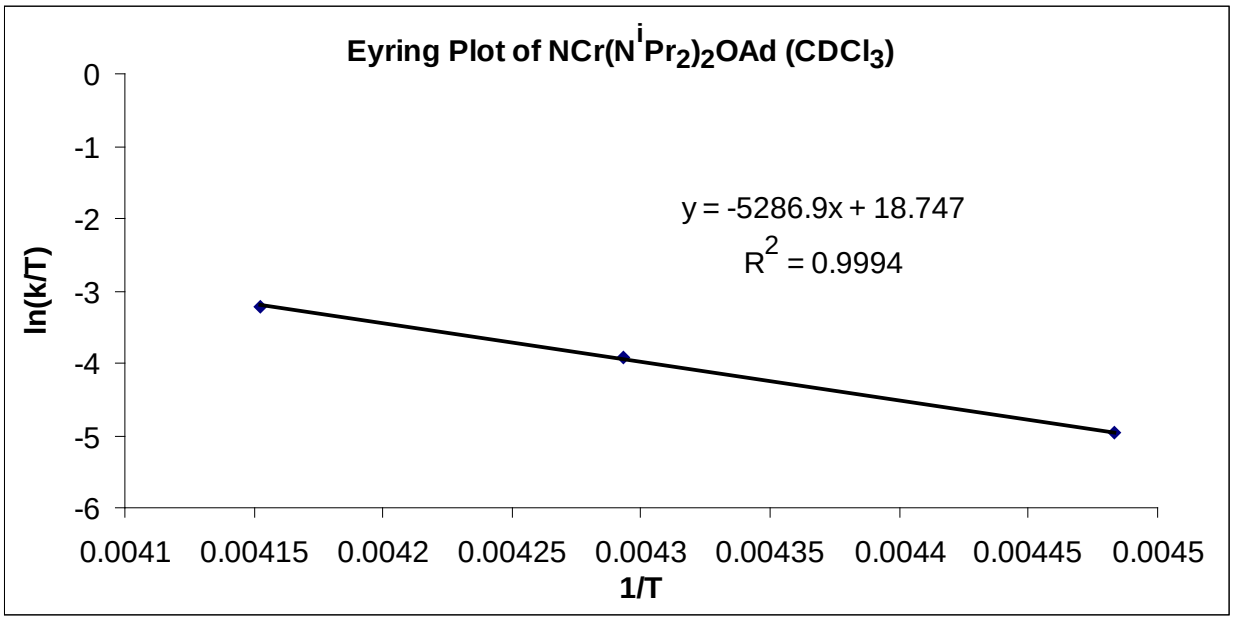


**Figure B1.4:** Eyring Plot of **6**

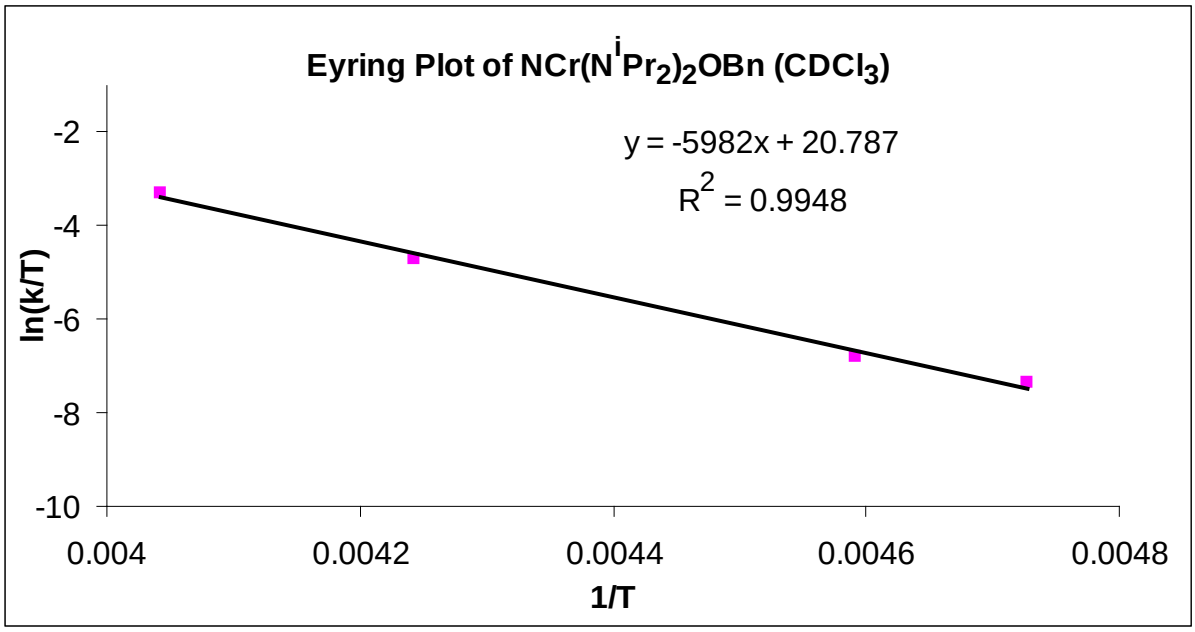


**Figure B1.5:** Eyring Plot of **20**

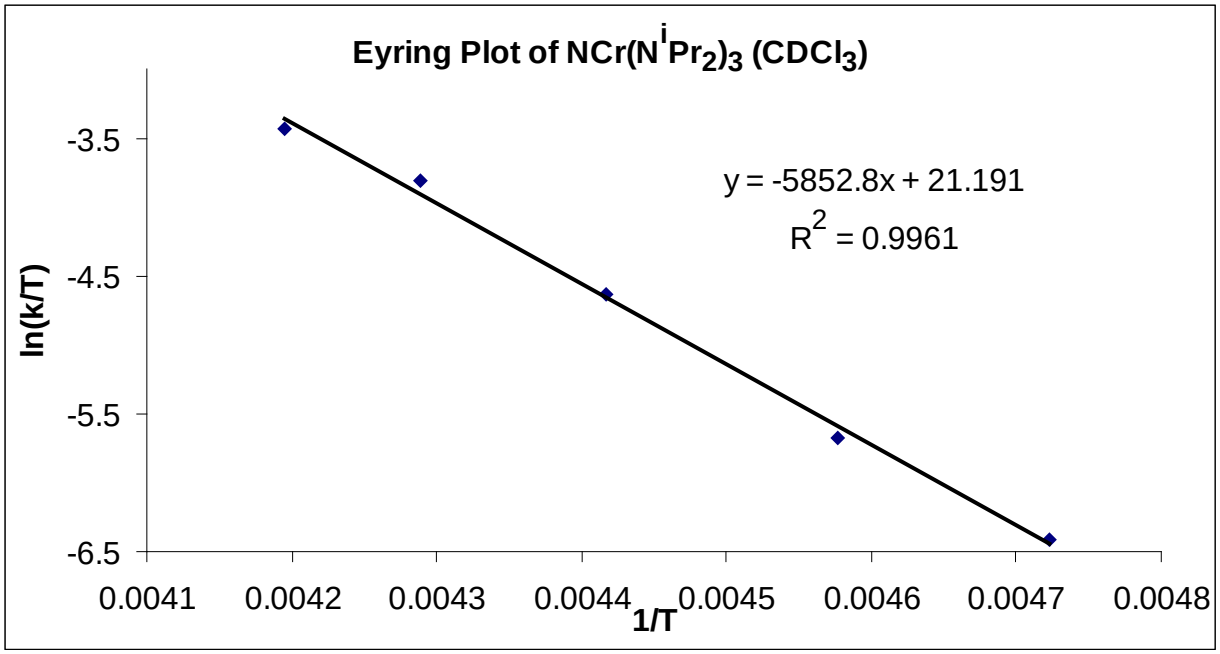


**Figure B1.6:** Eyring Plot of **1**

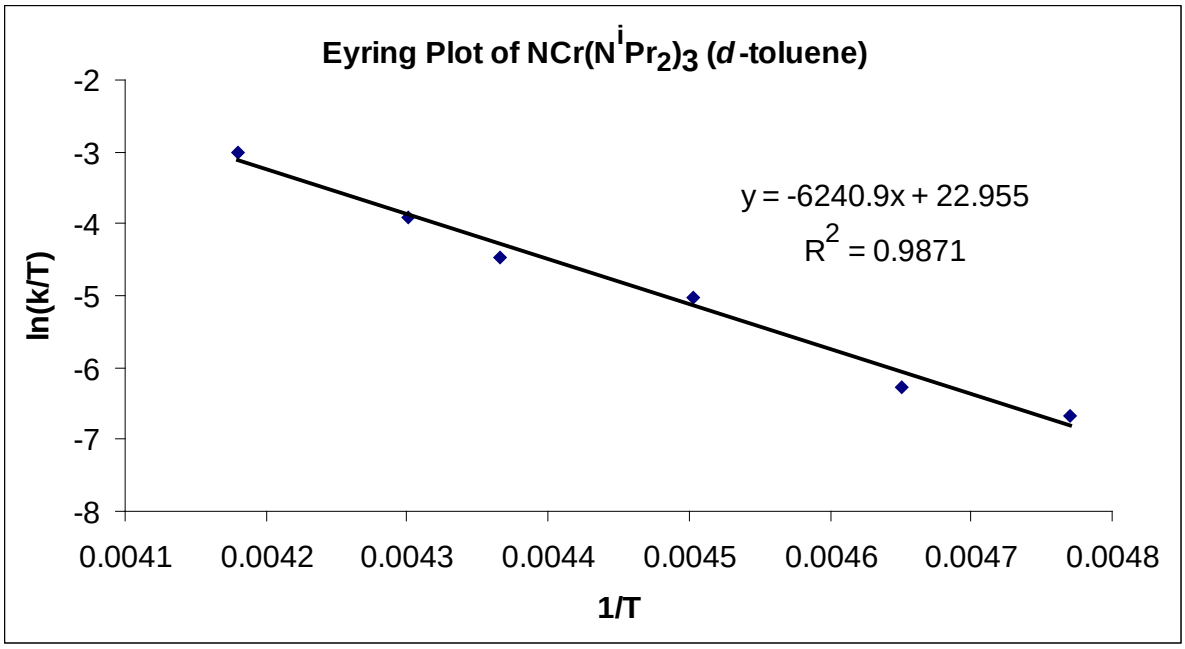


**Figure B1.7:** Erying Plot of **1** in *d*-toluene

**C1: Error Equations for SSMT**

The equation for relating the experimental observables to the rate constant, k, is Eqn 1 below. In Eqn 1, $M_{OA}$ is the integral before irradiation, which is set to 100, and $M_A$ is the observed integral after irradiation. The $T_1$ is found using the inversion recovery method, and the error in $T_1$ is calculated by Varian software VNMR 61c or VNMR J22d, both software gave similar results. The error in integration was set to 0.1 with the integration of the peak before irradiation set to 100. The error in temperature, $\varepsilon_T$, was ±1 ºC. The propagation of error in the system, error in k ($\varepsilon_k$), is found using Eqn 2.

$$k = \frac{1}{T_1}\left(\frac{M_{0A}}{M_A} - 1\right) \quad (1)$$

$$\varepsilon_k = k\sqrt{\left(\frac{\varepsilon_{1/T_1}}{T_1}\right)^2 + \left(\frac{\varepsilon_{M_{0A}/M_A}}{M_{0A}/M_A}\right)^2} \quad (2)$$

Where, $\varepsilon_{1/T1}$ and $\varepsilon_{MOA/MA}$ are found using Eqns 3 and 4, respectively.

$$\varepsilon_{1/T_1} = \frac{1}{T_1}\sqrt{\left(\frac{\varepsilon_{T_1}}{T_1}\right)^2} \quad (3)$$

$$\varepsilon_{M_{0A}/M_A} = \sqrt{\left(\frac{\varepsilon_{M_{0A}}}{M_{0A}}\right)^2 + \left(\frac{\varepsilon_{M_A}}{M_A}\right)^2} = \sqrt{1\times10^{-6} + \left(\frac{0.1}{M_A}\right)^2} \quad (4)$$

The free energy of amido rotation was found using Eyring equation in the form shown in Eqn 5. The error in $\Delta G$ was calculated as shown in Eqn 6.

$$\Delta G = RT\ln\left(\frac{k_B}{h}\right) + RT\ln T - RT\ln k \quad (5)$$

$$\varepsilon_{\Delta G} = \sqrt{\left(\varepsilon_T R\ln\left(\frac{k_B}{h}\right)\right)^2 + (R\varepsilon_{T\ln T})^2 + (R\varepsilon_{T\ln k})^2}$$

$$\varepsilon_{T\ln T} = T\ln T\sqrt{\left(\frac{\varepsilon_T}{T\ln T}\right)^2 + \left(\frac{\varepsilon_T}{T}\right)^2} \quad (6)$$

$$\varepsilon_{T\ln k} = T\ln k\sqrt{\left(\frac{\varepsilon_k}{k\ln k}\right)^2 + \left(\frac{\varepsilon_T}{T}\right)^2}$$

**D1: Eyring Plots for CLSA Experiments**

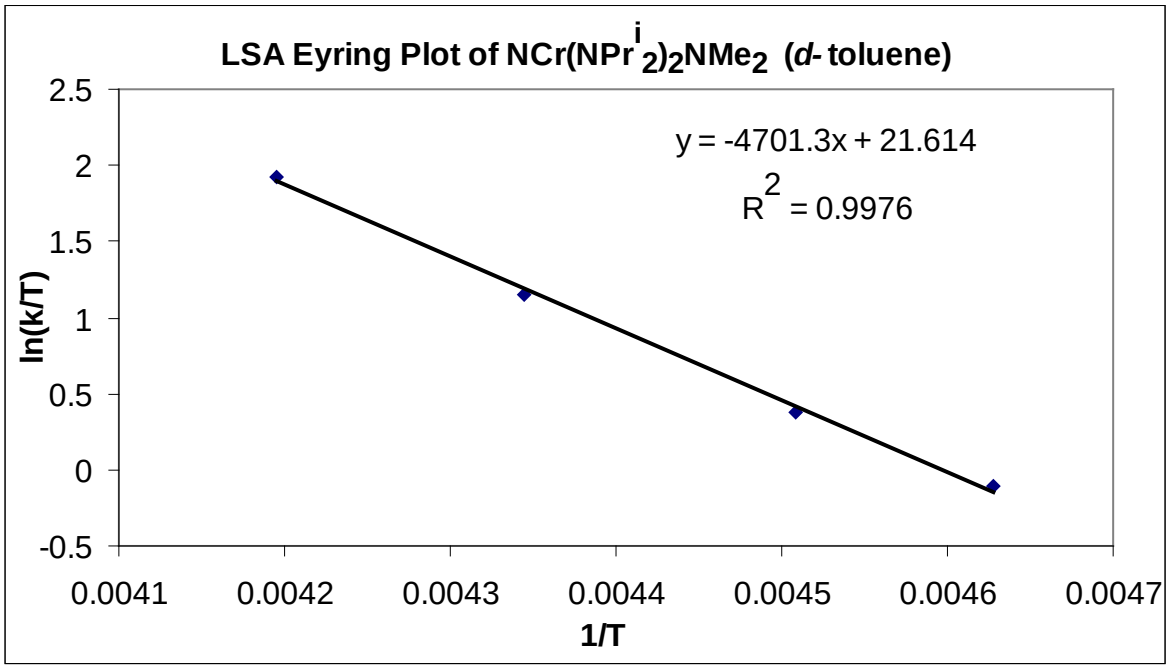


**Figure D1.1:** Eyring plot of **31**

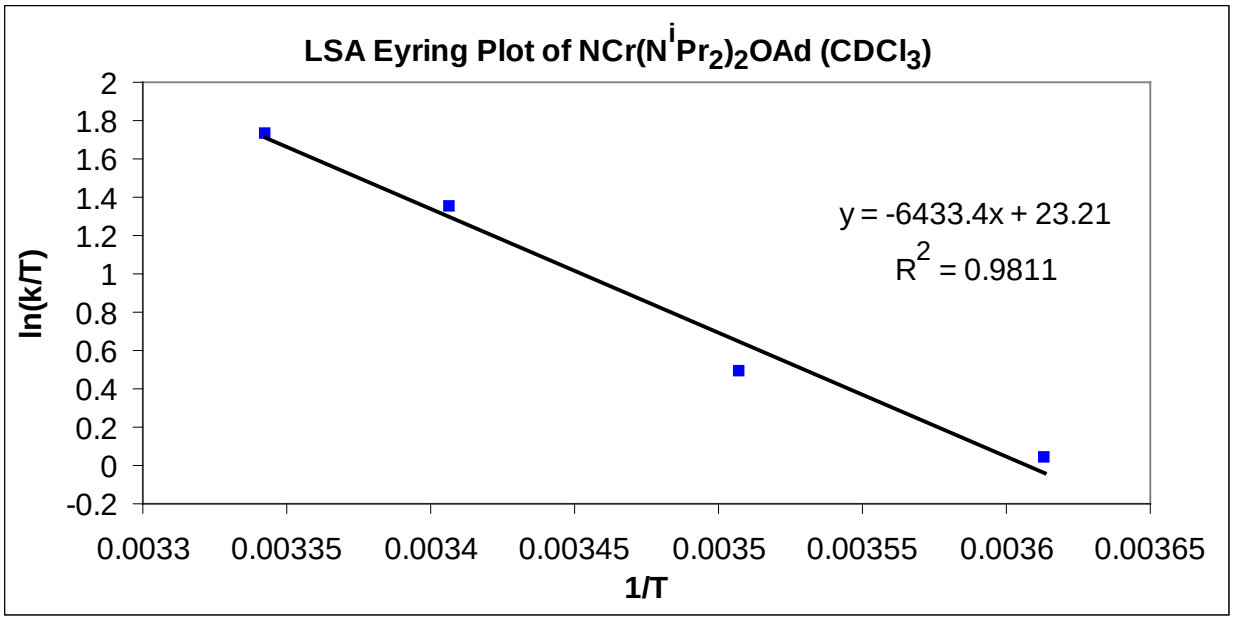


**Figure D1.2:** Eyring plot of **6**